TECHNISCHE UNIVERSITÄT MÜNCHEN

Fakultät für Medizin

Abteilung für Diagnostische und Interventionelle Neuroradiologie

# Neural mechanisms of cognitive control of motivated behavior

Felix Michael Brandl

Vollständiger Abdruck der von der Fakultät für Medizin der Technischen Universität München zur Erlangung des akademischen Grades eines Doctor of Philosophy (Ph.D.) genehmigten Dissertation.

Betreuer: Prof. Dr. Claus Zimmer

Vorsitzender: Prof. Dr. Arthur Konnerth

Prüfer der Dissertation:

1. Prof. Dr. Markus Ploner
2. Priv.-Doz. Dr. Christine Preibisch
3. Prof. Dr. Michael Ewers

Die Dissertation wurde am 30.11.2018 bei der Technischen Universität München eingereicht und durch die Fakultät für Medizin am 25.03.2019 angenommen.

# Abstract

This thesis investigated neural correlates of cognitive control of human motivated behavior. Cognitive control refers to the regulation of aversive emotions (like fear) or impulses towards rewarding stimuli (like food) based on cognitive models of long-term goals or societal norms. For example, one can suppress the craving towards a chocolate cake due to long-term weight considerations. Thus, cognitive control can be conceptualized as model-based decision making, i.e., as selection of context-appropriate behaviors based on internal models. On the other end of the decision making spectrum is model-free behavior, which only relies on previous experience. These decision making concepts can be used to describe fundamental mechanisms underlying all human motivated behaviors.

Macroscopic in-vivo imaging, namely magnetic resonance imaging (MRI) and positron emission tomography (PET), was used to study neural correlates of cognitive control in three projects:
Project 1 investigated whether brain activation patterns of cognitive control of (i) emotions and (ii) rewards overlap. Via coordinate-based meta-analysis of task functional MRI studies, an overlapping activation pattern focusing on prefrontal cortices was identified, suggesting a common model-based mechanism for the cognitive control of emotion and reward.
Project 2 tested theories that propose - additionally to such regional brain activations - increased global interaction of functional brain networks during cognitive control. This was done paradigmatically for cognitive emotion regulation via graph analysis of task functional MRI data. Increased global interaction of stable functional brain networks was observed during cognitive emotion regulation. The embedding of specific nodes overlapped with local activation patterns, suggesting complementary roles of global and local processes during cognitive control.
Project 3 focused on molecular aspects of cognitive control, namely the role of dopamine in the striatum for reward-based decision making and its impairments in schizophrenia. FDOPA-PET plus behavioral analyses was employed to analyze the link between model-based decision making and striatal dopamine transmission. Impaired decision making was then further studied in patients with schizophrenia, a disorder associated with abnormal dopamine transmission. Results showed a link between ventral striatal dopamine synthesis and the tendency towards model-based decision making. In schizophrenia, specifically model-free behavior was impaired, associated with aberrant dopamine transmission in the dorsal striatum.

Taken together, this work provides evidence for conceptualizations of cognitive control as model-based decision making, which relies on both local brain activation and global whole-brain interaction and is linked with dopamine transmission in the striatum. In schizophrenia, however, aberrant dopamine transmission in the striatum seems to impair rather model-free behavior.

# Zusammenfassung

Diese Arbeit untersuchte neurale Korrelate kognitiver Kontrolle von menschlichem motiviertem Verhalten. Kognitive Kontrolle bezeichnet die Regulation von aversiven Emotionen (wie Furcht) oder von auf belohnende Stimuli (wie Essen) gerichteten Impulsen auf der Basis von Langzeitzielen oder sozialen Normen. Kognitive Kontrolle kann also als Modell-basierte Entscheidungsfindung verstanden werden, d. h. als Auswahl von Kontext-entsprechenden Verhaltensweisen auf der Basis von internen Modellen. Am anderen Ende des Entscheidungsfindungs-Spektrums befindet sich Modell-freies Verhalten, das nur auf früheren Erfahrungen beruht. Diese Konzepte der Entscheidungsfindung können zur Beschreibung aller humanen motivierten Verhaltensweisen verwendet werden.

Magnetresonanztomographie (MRT) und Positronenemissionstomographie (PET) wurden benutzt, um neurale Korrelate kognitiver Kontrolle in drei Projekten zu studieren:
Projekt 1 untersuchte, ob Hirnaktivierungs-Muster kognitiver Kontrolle von Emotion und Belohnung überlappen. Eine Koordinaten-basierte Meta-Analyse Aufgaben-basierter funktioneller MRT-Studien zeigte ein überlappendes Aktivierungsmuster v. a. im Präfrontalkortex, was einen gemeinsamen Modell-basierten Mechanismus für die kognitive Kontrolle von Emotion und Belohnung nahelegt.
Projekt 2 testete Theorien über erhöhte globale Interaktion von funktionellen Hirnnetzwerken (zusätzlich zu regionaler Aktivierung) während kognitiver Kontrolle. Dazu wurde paradigmatisch für kognitive Emotionsregulation eine Graphenanalyse von task-fMRT Daten durchgeführt, die eine erhöhte globale Interaktion von stabilen funktionellen Netzwerken während kognitiver Emotionsregulation zeigte. Die Einbettung spezifischer Knoten überlappte mit lokalen Aktivierungsmustern, was komplementäre Rollen globaler und lokaler Prozesse bei kognitiver Kontrolle nahelegt.
Projekt 3 fokussierte auf molekulare Aspekte kognitiver Kontrolle, nämlich die Rolle von striatalem Dopamin für Belohnungs-basierte Entscheidungsfindung und ihre Störung bei Schizophrenie. FDOPA-PET und Verhaltensanalysen wurden verwendet, um die Verbindung zwischen Modell-basierter Entscheidungsfindung und Dopamintransmission zu analysieren. Weiter wurde gestörte Entscheidungsfindung bei Schizophrenie, einer mit veränderter Dopamintransmission assoziierten Erkrankung, untersucht. Die Ergebnisse zeigten eine Verbindung zwischen ventral-striataler Dopaminsynthese und der Tendenz zu Modell-basiertem Entscheiden. Bei Schizophrenie war spezifisch Modell-freies Verhalten beeinträchtigt und mit veränderter Dopamintransmission im dorsalen Striatum assoziiert.

Zusammengefasst zeigt diese Arbeit Evidenz für Konzeptionalisierungen von kognitiver Kontrolle als Modell-basierter Entscheidungsfindung, die sowohl auf lokaler Hirnaktivierung als auch globaler Hirninteraktion beruht und mit striataler Dopamintransmission assoziiert ist. Bei Schizophrenie scheint veränderte striatale Dopamintransmission jedoch eher Modell-freies Verhalten zu beeinträchtigen.

# Contents


**1 Introduction ... 1**

1.1 Theoretical background ... 1

1.1.1 Introduction to cognitive control ... 1

1.1.1.1 Cognitive control of aversive emotions ... 1

1.1.1.2 Cognitive control of impulses towards rewarding stimuli ... 2

1.1.2 Theories of cognitive control based on reinforcement learning ... 3

1.2 Neurobiological implementation of cognitive control ... 4

1.2.1 Possibly overlapping neural correlates for CRC and CER ... 4

1.2.2 Global models of cognitive control using the example of CER ... 5

1.2.3 Selection mechanisms underlying model-based decision making ... 5

1.2.3.1 Selection of competing behaviors in the striatum ... 6

1.2.3.2 Regional specificity and hierarchy of selections ... 7

1.2.3.3 Dopaminergic abnormalities in schizophrenia ... 7

1.3 Technical background of applied imaging methods ... 8

1.3.1 Functional magnetic resonance imaging (fMRI) ... 8

1.3.1.1 Physical basics of MRI ... 8

1.3.1.2 Blood oxygen level-dependent (BOLD) signal ... 9

1.3.1.3 Task-based fMRI ... 11

1.3.2 Positron emission tomography (PET) ... 12

1.3.2.1 Physical basics of PET ... 12

1.3.2.2 PET imaging of dopamine metabolism ... 12

**2 Objectives and Hypotheses ... 14**

2.1 Project 1: Overlapping model-based mechanisms of CRC and CER ... 14

2.2 Project 2: Increased global brain interaction during CER ... 15

2.3 Project 3: Dopamine and decision making in health and schizophrenia ... 17

2.4 Publication of projects in peer-reviewed journals ... 18

**3 Methods ... 19**

3.1 Project 1 ... 19

3.1.1 Coordinate-based meta-analysis of cognitive reward control ... 19

3.1.1.1 Literature search ... 19

3.1.1.2 Data extraction and meta-analysis ... 20

3.1.2 Coordinate based meta-analysis of cognitive emotion regulation ... 21

3.1.3 Conjunction analysis between CRC and CER ... 22

3.1.4 Post-hoc control analyses ... 22

3.2 Project 2 ... 23

3.2.1 Overview ... 23
3.2.2 Participants ... 23
3.2.3 Task paradigm ... 23
3.2.4 fMRI acquisition and preprocessing ... 24
3.2.5 Construction of connectivity matrices ... 26
3.2.6 Graph analysis ... 27
3.2.7 Node roles in the whole-brain community structure ... 29
3.2.8 Correlation of graph scores with CER success ... 30
3.2.9 Voxel-wise activation analysis ... 30
3.3 Project 3 ... 31
3.3.1 Participants ... 31
3.3.2 FDOPA-PET analysis ... 31
3.3.2.1 Imaging ... 31
3.3.2.2 Image analysis ... 32
3.3.3 Behavioral analysis ... 32
3.3.3.1 Decision making task ... 32
3.3.3.2 Analysis of stay-switch probability ... 34
3.3.3.3 Computational modeling of decision making behavior ... 34
3.3.4 Correlation between FDOPA-PET and decision making parameters ... 36

**4 Results ... 37**
4.1 Project 1 ... 37
4.1.1 Meta-analysis of cognitive reward control: CRC > Reward baseline ... 39
4.1.2 Meta-analysis of cognitive emotion regulation: CER > Emotional baseline ... 39
4.1.3 Common activation patterns of CRC and CER ... 39
4.1.4 Differential activation patterns of CRC and CER ... 39
4.1.4.1 (CER > Emotional baseline) > (CRC > Reward baseline) ... 40
4.1.4.2 (CRC > Reward baseline) > (CER > Emotional baseline) ... 40
4.1.5 Post-hoc control analyses for both CRC and CER ... 40
4.2 Project 2 ... 41
4.2.1 CER success ... 41
4.2.2 Increased global participation across network modules during successful CER ... 41
4.2.3 Nodal participation and connector hub analysis ... 42
4.2.3.1 Increased nodal participation of amygdala and cuneus during CER ... 42
4.2.3.2 Distinct nodes act as connector hubs in Regulate and Attend conditions ... 44
4.2.4 Spatial overlap of nodal functional embedding into the whole brain and specialized local activity during aversive emotional processing ... 45
4.3 Project 3 ... 47
4.3.1 Decision making and dopamine in healthy subjects ... 47

4.3.1.1 Stay-switch behavior ..... 47
4.3.1.2 Association between decision making and dopamine synthesis ..... 47
4.3.2 Impaired decision making and aberrant dopamine in schizophrenia ..... 48
4.3.2.1 Demographic and clinical characteristics ..... 48
4.3.2.2 Stay-switch behavior ..... 48
4.3.2.3 Computational modeling of decision making ..... 48
4.3.2.4 Striatal dopamine synthesis capacity ..... 48
4.3.2.5 Association between decision making and dopamine synthesis ..... 48

**5 Discussion ..... 49**
5.1 Project 1 ..... 49
5.1.1 Consistent activation in CRC across stimulus types ..... 49
5.1.2 Common activation in both CRC and CER ..... 50
5.1.3 Potential common model-based mechanisms of CER and CRC ..... 52
5.1.4 Cognitive control and intrinsic brain networks ..... 52
5.1.5 Limitations ..... 53
5.1.6 Conclusion ..... 53
5.2 Project 2 ..... 54
5.2.1 Increased global interaction of stable functional modules during CER ..... 54
5.2.2 Global interaction increase is pronounced in specific nodes ..... 55
5.2.3 Linking global and local theories of CER ..... 56
5.2.4 Clinical implications ..... 56
5.2.5 Limitations and future directions ..... 57
5.2.6 Conclusion ..... 58
5.3 Project 3 ..... 59
5.3.1 Decision making and striatal dopamine synthesis in healthy subjects ..... 59
5.3.2 Model-based/model-free decision making in schizophrenia ..... 59
5.3.3 Decision making and striatal dopamine synthesis in schizophrenia ..... 60
5.3.4 Conclusion ..... 60

**6 Conclusion ..... 61**

**7 References ..... 62**

**8 Acknowledgments ..... 72**

**9 List of figures and tables ..... 73**

**10 Publications related to this thesis ..... 74**

# Abbreviations

| | |
|---|---|
| BOLD | Blood oxygen level-dependent |
| CER | Cognitive emotion regulation |
| CRC | Cognitive reward control |
| dlPFC | Dorsolateral prefrontal cortex |
| EPI | Echoplanar imaging |
| FDOPA | 6-[$^{18}$F]Fluoro-L-DOPA |
| FDR | False discovery rate |
| fMRI | Functional magnetic resonance imaging |
| FWER | Family-wise error rate |
| GABA | γ-aminobutyric acid |
| GLM | General linear model |
| gPPI | Generalized psychophysiological interaction |
| IAPS | International Affective Picture System |
| L-DOPA | L-3,4-dihydroxyphenylalanine |
| MKDA | Multilevel Kernel Density Analysis |
| MNI | Montreal Neurological Institute |
| mPFC | Medial prefrontal cortex |
| MPRAGE | Magnetization Prepared Rapid Acquisition Gradient Echo |
| MRI | Magnetic resonance imaging |
| MSN | Medium spiny neuron |
| PANSS | Positive and Negative Syndrome Scale |
| PCC | Posterior cingulate cortex |
| PET | Positron emission tomography |
| PFC | Prefrontal cortex |
| PPI | Psychophysiological interaction |
| ROI | Region of interest |
| SMA | Supplementary motor area |
| TE | Echo time |
| TR | Repetition time |
| vlPFC | Ventrolateral prefrontal cortex |

# 1 Introduction

## 1.1 Theoretical background

### 1.1.1 Introduction to cognitive control

#### *1.1.1.1 Cognitive control of aversive emotions*

Let us start with an example: imagine encountering a venomous snake in the jungle. In humans, this sight usually triggers certain physiological reactions: an increase in heart rate, respiration rate, skin conductibility, and pupil diameter, accompanied by facial expressions (e.g., wide opening of the eyes, screaming) and flight behavior. When you experience these processes simultaneously, you will interpret your reaction to this situation as "fear" or "fearful emotion".

Now imagine viewing the same snake in a terrarium. In this case, the physiological reaction will be much less pronounced or even absent. Even if you experience some "fearful emotion" in the first moment, you will be able to intentionally downregulate the reaction, for example by telling yourself that the terrarium glass provides effective protection.

This example shows that emotions can be cognitively controlled or regulated. According to current views, an emotion can be defined as a psychological state that comprises physiological reactions (e.g., increasing heart rate), expressive behavior (e.g., screaming or running away), and subjective experience [Gross & Barrett, 2011]. In this way, emotions could be seen as "situated conceptualizations": the brain conceptualizes, i.e., makes meaning of, a specific situation that combines external (e.g., a snake) and internal (e.g., heart rate increase) stimuli using knowledge about previous similar situations [Barrett et al., 2014]. This process is also described as "perception-valuation-action sequence": the brain perceives a stimulus, evaluates it, and acts based on this evaluation [Etkin et al., 2015].

Cognitive control of emotions or cognitive emotion regulation (CER), in turn, refers to the cognitive modulation of emotional responses [Gross, 1998]. Of note, every single step of the perception-valuation-action sequence can be modified, for example, the bodily response can be suppressed [Gross, 1998]. But the term "CER" is specifically restricted to the evaluation/interpretation part; in Gross's process model of emotion regulation, this is called "antecedent-focused" as opposed to "response-focused" strategies [Gross, 1998]. Popular CER strategies include self-distancing (i.e., telling yourself that the situation does not affect you)

and reappraisal (i.e., re-appraising the situation as unreal or movie scene) [Buhle et al., 2014; Gross, 1998]. The clinical importance of studying CER lies in its being a core symptom of several psychiatric disorders, for example major depressive disorder [Joormann & Gotlib, 2010], schizophrenia [Grezellschak et al., 2015], or anxiety disorders [Hofmann et al., 2012].

This relevance has led to the development of research paradigms to study CER. Commonly, subjects lie in a magnetic resonance imaging (MRI) scanner while they are presented with emotional pictures. In one condition of the experiment, they are instructed to just "naturally" attend to the pictures and not alter their emotional responses. In the other condition, they are told to cognitively change their emotional reaction, for example by reappraisal. To cite one study, Ochsner et al. showed aversive photos to subjects during functional MRI (fMRI) acquisition. The participants were instructed to either not alter their emotional response ("Attend" condition) or to reinterpret the photos to decrease the negative feeling ("Reappraise" condition) [Ochsner et al., 2002].
Across many studies, images of both positive and negative valence (i.e., both pleasant and aversive pictures) have been used, and subjects were instructed to both up- or downregulate their emotional responses [Morawetz et al., 2017b]. In this thesis, however, usage of the term "CER" will be restricted to the cognitive downregulation of negative emotions.

#### *1.1.1.2 Cognitive control of impulses towards rewarding stimuli*

Let us continue with another example: coming home from work in a hungry state, you can decide between eating vegetables or a chocolate cake. You will almost certainly feel an urge (or impulse) to eat the cake in order to replenish your glucose storages. However, thinking about long-term health consequences or societal weight norms might make you reconsider your choice. In this way, you may overcome the craving towards the cake and instead select the vegetables.
This example shows that impulses, just like emotions, can be cognitively controlled. An impulse can be defined as a temporally and spatially immediate urge to approach or consume a hedonic (rewarding) stimulus (e.g., food, sex, drugs) [Hofmann et al., 2009]. As impulses are usually directed towards attainment of short-term gratifications, they often collide with long-term goals or societal norms. Therefore, suppression of such unwanted behaviors is necessary for everyday life [Hofmann et al., 2009]. Like for emotion regulation, one could also think of the modulation of distinct steps in the impulse-generating process. Again, this thesis focuses only on *cognitive* control of impulses rewarding stimuli, for example by thinking about long-term

health consequences. This concept will be called "cognitive reward control" (CRC) in the following - it is related to concepts called "self-regulation" or "self-control" [Heatherton, 2011; Hofmann et al., 2009; Kelley et al., 2015].

Failure of CRC can have severe health consequences such as addiction [Heatherton, 2011]. For this reason, fMRI paradigms were developed to study human CRC in-vivo. Usually, subjects are shown pictures of tempting cues (e.g., high-calorie food). In one condition, they shall react naturally towards the stimulus; in the other condition, they have to cognitively down- (or up-) regulate their impulse towards the stimulus (as with CER, this thesis will only focus on downregulation). To cite one study, Brody et al. presented subjects with cigarette videos. In one condition, participants should allow themselves to crave the cigarettes; in the other condition, they were instructed to resist the craving [Brody et al., 2007].

### 1.1.2 Theories of cognitive control based on reinforcement learning

How can CER and CRC be brought together? In other words, might there be an overarching neural mechanism underlying distinct instances of cognitive control?

Building on concepts from reinforcement learning, recent models suggest that similar model-based decision making mechanisms underlie both CER and CRC [Etkin et al., 2015]. In the realm of motivated behavior, decision making refers to the selection of context-appropriate behaviors from competing alternatives; this selection is based on prior knowledge and current context [Striedter, 2016]. When the selection probability of a certain behavior changes over time, this is called learning. As such changes in behavior are usually driven by rewarding/reinforcing (i.e., leading to an increased selection probability) or punishing action outcomes, this learning process is called reinforcement learning [Maia, 2009; Sutton & Barto, 2018]. The modern field of reinforcement learning developed in the 1980s as a synthesis of approaches dealing with optimal control in dynamical systems, such as dynamic programming [Bellman, 1957], and animal trial-and-error learning research [Pavlov, 1927; Thorndike, 1898; Tolman, 1932].

Drawing on reinforcement learning theories, human decision making strategies can be described as being located in a continuum between "model-free" and "model-based" [Daw et al., 2005]. "Model-based" means that a subject employs a complex cognitive model of the "decision tree" (i.e., which decision leads to which next stage?) to guide her/his selections. For this reason, it is sometimes called reflective or prospective control [Dolan & Dayan, 2013]. "Model-free", in contrast, means that decisions are driven solely by previous experience. Therefore, it is sometimes called reflexive or retrospective control [Dolan & Dayan, 2013]. In mathematical

descriptions of model-free learning such as "temporal difference learning", it is assumed that prediction errors (i.e., the difference between predicted and actual outcome) serve to update the subjects' reward predictions and therefore influence future choices [Sutton, 1988].
Historically, concepts of model-free decision making are related to theories of stimulus-response associations and habit behavior [Dolan & Dayan, 2013; Thorndike, 1898]. Model-based concepts, on the other hand, are related to early theories of goal-directed learning and cognitive maps [Dolan & Dayan, 2013; Tolman, 1932, 1948].
It is important to understand that model-based and model-free decision making are part of a continuum. Nobody employs either of them; they are always used both - however, the degree to which each strategy is applied, i.e., their balance, can vary.

These considerations can now be used to describe cognitive control processes with more precision. According to a recent model, both CER and CRC can be seen as model-based decision making [Etkin et al., 2015]. This concept assumes that in CER, an internal model is applied to select the appropriate emotion-regulatory action for achieving a desired emotional state. Likewise, in CRC, a cognitive model of long-term goals or societal norms is employed to regulate one's craving towards a rewarding stimulus, e.g., food, sex, or drugs. Taken together, computational models and underlying neural mechanisms of CRC and CER might resemble each other: both model-based control strategies involve decisions about actions, which alter either one's emotional state or one's craving towards consumption of a rewarding stimulus.

## 1.2 Neurobiological implementation of cognitive control

### 1.2.1 Possibly overlapping neural correlates for CRC and CER

On a neurobiological level, concepts of similar mechanisms for CRC and CER suggest that neural correlates of CER should resemble neural correlates of CRC. Such an overlap of neural substrates would in turn indicate similar generating neural mechanisms. Previous literature suggests a widespread overlap of neural activation across CER and CRC in ventromedial and dorsolateral prefrontal cortices as well as in supplementary motor cortex [Etkin et al., 2015]. However, this hypothesis has not been tested across single studies with possibly varying methodology. Therefore, part of the current thesis addressed this question by use of coordinate-based meta-analysis of task-fMRI studies concerning CRC and CER (Project 1).

### 1.2.2 Global models of cognitive control using the example of CER

As described above, previous studies report widespread regional brain activation during cognitive control. However, theories differ with regard to the spatial extent of brain changes underlying cognitive control. In the following, this question is paradigmatically restricted to CER. While local theories view CER as a regionally confined process, global models point to increased whole-brain interactions across functional brain networks during CER. More specifically, local and related 'intermediate' models of CER emphasize that circumscribed cortical areas, like in the medial and lateral prefrontal cortices, control activity in spatially more-or-less distinct brain regions such as in amygdala and orbitofrontal-insular cortices [Ochsner et al., 2002; Wager et al., 2008]. Global theories, in contrast, propose that larger functional brain modules, which comprise brain regions of local/intermediate theories, underlie emotional processes both with and without CER, but with increased global across-module interactions during CER [Barrett, 2009; Barrett et al., 2014; Lindquist & Barrett, 2012]. While evidence for local/intermediate views is overwhelming (for recent meta-analyses, see [Buhle et al., 2014; Frank et al., 2014]), evidence for global theories is scarce.

For this reason, part of this thesis tested key predictions of global CER theories by combining a typical CER paradigm on aversive emotional pictures during fMRI with a graph theory-based approach to brain activity (Project 2).

### 1.2.3 Selection mechanisms underlying model-based decision making

As described above, cognitive control strategies like CRC and CER can be conceptualized as model-based decision making. Several studies have shown that model-based decision making depends on dopamine levels. Wunderlich et al. presented evidence that application of L-DOPA (a precursor of dopamine) leads to increased model-based decision making in a sequential learning task [Wunderlich et al., 2012]. However, the design of this study prevented any conclusions about the regional specificity of dopamine effects. This gap was closed by the study of Deserno et al.: they combined a sequential decision making task with FDOPA positron emission tomography (PET) [Deserno et al., 2015]. Results indicated that dopamine synthesis in the nucleus accumbens is positively correlated with a tendency towards model-based behavior.

The following paragraphs will elaborate on dopamine's role in selection processes underlying decision making (remember that decision making can be defined as selection of context-appropriate behaviors from a repertoire of competing behaviors).

### *1.2.3.1 Selection of competing behaviors in the striatum*

Current neurobiological models emphasize the role of the striatum in selection processes. Such hypotheses are based on the underlying anatomy and physiology of the striatum as part of the basal ganglia. The striatum is part of topographically arranged parallel and largely segregated cortico-striato-pallido-thalamo-cortical loops [Alexander et al., 1986; Haber, 2016]. Since the cortico-striatal input arrives mostly from frontal cortices, sometimes the term "frontostriatal system" is used [Striedter, 2016]. The net effect of these loops is positive feedback to the cortex [Striedter, 2016]. Their supposed function is the selection of context-appropriate behaviors from competing alternatives, or more general: the selection of cortical co-activation patterns, which then lead to specific behaviors.

The main mechanism of selection is thought to be the strength (and/or simultaneity) of cortical input onto direct pathway GABAergic medium spiny neurons (MSNs) in the striatum. Direct pathway means that these inhibitory neurons project directly onto GABAergic neurons in the pallidum, which in turn tonically inhibit the thalamus. Thus, activation of a striatal MSN leads to selective disinhibition of the thalamus as net effect [Striedter, 2016].

Further mechanisms supporting and sharpening selections are:

(i) a winner-takes-all mechanism: active MSNs inhibit less active MSNs via axon collaterals, which makes the selection more precise;

(ii) the so-called indirect pathway leading to a diffuse excitation of pallidum via globus pallidus externus and subthalamic nucleus. The effect is a diffuse inhibition of non-selected co-activation patterns and therefore a more precise selection;

For the next two points, a short introduction of the human dopaminergic system is needed. The bodies of dopaminergic neurons are located in the midbrain, more specifically in substantia nigra pars compacta and ventral tegmental area. The densest projection of dopaminergic cells is towards the striatum. However, other brain areas are targeted too, for example pallidum, thalamus, and cortex (particularly frontal regions) [Sanchez-Gonzalez et al., 2005; Weinstein et al., 2017]. The two basic firing modes of dopamine neurons are tonic (regular, low-frequency "pacemaker" firing) and phasic (high-frequency spike bursts) [Grace & Bunney, 1984a, b].

(iii) tonic or spontaneously phasic dopamine release in the striatum. Dopaminergic synapses are located at dendritic spines of MSNs "below" cortico-striatal synapses and excite the direct pathway via D1 receptors while inhibiting the indirect pathway via D2 receptors. Thus, this input facilitates the selection of specific co-activation patterns in the striatum;

(iv) stimulus-associated phasic dopamine bursts, at first during the consumption of a reward achieved by a certain action. After classical conditioning, however, the burst moves forward to the time point when a cue associated with the reward is presented. Thus, stimulus-associated phasic dopamine bursts act as teaching signals to learn sequences of actions. They further alter selection probabilities of specific co-activation patterns over time via long-term potentiation/depression at cortico-striatal synapses [Striedter, 2016].

#### *1.2.3.2 Regional specificity and hierarchy of selections*

Current models suggest that topographical conservation of cortico-striato-pallido-thalamo-cortical loops gives rise to a regional specificity of selection processes underlying decision making. The orbital prefrontal cortex (PFC) projects primarily to the ventral striatum (including mainly nucleus accumbens), supporting the selection of high-level goals. Lateral and medial PFC project to dorsomedial striatum (caudate nucleus), leading to the selection of actions to achieve the selected goals. Finally, (pre-)motor cortices project to dorsolateral striatum (putamen), subserving the selection of movements to perform the selected actions. Such theories assume a hierarchy from the ventral over the dorsomedial to the dorsolateral frontostriatal system. The ventral system is active over longer time scales since it represents high-level decisions, the dorsal system over shorter time scales [Striedter, 2016].

Consequently, it has been suggested that model-based decision making is represented mainly in ventral striatum since it is based on high-level cognitive decisions requiring input from orbital PFC [Daw et al., 2005; Dolan & Dayan, 2013]. This assertion is supported by fMRI studies showing brain activation in the nucleus accumbens to be associated with model-based decisions [Daw et al., 2011; Deserno et al., 2015]. Model-free behavior, on the other hand, seems to be represented by the whole striatum with focus on dorsal regions, because model-free behaviors rely mostly on somehow automatized actions and movements. Support for such claims comes from studies showing that activity shifts from ventral to dorsolateral striatum as actions are learned, indicating a transition from goal-directed to habit behavior or from model-based to model-free decision making [Graybiel, 2008].

#### *1.2.3.3 Dopaminergic abnormalities in schizophrenia*

As we have seen, dopamine plays an important role in the selection of competing behaviors in the striatum and thus in decision making. Schizophrenia has long been associated with aberrant dopamine transmission [Howes & Kapur, 2009]. It is a disease that affects about 1% of the

world's population and usually begins in young adulthood [Owen et al., 2016]. Its symptoms are generally categorized into positive (including delusions and hallucination), negative (including anhedonia, loss of motivation, asociality etc.), and cognitive (e.g., impaired working memory, cognitive speed, task switching etc.) symptoms.

First theories of excessive dopamine transmission in schizophrenia emerged from findings that antipsychotic drugs exert their effect through blockade of dopamine D2 receptors [Carlsson et al., 1957; Creese et al., 1976; van Rossum, 1966] and that dopamine agonists like amphetamine can cause psychotic symptoms [Lieberman et al., 1987]. These theories were later modified, now suggesting prefrontal cortical hypodopaminergia versus subcortical hyperdopaminergia [Davis et al., 1991]. The advent of in-vivo imaging tools like PET then demonstrated that particularly presynaptic dopamine synthesis in the striatum is reliably elevated in schizophrenia [Howes et al., 2012]. Of note, however, these data were almost exclusively acquired from patients during psychotic episodes; such a primary association between increased presynaptic dopamine and psychosis in general is supported by similar findings in subjects at risk for psychosis [Howes et al., 2009] and patients with psychotic bipolar disorder [Jauhar et al., 2017].
Therefore, the question arises whether abnormal dopamine transmission in schizophrenia is associated with an impaired balance between model-based and model-free decision making. The study of Culbreth et al. has hinted at such an imbalance [Culbreth et al., 2016]; however, as they did not acquire in-vivo dopamine imaging data, evidence for associations with dopamine transmission is still missing. This problem is addressed by Project 3.

## 1.3 Technical background of applied imaging methods

### 1.3.1 Functional magnetic resonance imaging (fMRI)

#### *1.3.1.1 Physical basics of MRI*

MRI is a non-invasive in-vivo imaging technique based on the spin of hydrogen nuclei, i.e., protons. "Spins" are spinning or rotating electrical charges, for example protons, that generate a magnetic dipole moment.
In an MRI tomograph, a static magnetic field $B_0$ leads to alignment of proton spins with the direction of the field along the z-axis (longitudinal magnetization). More precisely, the protons precess around the direction of $B_0$ with the Larmor frequency (defined by the field strength of $B_0$ and the gyromagnetic ratio of the proton). Then a radiofrequency pulse equaling the Larmor

frequency excites the protons and flips them by 90° (transverse magnetization), which causes a spinning of the net magnetization vector (the sum of all proton spins) in the x-y-axis. Such a magnetization shift induces an electrical current in the receiver coils of the MRI machine. After the end of the radiofrequency pulse, the net magnetization vector returns to the alignment with $B_0$. This so-called relaxation is determined by two time constants: T1 describes the recovery of longitudinal magnetization, while T2 describes the loss of transverse magnetization due to spin dephasing caused by spin-spin-interactions. However, inhomogeneities in the external magnetic field accelerate the dephasing; this process is described by the T2* relaxation time, which is shorter than T2.

Body tissues differ in their T1 and T2 times. Thus, one can define contrasts by varying repetition time (TR, time between two radiofrequency pulses) and echo time (TE, time between radiofrequency pulse and measurement of MRI signal). A short TR leads to T1 weighting, because differences in the recovery speed of longitudinal magnetization are emphasized. A long TE causes T2 weighting, since differences in dephasing speed are accentuated.

For three-dimensional spatial encoding of spin excitation, several strategies are used. On the one hand, frequency encoding uses gradient coils. This leads to different Larmor frequencies along a certain axis, which can then be selectively excited by specific radiofrequency pulses. Usually, this strategy is used for slice selection and for encoding in x-direction. On the other hand, phase encoding applies a short magnetic gradient pulse that causes phase difference of transverse magnetization vectors. This is usually employed for encoding in y-direction [Weishaupt et al., 2009].

#### *1.3.1.2 Blood oxygen level-dependent (BOLD) signal*

fMRI is based on the measurement of T2* relaxation time, which is influenced by the ratio of oxygenated versus deoxygenated hemoglobin. For this reason, the measured signal is called "blood oxygen level-dependent" (BOLD) [Ogawa et al., 1990]. The BOLD signal is an indirect marker for neuronal activity and, according to current understanding, arises from the following process: Neuronal activity consumes energy, e.g., for the reuptake and recycling of transmitters of for the restoration of membrane potentials [Shulman et al., 2004]. This energy in form of adenosine triphosphate (ATP) is provided by oxidative glucose metabolism [Sibson et al., 1998]. Therefore, neuronal activity leads to increased consumption of oxygen, which is brought to neurons by hemoglobin via the blood. Initially, neuronal activity causes a decrease in the local concentration of oxygenated hemoglobin. After a short time, however, a process called neurovascular coupling leads to a local increase of cerebral blood flow. The exact mech-

anisms are still unclear; possible candidates include interneurons [Cauli et al., 2004], astrocytes [Takano et al., 2006], and pericytes [Peppiatt et al., 2006]). The increase in cerebral blood flow leads to a supply of oxygen that exceeds its consumption, so the net effect is an increasing ratio of oxygenated versus deoxygenated hemoglobin [Logothetis, 2008]. The temporal dynamics of this process follow the "Hemodynamic Response Function": it starts about 500 ms after onset of a stimulus and peaks at 3-5 s after stimulus onset (***Fig. 1***) [Hillman, 2014; Logothetis & Wandell, 2004]. Oxyhemoglobin and deoxyhemoglobin differ in their magnetic susceptibility: deoxyhemoglobin is paramagnetic and shortens T2* relaxation, whereas oxyhemoglobin is diamagnetic and has no or only minimal influence on T2* relaxation. Thus, an increase in the concentration of oxyhemoglobin causes an increased signal in T2*-weighted MRI sequences like echoplanar imaging (EPI) [Logothetis, 2008; Schneider & Fink, 2013; Weishaupt et al., 2009].

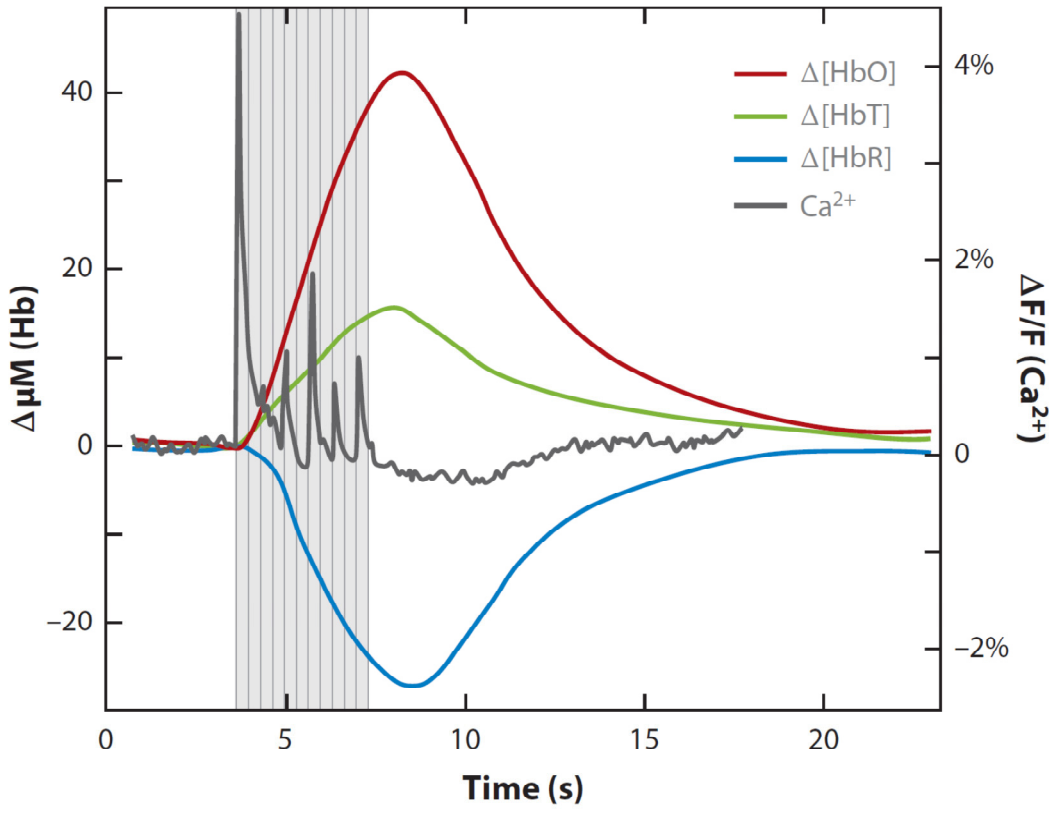


***Figure 1: Hemodynamic response.***

*Temporal dynamics of increase in oxygenated hemoglobin (HbO, red line) and its association with calcium response ($Ca^{2+}$, dark grey line). The HbO increase reaches its peak about 3-5 seconds after stimulus onset (stimulus is indicated by grey shading). Data show a stimulus-evoked response in the rat somatosensory cortex. Figure taken from [Hillman, 2014].*

The neurophysiological basis of the BOLD signal is still poorly understood, particularly concerning neurovascular coupling mechanisms [Attwell et al., 2010; Hillman, 2014] and whether vascular dynamics not precisely related to neuronal activity contribute to the signal [Girouard & Iadecola, 2006; O'Herron et al., 2016]. However, multiple animal studies showed a high correlation of BOLD signal and underlying neuronal activity, justifying its use in neuroimaging research (***Fig. 1***) [Logothetis et al., 2001; Matsui et al., 2016; Pan et al., 2013]. Possible candidates for neural sources of the BOLD signal are local field potentials, reflecting mostly synaptic activity [Logothetis et al., 2001; Pan et al., 2013], and local spiking activity [Cardoso et al., 2012; Lima et al., 2014]. In any case, it has to be kept in mind that the fMRI signal reflects a population or mass signal, since a typical MRI voxel contains about 5 million neurons and 50 billion synapses [Logothetis, 2008].

#### *1.3.1.3 Task-based fMRI*

Tasks used in fMRI studies range from simple (e.g., eyes open/closed, finger tapping) to complex (e.g., learning tasks). Two basic types of designs are distinguished: in blocked designs, a certain period of one experimental condition (e.g., eyes open) is followed by a period of another condition (e.g., eyes closed). In event-related designs, in contrast, discrete single events occur multiple times with fixed or variable intervals (e.g., a picture is shown for 3 seconds). The whole sequence comprising one event is usually called a trial, which is repeated multiple times during one experimental run. One such run in an event-related design can contain only trials of one condition (e.g., watching an aversive picture without emotion regulation) or alternating trials of several conditions (e.g., watching an aversive picture with or without emotion regulation).

In common experimental setups, the subject is presented with certain stimuli during acquisition of an fMRI sequence. For example, these stimuli can be visual (pictures/videos shown on a screen at the end of the scanner, which can be watched by the subject through a mirror above her/his head) or auditory (via headphones). If the task includes decision making or feedback by the subject, a set of buttons is provided through which the subject can give a response via button press. Furthermore, physiological data can be recorded, e.g., electrodermal activity, heart rate, or pupil diameter.

## 1.3.2 Positron emission tomography (PET)

### *1.3.2.1 Physical basics of PET*

PET is an invasive in-vivo functional imaging technique based on the emission of positrons by a radionuclide. A radionuclide is an atom that exhibits radioactive decay. For example, the most commonly used radionuclide in nuclear medicine is the radioactive fluorine isotope $^{18}F$ (half-life: 110 min [Conti & Eriksson, 2016]). Such a radionuclide is chemically inserted in a certain molecule, which usually occurs naturally in the human body. The product is called radiotracer and allows for the investigation of a specific metabolic process. For example, glucose metabolism can be analyzed using fluorodeoxyglucose (FDG). In PET imaging, the radiotracer is intravenously applied to the subject and taken up by the tissues that normally take up this specific molecule.

Within these tissues, the radionuclide emits positrons ($\beta^+$ radiation) which, after a short distance of "traveling" (about 1 mm for $^{18}F$ [Conti & Eriksson, 2016]), annihilate with an electron. Annihilation leads to the emission of two photons (γ radiation) with a characteristic energy of 511 keV in opposite directions (i.e., with an angle of 180°). These coincident pairs of photons are then detected by PET detectors positioned in a ring around the subject. Such coincidences allow for the reconstruction of the location of annihilation [Reiser et al., 2011].

### *1.3.2.2 PET imaging of dopamine metabolism*

Several aspects of dopamine metabolism can be investigated by in-vivo molecular imaging in humans. The most widely used techniques are PET and single-photon emission computed tomography (SPECT); due to the focus of this thesis, the discussion will be restricted to PET. PET is used to study dopamine synthesis, release, postsynaptic receptor binding, and transport [Weinstein et al., 2017].

First, dopamine synthesis capacity can be measured with the tracer FDOPA, which is L-DOPA radioactively labeled with $^{18}F$ [Garnett et al., 1983]. L-DOPA, in turn, is a precursor of dopamine that can, contrary to dopamine itself, cross the blood-brain barrier. In the brain, FDOPA is taken up by dopaminergic neurons in substantia nigra and ventral tegmentum and transported to axon terminals. Then, FDOPA is converted by the enzyme amino acid decarboxylase (AADC) into 6-[$^{18}F$]Fluorodopamine, which is stored in presynaptic vesicles [Weinstein et al., 2017]. In this way, the uptake of FDOPA in a specific brain area can be used to quantify dopamine synthesis (for the biophysical models used in the quantification process, e.g., Patlak modeling, see the Methods section).

Second, availability of postsynaptic dopamine receptors is measured with tracers that bind to these receptors (i.e., radioligands). For example, [$^{11}$C]NNC 112 binds to D1 receptors [Abi-Dargham et al., 2000], while [$^{11}$C]raclopride binds to D2 receptors [Farde et al., 1986]. The outcome measure of these studies is binding potential, which corresponds to receptor availability. However, it has to be kept in mind that a considerable number of receptors might be occupied by endogenous dopamine and are therefore not available for radioligands. Depletion paradigms try to circumvent this issue: alpha-methyl-para-tyrosine suppresses endogenous dopamine synthesis (via blockade of the enzyme tyrosine hydroxylase) and in this way "unmasks" occupied dopamine receptors, revealing the "true" receptor density [Laruelle et al., 1997; Verhoeff et al., 2001]. The reduction in binding potential is interpreted as baseline synaptic dopamine [Weinstein et al., 2017].

Third, D2 receptor tracers can also be used to study dopamine release. In order to do so, subjects undergo two PET scans: once at baseline and once after application of amphetamine, an agent that stimulates dopamine release [Breier et al., 1997; Laruelle et al., 1995]. The change in binding potential across the two conditions is then taken as proxy for dopamine release.

Finally, dopamine reuptake via presynaptic dopamine transporters can be investigated using tracers binding to these transporters, for example [$^{18}$F]CFT [Laakso et al., 1998]. The outcome measure (binding potential) quantifies transporter availability.

# 2 Objectives and Hypotheses

## 2.1 Project 1: Overlapping model-based mechanisms of CRC and CER

This project addresses two questions. First, is there a consistent pattern of brain activation for cognitive reward control (CRC) across a wide range of reinforcing stimuli, e.g., food, sex, drugs? Although multiple fMRI studies have investigated task activation patterns during CRC via changes in blood oxygenation [Brody et al., 2007; Crockett et al., 2013; Kober et al., 2010], due to heterogeneous methods and results no consistent pattern across studies and stimulus types has been identified so far. A recent meta-analysis has shown consistent brain activation in dietary reward control across insular, prefrontal, and parietal cortices [Han et al., 2018]. However, it is unclear whether this pattern generalizes also for other stimulus types.

This question was addressed using coordinate-based meta-analysis of task-fMRI studies in CRC as an experimental proxy for reward-related model-based decision-making. Meta-analysis is a powerful tool to detect consistent neural correlates across methodologically heterogeneous studies. We included all fMRI studies using tasks in which subjects cognitively controlled hedonic impulses towards rewarding cues (e.g., food, sex, cigarettes, money) and synthesized results using Multilevel Kernel Density Analysis (MKDA) [Wager et al., 2007]. We hypothesized consistent activation in ventrolateral and dorsolateral prefrontal cortex, parietal, and (pre-) supplementary motor areas (pre-SMA, SMA) [Etkin et al., 2015; Kelley et al., 2015].

Second, we investigated whether the extension of computational models based on reward-related decision making onto cognitive emotion regulation (CER) is justified. Based on theories drawn from reinforcement learning, Etkin et al. had suggested that CRC and CER can both be described as model-based decision making strategies [Etkin et al., 2015]. Consequently, their neural activation patterns should overlap.

We tested this hypothesis by complementing the CRC meta-analysis with a coordinate-based meta-analysis of task-fMRI studies in CER, i.e., studies in which subjects cognitively downregulated negative emotional responses elicited by aversive pictures via reappraisal [Goldin et al., 2008; Gross, 2002; Ochsner et al., 2002]. Then we tested for common and distinct activation patterns across CRC and CER via meta-analytic contrasts and conjunction analysis [Radua et al., 2013]. We expected common activation in ventrolateral PFC, dorsolateral PFC, SMA, pre-SMA, and parietal cortices [Etkin et al., 2015].

## 2.2 Project 2: Increased global brain interaction during CER

The second part of this thesis investigates global processes (complementing locally confined activation) during cognitive control, paradigmatically for the example of CER. Such global models point to increased whole-brain interactions across functional brain networks during CER [Barrett, 2009; Barrett et al., 2014; Lindquist & Barrett, 2012]. We addressed this question by graph analysis of fMRI data acquired during a CER paradigm.

Graph-based analysis is a powerful tool to investigate interaction patterns among large-scale brain networks, covering the whole brain [Bullmore & Sporns, 2009]. A graph consists of nodes and edges; in the context of emotion-related brain activity, a graph consists of regions-of-interest (ROIs) representing the whole brain as nodes and emotion-related functional connectivity between these ROIs as edges between nodes (for a glossary of graph terms, see ***Table 1***). The topology of such a whole-brain graph can be described both at global and nodal levels by measures of integration, segregation, and community structure [Rubinov & Sporns, 2010]. Particularly, the community or modular structure describes how the whole graph can be subdivided into functional network modules with high intra-modular but low inter-modular connectivity [Girvan & Newman, 2002]. More specifically, global community structure has two characteristics: modularity quantifies how 'easily' a graph can be decomposed into separate modules [Newman, 2004]; global participation quantifies how 'strongly' each node of the graph is connected to nodes in other modules [Guimera & Amaral, 2005b].

Applying these concepts to the global CER perspective, we expected stable functional brain network modularity across the two emotional states with and without CER, due to the idea that similar functional networks subserve emotional processing with and without CER. On the other hand, we expected increased global participation across these networks during CER, reflecting an increased interaction across modules during CER, compared to without CER. Complementary, at nodal level we expected that nodes driving increased global participation across modules are also part of known regions from local/intermediate perspectives on CER, such as amygdala or prefrontal cortex. This suggestion was based on the idea that altered local activity, which shows the strongest activation-based change during CER, might also affect these nodes' functional embedding into the whole-brain graph.

| Graph term | Definition |
|---|---|
| **Graph** | Set of nodes linked by edges |
| **Node** | In this thesis: spherical brain regions of interest |
| **Edge** | In this thesis: functional connectivity during emotion or cognitive emotion regulation |
| **Cost** | Number of edges divided by the maximal possible number of edges |
| **Module** | Group of densely interconnected nodes with only sparse connections to other modules |
| **Within-module connectivity** | Connectivity of a node with all other nodes in its module |
| **Between-module connectivity** | Connectivity of a node with all nodes *outside* of its module |
| **Modularity** | Quantifies the degree to which a graph can be subdivided into non-overlapping modules |
| **Participation coefficient** | Quantifies the between-module connectivity on nodal and global levels |
| **Within-module degree** | Quantifies the within-module connectivity of a node |
| **Functional segregation** | Ability for specialized processing within densely connected clusters |
| **Clustering coefficient** | Fraction of interconnected neighbors around a node; quantifies segregation |
| **Functional integration** | Ability for rapid combination of spatially distributed information |
| **Characteristic path length** | Average shortest path length across all pairs of nodes; quantifies integration |

***Table 1: Glossary of graph terms.***

*Definitions were largely derived from [Bullmore & Sporns, 2009; Rubinov & Sporns, 2010]*.

## 2.3 Project 3: Dopamine and decision making in health and schizophrenia

This project investigates two questions. First, does presynaptic dopamine synthesis, as measured by FDOPA-PET, influence the balance of model-based and model-free decision making? Dopamine modulates selection processes in the striatum that underlie decision making. This suggests that it affects model-based decisions such as cognitive control. Indeed, Wunderlich et al. could show that application of L-DOPA (a dopamine precursor) increases the tendency towards model-based decision making [Wunderlich et al., 2012]. Deserno et al. further specified this finding by showing that specifically presynaptic dopamine synthesis in the nucleus accumbens correlates with the tendency towards model-based behavior [Deserno et al., 2015]. In a first step, we sought to confirm these results in healthy subjects.

Second, we tested whether the association between dopamine and decision making is impaired in patients with schizophrenia. Previous results suggest an impaired balance between model-based and model-free decision making in schizophrenia [Culbreth et al., 2016]. However, the relationship with dopamine metabolism remains unclear. We addressed this issue by conducting a decision making task plus FDOPA-PET in patients with chronic schizophrenia (at least 2 psychotic episodes) and healthy controls. Of note, patients were in a state of psychotic remission during the study, meaning that positive symptoms were absent, but negative and cognitive symptoms present [Andreasen et al., 2005]. In this way, any bias from psychotic symptoms can be avoided. Subjects' decision making behavior in the task was described by mathematical models allowing for the quantification of model-based and model-free behavior. Presynaptic dopamine synthesis capacity in the striatum, on the other hand, was quantified by graphical Patlak analysis of FDOPA-PET data. The outcome of this analysis is the influx constant $k_i^{cer}$ that quantifies the uptake/accumulation of the radiotracer in a certain brain region. Decision making parameters were compared across groups and correlated with $k_i^{cer}$ measures.

## 2.4 Publication of projects in peer-reviewed journals

Project 1 was published in "Cerebral Cortex" in the following article:

Brandl F, Mulej Bratec S, Xie X, Wohlschläger AM, Riedl V, Meng C, Sorg C:

*Increased Global Interaction Across Functional Brain Modules During Cognitive Emotion Regulation.*

Cereb Cortex. 2018 Sep 1;28(9):3082-3094.

Project 2 has been revised according to reviewer comments from a submission to "Neuroscience and Biobehavioral Reviews" and is currently under peer review at "NeuroImage" with the following title:

Brandl F, Le Houcq Corbi Z, Mulej Bratec S, Sorg C:

*Cognitive reward control recruits medial and lateral frontal cortices, which are also involved in cognitive emotion regulation - A coordinate-based meta-analysis of fMRI studies.*

Project 3 has been presented as poster at the conferences "Annual Meeting of the Society of Biological Psychiatry 2018" and "FENS Forum of Neuroscience 2018". It is now prepared for publication under the following title:

Brandl F, Avram M, Cabello J, Leucht C, Scherr M, Mustafa M, Leucht S, Ziegler S, Wunderlich K, Sorg C:

*Association between impaired model-free decision making and dopamine synthesis in schizophrenia.*

# 3 Methods

## 3.1 Project 1

### 3.1.1 Coordinate-based meta-analysis of cognitive reward control

#### *3.1.1.1 Literature search*

PubMed and Web of Science were searched until May 01, 2018 using the keywords *(self-regulat* OR impulse control OR self-control OR restrain) AND (fMRI OR neuroimaging)* (***Fig. 2A***). Additional relevant studies were identified using reviews and reference lists.

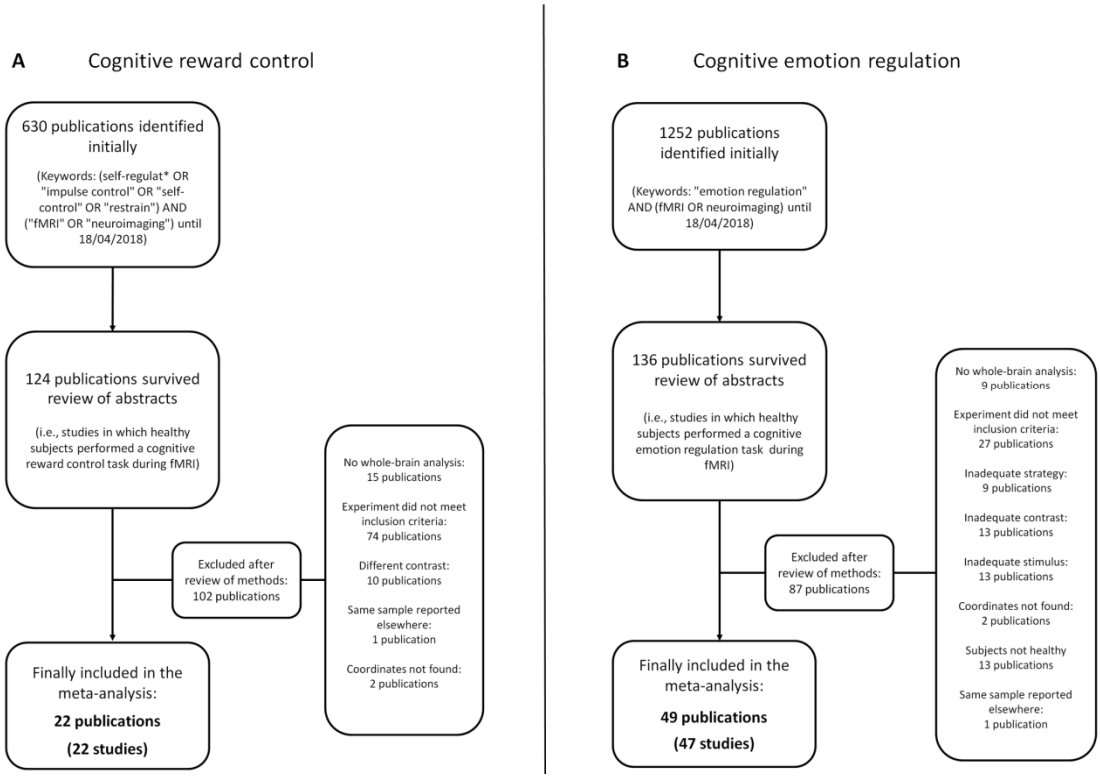


***Figure 2: Flow diagram of literature search.***

*Literature search for cognitive reward control (A), yielding a total of 22 publications (22 studies) and 741 subjects, and for cognitive emotion regulation (B), yielding a total of 49 publications (47 studies) and 1455 subjects. Keywords and exclusion criteria are indicated. Publications using identical subject samples were counted as one single study; this resulted in less included studies than included publications.*

CRC is usually studied by instructing subjects to control their craving towards rewarding stimuli (e.g., food, money, or sex), whose consumption is not compatible with internal long-term goals or societal norms. For example, when feeling the impulse of eating a chocolate dessert, an internal model of long-term health consequences may inhibit this impulse [Hare et al., 2011]. Thus, the experiment design in the selected CRC studies contrasted two conditions: *"Reward baseline"*, in which subjects were asked to allow themselves to crave a desirable reward cue they were viewing, e.g., cigarettes or tasty food, and *"CRC"*, in which participants should resist any desirable reward by, for example, thinking about long-term consequences of repeatedly consuming the substance [Brody et al., 2007; Crockett et al., 2013; Kober et al., 2010]. We only included studies using visual stimuli such as pictures and videos [Buhle et al., 2014; Kohn et al., 2014]. Furthermore, only studies in which subjects were instructed to downregulate their hedonic impulses towards reinforcing cues were considered; studies with different goals like upregulation were not included. Further exclusion criteria were: (i) use of subjects with mental disorders, (ii) no whole-brain analysis (restriction to predefined regions of interest), (iii) no report of coordinates in MNI or Talairach space. Publications using identical subject samples were counted as one single study; thus, there were less included studies than included publications.

#### *3.1.1.2 Data extraction and meta-analysis*

Peak coordinates of activation differences between the two conditions (CRC vs. Reward baseline) were extracted from the studies and converted to Montreal Neurological Institute (MNI) space if necessary. For coordinate-based meta-analysis, we used Multilevel Kernel Density Analysis (MKDA) [Etkin & Wager, 2007; Wager et al., 2007], which comprises the following steps: first, peak coordinates of each study contrast map were convolved separately with a spherical kernel (radius = 15mm) to create a so-called comparison indicator maps. In these indicator maps, each voxel had either the intensity value 1 (= at least one peak within 15mm of this voxel) or 0 (= no peak within 15mm of this voxel). Subsequently, indicator maps were weighted by sample size and averaged across studies to yield so-called density maps, showing the weighted proportion of contrast maps reporting a peak within 15mm of each voxel (= density statistic). In this step, the hypoactivation map was subtracted from the hyperactivation map in order to identify brain regions which are specifically hyperactivated, but not hypoactivated during CRC. Due to our hypothesis, we only investigated the meta-analytic contrast "CRC > Reward baseline".

To test for statistical significance of meta-analytic result clusters in the density maps, a Monte Carlo simulation with 15,000 iterations was performed to establish a family-wise error rate (FWER) threshold. Significant result clusters were detected for $p<0.05$ (FWER-corrected), both based on voxel-wise density statistic (height-based threshold) and cluster size (extent-based threshold) [Wager et al., 2007]. Both thresholds were reported since they provide complementary information [Kaiser et al., 2015]. To control for potential confounding effects (like disproportionate influence of single studies) on our meta-analytic results, several post-hoc control analyses were performed, which are presented in detail below after the description of the CER meta-analysis.

### 3.1.2 Coordinate based meta-analysis of cognitive emotion regulation

PubMed and Web of Science were searched until May 01, 2018 using the keywords *emotion regulation AND (fMRI OR neuroimaging)*. Additional relevant studies were identified using reviews and reference lists (***Fig. 2B***). CER is typically studied by contrasting *'pure'* emotional stimulation (e.g., viewing aversive pictures) with emotional stimulation *during* CER (i.e., while reappraising the stimulus). For example, when seeing the picture of a snake, re-appraising the situation as being part of an experiment typically decreases induced fear [Eippert et al., 2007]. Thus, the experiment design in the selected CER studies contrasted two conditions: *"Emotional baseline"*, in which subjects watched aversive pictures and were asked to naturally experience the emotional state elicited by the picture, and *"CER"*, in which participants attempted to down-regulate their negative emotional responses towards the aversive pictures using reappraisal [Goldin et al., 2008; Gross, 2002; Ochsner et al., 2002].

Inclusion and exclusion criteria for studies were the same as for CRC (only visual stimuli, only downregulation). Note that only studies using aversive stimuli were included. Furthermore, we selected only studies that employed reappraisal to modulate emotional responses; studies that used suppression or manipulation of attention such as distraction were excluded. These strict criteria were selected to achieve design homogeneity across CER and CRC studies, resulting in a smaller number of included studies than in other meta-analyses of CER [Morawetz et al., 2017b]. Publications using identical subject samples were counted as one single study; thus, there were less included studies than included publications.

Data extraction, meta-analysis, and post-hoc control analyses (see below for details) were conducted as for CRC, using MKDA [Wager et al., 2007]. Due to our hypothesis, we only investigated the meta-analytic contrast "CER > Emotional baseline".

### 3.1.3 Conjunction analysis between CRC and CER

In order to find overlapping brain regions activated during both CRC and CER, we performed a conjunction analysis of the two individual meta-analyses, i.e., "CRC > Reward baseline" and "CER > Emotional baseline". To do so, we computed the union of p-value result maps of both individual analyses, correcting for potential errors in the estimation of p-values during individual meta-analyses ($p<0.005$) [Radua et al., 2013].

In order to find differential activation patterns between CRC and CER, we investigated the meta-analytic contrast "(CER > Emotional baseline) > (CRC > Reward baseline)" and vice versa. Results were conjuncted with results of individual meta-analyses to ensure that activation differences were located in areas of significant activation.

### 3.1.4 Post-hoc control analyses

Several control analyses were conducted for both the CRC and the CER meta-analysis.

Jackknife analyses were performed to test for disproportionate effects of any single study on the results. The density statistic of each significant meta-analytic result cluster was iteratively recalculated (each time leaving out one study) and then compared to the original density statistic via $\chi^2$-test [Etkin & Wager, 2007].

Furthermore, we conducted post-hoc analyses to test for disproportionate influences of the following variables on the results: (i) gender (only female, only male, or mixed), (ii) age (child [0 to 18 years], young adult [18 to 30 years], or older adult [more than 30 years]), (iii) cognitive control strategy subtypes (antecedent-focused, i.e., instruction was given before stimulus, or postcedent-focused, i.e., instruction was given during or after stimulus), and (iv) stimulus type (e.g., food vs. non-food pictures). For each variable, studies were divided into categories as described above. Then the density statistic of each significant cluster was recalculated for each category and compared to the other categories of this variable via $\chi^2$-test [Kaiser et al., 2015].

## 3.2 Project 2

### 3.2.1 Overview

This project tested the hypothesis of increased global participation during CER (***Fig. 3A***) by applying graph analysis to fMRI data acquired during a CER task [Mulej Bratec et al., 2015]. Participants faced aversive emotional pictures in two conditions: Attend and Regulate. A single trial of the task started with a fixation cross, followed by the instruction of whether to simply attend to the stimulus or to regulate the emotions induced by the upcoming picture, employing a cognitive reappraisal strategy (***Fig. 3B***) [Gross, 2002]. Regulation strategy defined the contrasting conditions of our analysis (Attend vs. Regulate), which focused on graph-scores derived from emotion-related functional connectivity in response to aversive pictures (***Fig. 3C***).

### 3.2.2 Participants

19 healthy female subjects (mean age 24.8 ± 2.4 years) were recruited for the fMRI-based CER experiment. Subjects had to be free of any current or past neurological or psychiatric disorders, as verified by interview and psychometrics (Beck Depression Inventory and State-Trait Anxiety Inventory), and without any psychotropic medication. Only females were selected to exclude any gender bias in emotion processing and regulation [McRae et al., 2008b]. The study was approved by the ethics committee of Technische Universität München, and written informed consent was obtained from all participants. Furthermore, all subjects were right-handed native German speakers with normal or corrected-to-normal vision.

### 3.2.3 Task paradigm

After a 20 min training of the paradigm outside the scanner, each participant completed 2 task runs in the MRI scanner [Mulej Bratec et al., 2015]. Each run comprised one task condition defined by the regulation strategy and consisted of 80 trials. Runs/tasks were counterbalanced across subjects. In the Attend condition, subjects were instructed to attentively look at the pictures and to not change the evoked emotional feelings. In the Regulate condition, subjects were instructed to down-regulate their emotions using a so-called antecedent-focused strategy of cognitive reappraisal in the form of self-distancing (e.g. 'The content of the images has nothing to do with me or my situation. I am not affected and none of my loved ones is affected'). Each trial started with a fixation cross presented for 1s, followed by 1) the instruction (2s) of whether to simply attend to the stimulus or to regulate the emotions induced by the up-

coming picture; 2) an anticipation phase (6s), during which participants prepared for the emotional stimulus; 3) a picture presentation phase (6s), to induce negative emotions; and 4) a rating phase (3s), in which participants rated the intensity of their emotional feelings (on a 7-point scale ranging from -3 = very negative to +3 = very positive). Negative emotional intensity scores describe a negative emotional feeling, positive emotional intensity scores a positive emotional feeling. This means that the higher (i.e., less negative) this score in the Regulate condition compared to the Attend condition, the greater the success of emotion regulation. Finally, a black screen was presented for a jittered inter-trial interval (3 ± 2s) (***Fig. 3B***). During the picture presentation phase, aversive pictures from the International Affective Picture System (IAPS) were presented to elicit negative emotions [Lang et al., 1997]. Overall, pictures were presented in 40 trials (i.e., in 50% of the 80 trials per condition); in the other 50% of trials, no picture was shown. The psychological factor in the subsequent psychophysiological interaction analysis was the presence of a picture (i.e., contrast picture present vs. baseline) in order to specifically investigate emotion-related brain activity.

### 3.2.4 fMRI acquisition and preprocessing

The experiment was conducted on a 3T Siemens MRI scanner at Klinikum rechts der Isar, Technische Universität München. Stimuli were presented using Presentation software (Neurobehavioral Systems) and were back-projected onto a screen behind the scanner. Subjects could see the screen through an adjustable mirror mounted to the head coil. T1-weighted anatomical images were obtained using an MPRAGE sequence (1 × 1 × 1 mm resolution). Functional T2* images were acquired using a gradient-echo EPI sequence (repetition time: 2 s, echo time: 30 ms, flip angle: 90°, acquisition matrix: 64 × 64, 35 slices, slice thickness: 3 mm, inter-slice gap: 0.6 mm; 3x3x3 mm resolution). In each of the two task conditions, 881 functional images were obtained per subject.

Data preprocessing was performed using SPM8 (Wellcome Department of Cognitive Neurology, London, UK). For each subject, the first two volumes of each session were discarded to account for magnetization effects. The remaining functional images were slice-timed, head motion corrected, coregistered to T1 images, spatially normalized into MNI standard space through T1-based segmentation, and spatially smoothed with a Gaussian kernel of 8mm FWHM (full width at half maximum). To control for confounding influences of spatial smoothing (especially in subcortical ROIs, some of which were less than 8mm apart), we repeated the complete analysis with smoothing kernels of 6mm, 4mm, and 2mm FWHM.

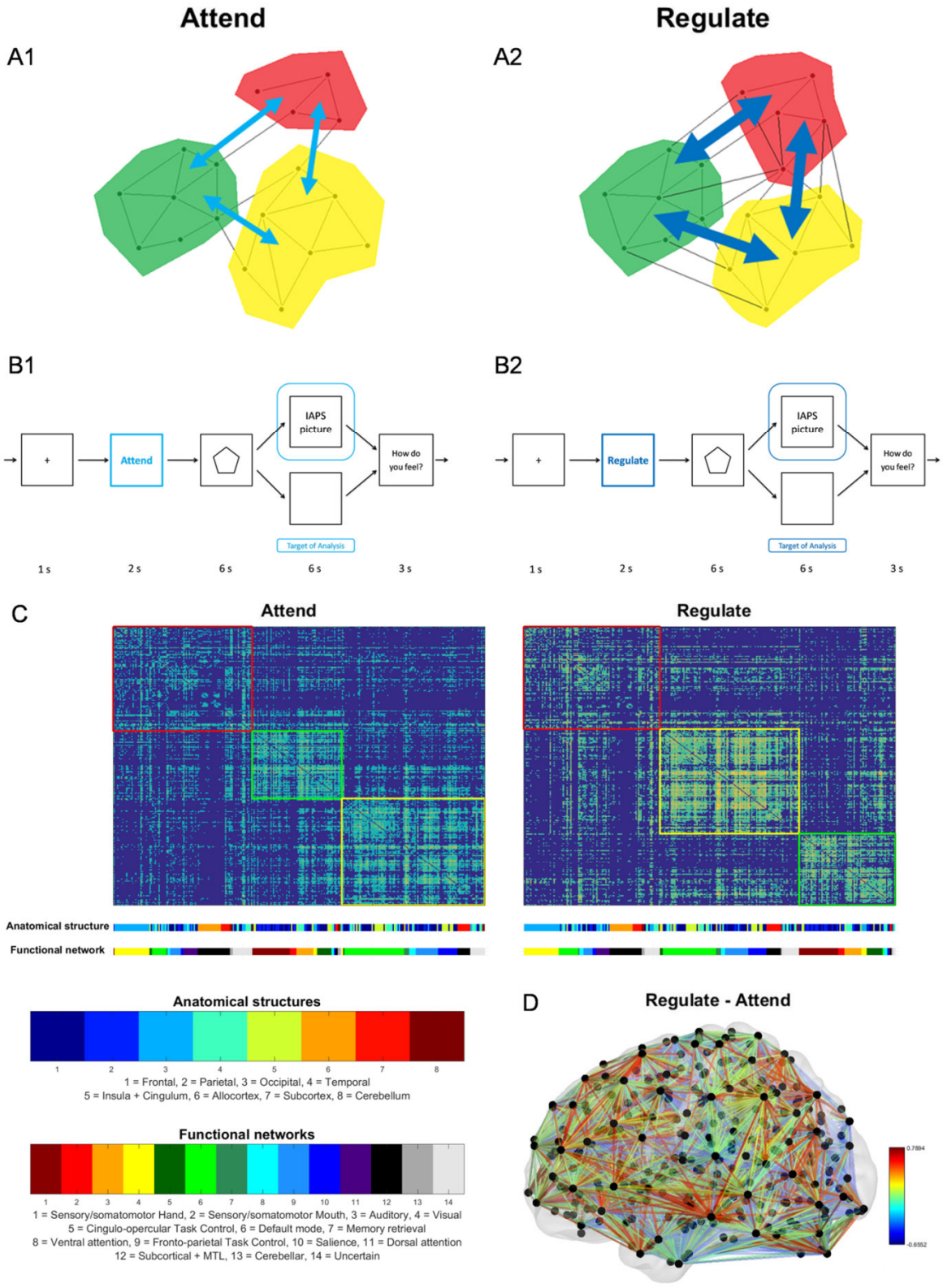


***Figure 3: Hypothesis, design, and functional brain network modules during emotions with and without CER.***

*(A) Illustration of the study hypothesis for conditions Attend (A1) and Regulate (A2). Across conditions, functional brain modules were expected to remain stable, but to increase interaction among each other. (B) Experimental paradigm for each trial. (B1) shows the task paradigm*

*for the Attend condition, (B2) for the Regulate condition. After instructing (2s) and preparing (6s) the regulation strategy, an aversive picture from the International Affective Picture System (IAPS; Lang et al., 1997) was presented (6s) in 50% of trials. Finally, subjects had to evaluate their emotion intensity on a scale from -3 to +3. (C) Group-level connectivity matrices for Attend and Regulate conditions, with nodes grouped into functional brain network modules. Module borders are indicated by colored frames; corresponding modules (i.e., modules with similar functional composition across conditions) are marked with the same color. Below the matrices, color bars show the anatomical and functional affiliation of each node (functional networks were derived from Power et al. (2011)). Color legends of anatomical structures and functional networks are printed in the lower left part of the figure. MTL = medial temporal lobe. (D) Differences in functional connectivity between conditions (Regulate - Attend). Connectivity differences were calculated by subtracting the two group-level matrices shown in (C). Hot colors depict stronger, cool colors weaker connectivity in Regulate than Attend. Plots are overlaid on a reference surface projection of the brain using BrainNet Viewer [Xia et al., 2013].*

### 3.2.5 Construction of connectivity matrices

Nodes were defined by 286 cortical and subcortical spherical ROIs. 241 isocortical and 8 cerebellar ROIs with 4 mm radius each, as well as 5 thalamic ROIs with 3 mm radius, were taken from Power and colleagues (2011); these ROIs were asymmetrically distributed across the brain. ROI labels were in line with brain anatomy, by matching the ROI center coordinates to the Harvard-Oxford brain atlas implemented in FSL (FMRIB, Oxford University). For other cortical and subcortical structures, we relied on different sources to ensure better brain coverage, including brain regions potentially relevant for emotions. For each hemisphere, 8 hippocampus ROIs with 2 mm radius and 6 striatum ROIs with 3 mm radius were created, based on the coordinates reported by Kahn et al. [Kahn et al., 2008] and Di Martino et al. [Di Martino et al., 2008], respectively. For the amygdala, 2 ROIs (basolateral and centromedial amygdala) with 2 mm radius were generated in each hemisphere, based on center coordinates from the SPM Anatomy toolbox [Amunts et al., 2005].

Edges were calculated by connectomic psychophysiological interactions (PPI) using the generalized PPI (gPPI) method, which is believed to be superior to the standard PPI approach in examining inter-individual functional connectivity differences, by allowing greater model flexibility and improving model fit, sensitivity and specificity of findings [Cisler et al., 2014; McLaren et al., 2012]. Connectomic PPI, in which one gPPI analysis is conducted for each pair of nodes, captures task-dependent changes in whole-brain functional connectivity [Gerchen et al., 2014].

GPPI is a special type of multiple regression that includes a psychological regressor (in our case presentations of aversive pictures), a physiological regressor (BOLD time course of the "seed" node), and a condition-specific interaction regressor (product of the psychological and the deconvolved physiological regressor). To control for nuisance variables, we additionally added 6 head motion regressors to the model, specifically rotation and translation in 3 directions each. Seed time-courses for each node were obtained by extracting voxel-wise BOLD time series and then averaging them across all voxels in the ROI. Absolute beta values of PPI interaction regressors, reflecting the strength of task-dependent functional connectivity between each pair of ROIs, were then entered as edge weights into the connectivity matrix.

As the connectomic PPI analysis was performed separately for each regulation condition, it resulted in two condition-specific 286 x 286 whole-brain connectivity matrices for each subject. Since we did not assume any directionality of the connections, the two triangles of each matrix were then averaged to create symmetric connectivity matrices. To improve inter-subject comparability, matrices were normalized by rescaling the edge weights to the range [0,1] [Rubinov & Sporns, 2010]. For purposes of visualization and analysis of topological node roles, two group-level connectivity matrices were generated (one for the Attend and one for the Regulate condition) by averaging the individual condition-specific matrices and again rescaling them to the range [0, 1].

### 3.2.6 Graph analysis

Connectivity matrices were thresholded by cost (i.e., connection density) following previous graph-based studies of task-related brain connectivity [Godwin et al., 2015; Kinnison et al., 2012]. Cost equals the number of existing edges divided by the maximal possible number of edges in a graph; thus, a cost of x% means that only the x% of strongest edges are kept. The term "cost" derives from economical constraints of wiring costs [Bullmore & Sporns, 2009]. We investigated the cost range between 10% and 50% (with intervals of 5%) since at lower costs, graphs become increasingly unstable and fragmented and at higher costs, topology becomes increasingly random [Bullmore & Bassett, 2011; Humphries et al., 2006]. Graph scores were stable over the entire cost range; we report results for the cost of 30%, because at this cost, the number of modules was most stable across subjects. However, to ensure that results did not depend solely on one cost, we also calculated for each graph score the area under the curve over the entire cost range [Spielberg et al., 2015].

Functional segregation, integration, and community structure were assessed by calculating several global and nodal graph scores for the individual connectivity matrices. Functional seg-

regation was quantified by global clustering coefficient, functional integration by characteristic path length, and community structure by modularity, participation coefficient and within-module degree. All graph scores were calculated using the Brain Connectivity Toolbox [Rubinov & Sporns, 2010].

Brain modules were identified by maximizing modularity, i.e., the degree to which a graph can be subdivided into non-overlapping sub-graphs or modules. Modularity thus quantifies the ratio of within-module edges to between-module edges [Newman, 2004]. Modularity was maximized using Newman's algorithm [Newman, 2006] followed by the Kernighan-Lin fine-tuning algorithm [Kernighan & Lin, 1970], and averaged over 100 repetitions.

Participation coefficient, which quantifies the between-module connectivity of a graph, was calculated based on the modular partition with highest modularity [Guimera & Amaral, 2005b]. For node *i*, the nodal participation coefficient $P_i^w$ ranges between 0 and 1: values close to 1 indicate that node *i* is uniformly connected among all modules; a value of 0 means that it is only linked to nodes in its own module [Guimera & Amaral, 2005b]. Thus, nodes with high nodal participation are likely to facilitate global inter-modular integration [Rubinov & Sporns, 2010]. The global participation coefficient of a network is then computed as the average nodal participation coefficient across all nodes [Godwin et al., 2015].

To characterize functional segregation in the whole-brain network, global clustering coefficient was calculated [Watts & Strogatz, 1998]. Finally, functional integration was quantified by characteristic path length [Watts & Strogatz, 1998].

The following formulas were used to calculate graph scores:

***Modularity.*** We calculated the weighted modularity $Q^w$ [Newman, 2004] by

$$Q^w = \frac{1}{l^w} \sum_{i,j \in N} \left[ w_{ij} - \frac{k_i^w k_j^w}{l^w} \right] \delta_{m_i,m_j} ,$$

where $l^w$ is the sum of all edge weights and *N* the set of all nodes in the network, $w_{ij}$ the connection weight of the edge linking nodes *i* and *j*, $k_i^w$ the weighted degree of node *i*, and $m_i$ the module containing node *i*; $d_{m_i,m_j}$ = 1 if *i* and *j* are in the same module, otherwise $d_{m_i,m_j}$ = 0.

***Participation coefficient.*** For node *i*, the nodal participation coefficient $P_i^w$ was calculated by

$$P_i^w = 1 - \sum_{m \in M} \left( \frac{k_i^w(m)}{k_i^w} \right)^2 ,$$

with *M* being the set of all modules and $k_i^w(m)$ the connection weight of edges linking node *i* and all nodes in module *m* [Guimera & Amaral, 2005b].

***Global clustering coefficient.*** Global clustering coefficient $C^w$ was calculated by

$$C^w = \frac{1}{n}\sum_{i\in N}\frac{2t_i^w}{k_i(k_i-1)},$$

where *n* is the number of nodes in the network and $t_i^w$ the connection weight of the triangles around node *i* [Watts & Strogatz, 1998].

***Characteristic path length.*** Characteristic path length $L^w$ was calculated using the following formula [Watts & Strogatz, 1998]:

$$L^w = \frac{1}{n}\sum_{i\in N}\frac{\sum_{j\in N, j\neq i} d_{ij}^w}{n-1},$$

with $d_{ij}^w$ being the weighted shortest path length between nodes *i* and *j*.

All global graph scores were normalized at the subject level by dividing them by the respective average graph score across 100 random graphs with conserved size, cost and degree distribution of the original graph [Bullmore & Sporns, 2009]. Statistical comparison of graph scores across conditions was performed using Wilcoxon's signed-rank test ($p<0.05$), as no assumptions about the normal distribution of data were made [Bullmore & Sporns, 2009]. For nodal scores, an false discovery rate (FDR) correction was applied to account for multiple comparisons [Benjamini & Hochberg, 1995]. To control for the testing procedure, we re-evaluated our findings with a permutation test (100,000 permutations) [Spielberg et al., 2015].

### 3.2.7 Node roles in the whole-brain community structure

To assess the role of nodes in the community structure of the functional whole-brain network, we assigned them to different categories based on their pattern of within- and between-module connectivity. For this step, the two condition-specific group-level graphs were used.
Within-module connectivity was measured by within-module degree, which is large for nodes with a large number of intra-modular connections. The within-module degree of node *i* is normalized as the z-score over all nodes in *i*'s module, and therefore quantifies how well connected node *i* is within its own module [Guimera & Amaral, 2005a]:

$$z_i^w = \frac{k_i^w(m_i) - \bar{k}^w(m_i)}{\sigma_{k^w(m_i)}},$$

where $\bar{k}^w$ is the mean and $\sigma_{k^w}$ the standard deviation of the within-module degree of all nodes in module $m_i$.
Between-module connectivity, in contrast, was measured by nodal participation coefficient.

Within-module degree $z_i^w$ and nodal participation coefficient $P_i^w$ define a two-dimensional parameter space, the *z-P* plane, on which all nodes can be plotted. Depending on its position on the *z-P* plane, each node is then assigned to one of seven categories [Guimera & Amaral, 2005b]. According to the within-module degree, nodes with $z \geq 2.5$ are classified as "hubs" and nodes with $z < 2.5$ as "non-hubs". According to the nodal participation coefficient, non-hubs are further subdivided into "ultra-peripheral nodes" ($P \leq 0.05$), "peripheral nodes" ($0.05 < P \leq 0.62$), "connector nodes" ($0.62 < P \leq 0.80$), and "kinless nodes" ($P > 0.80$). Hubs are further subdivided into "provincial hubs" ($P \leq 0.30$), "connector hubs" ($0.30 < P \leq 0.75$), and "kinless hubs" ($P > 0.75$) [Guimera & Amaral, 2005b]. Thus, connector hubs have both high within- and high between-module connectivity and play a key role in inter-modular communication, as they can mediate information flow between their own module and other modules.

In networks with $m \geq 2$ modules, the maximal possible $P$ is $1 - (1/m)$ [Fuertinger et al., 2015]. The group-level graphs for the Attend and Regulate condition both have 3 modules, so the maximal possible $P$ is 0.67. Therefore, kinless nodes and kinless hubs cannot occur in the condition-specific group-level graphs. The "highest" possible node categories are "connector nodes" ($z < 2.5$; $0.62 < P \leq 0.80$) and "connector hubs" ($z \geq 2.5$; $0.30 < P \leq 0.75$).

### 3.2.8 Correlation of graph scores with CER success

To evaluate the specificity of global interaction for CER outcome, correlation analysis with emotional intensity rating scores was performed. Pearson correlations were calculated between the averaged emotional intensity scores of the Regulate condition and the global participation coefficient during Regulate.

### 3.2.9 Voxel-wise activation analysis

To detect potential overlaps between nodes with increased functional embedding during CER and clusters of specialized local activity during emotional processing with and without CER, an activation analysis based on a general linear model (GLM) was conducted. The GLM contained the following regressors convolved with the hemodynamic response function: regulation strategy, preparatory cue, aversive picture, blank screen (no-picture trials), and emotion intensity scale. Additionally, 6 movement regressors derived from realignment were included as regressors of no interest. On the group level, β-maps for aversive picture presentation in picture trials were entered into paired t-tests. Activation maps were generated for contrasts Attend - Regulate ($p<0.005$, uncorrected) and Regulate - Attend ($p<0.005$, uncorrected).

## 3.3 Project 3

### 3.3.1 Participants

15 patients with schizophrenia (42.1±12.5 years; 6 female) and 15 healthy controls (43.3±10.1 years; 6 female) were included in the study. Patients met DSM-IV criteria for schizophrenia based on the Structured Clinical Interview for DSM-IV (SCID). and were recruited from the Department of Psychiatry of Klinikum rechts der Isar, Munich, Germany. Inclusion criteria comprised at least 2 psychotic episodes and a state of symptomatic remission of positive symptoms at the time of study. This latter criterion was defined based on Andreasen et al. [Andreasen et al., 2005]: Positive and Negative Syndrome Scale (PANSS) items 'hallucinations' (P2), 'delusions' (P3), 'bizarre behavior' (G5), and 'thought disorder' (G9) had to be ≤3 [Andreasen et al., 2005; Wils et al., 2017]. For negative and general symptoms, no remission criteria had to be fulfilled. Antipsychotic medication was kept stable for at least 2 weeks before scanning. All participants gave informed consent after receiving a complete description of the study. The study was approved by the Ethics Review Board of the Klinikum Rechts der Isar, Technische Universitat München, Germany. Approval to administer radiotracers was obtained from the Bundesamt für Strahlenschutz. Clinical assessments were performed by trained psychiatrist C.L. Schizophrenic symptom severity was quantified by PANSS [Kay et al., 1987].

### 3.3.2 FDOPA-PET analysis

#### *3.3.2.1 Imaging*

FDOPA-PET data were acquired with a hybrid whole-body mMR Biograph PET/MRI scanner (Siemens Healthcare, Erlangen, Germany) using a vendor-supplied 12-channel phase array head coil. Participants were instructed not to smoke or drink coffee or alcohol for 12 hours before scanning [Bloomfield et al., 2014]. 150 MBq of FDOPA were administered by bolus intravenous injection 30s before scan start. The PET acquisition lasted 70min. Ordered subset expectation maximization (OSEM) (21 subsets, 3 iterations) was used to reconstruct PET data with a voxel size of 1.7×1.7×2mm$^3$, with a 3 mm Gaussian post-reconstruction filter, corrected for attenuation and scatter based on anatomical MRI information. PET data were framed into 30 dynamic frames (1×30s, 10×15s, 3×20s, 2×60s, 2×120s, 12×300s). Anatomical T1-weighted MRI data were acquired simultaneously with the PET data (TR/TE/flip angle: 2,300 ms/2.98 ms/9°; 160 slices (gap 0.5 mm) covering the whole brain; FoV: 256 mm; matrix size: 256×256; voxel size: 1.0×1.0×1.0 mm3).

#### *3.3.2.2 Image analysis*

FDOPA-PET data were analyzed with SPM12 (Wellcome Trust Centre for Neuroimaging, London, UK). First, PET data were corrected for motion by realigning all PET frames to the last frame. Since anatomical information is fuzzy in the first frames, the transformation matrix of the frame at minute 5 was applied to all preceding frames [Deserno et al., 2015]. The individual T1 image was coregistered to the last PET frame and then spatially normalized into MNI space. The inverse transformation matrix of this normalization was then used for the transformation of striatum and cerebellum ROIs (see below for details) into individual PET space. Next, we calculated the influx constant $k_i^{cer}$, a quantitative measure reflecting dopamine synthesis capacity, in a voxel-wise manner using Gjedde-Patlak linear graphical analysis with cerebellum as reference region [Patlak et al., 1983]. The formula of the Patlak plot is the following:

$$\frac{C_{vox}(t)}{C_{ref}(t)} = k_i \frac{\int_0^t C_{ref}(\tau)d\tau}{C_{ref}(t)} + V_0$$

where $C_{vox}(t)$ is the tracer blood plasma concentration in a certain voxel at time t, $C_{ref}(t)$ is the tracer blood plasma concentration in a reference region at time t, and $V_0$ is the distribution volume of the central compartment. $k_i$ and $V_0$ are estimated using linear regression fitting. When using cerebellum as reference region, $k_i$ is called $k_i^{cer}$.

The time activity curve of the cerebellum (excluding vermis) was extracted using an anatomical mask created in FSLview from the Probabilistic cerebellar atlas [Diedrichsen et al., 2009]. PET frames acquired between 20 and 60min were used for linear fitting [Deserno et al., 2015], resulting in whole-brain voxel-wise $k_i^{cer}$ maps.

Mean $k_i^{cer}$ values of limbic, associative, and sensorimotor subdivisions of the striatum were extracted (by averaging over all voxels in each ROI) from individual maps using functionally defined masks from the Oxford-GSK-Imanova connectivity atlas.

### 3.3.3 Behavioral analysis

#### *3.3.3.1 Decision making task*

Model-based/model-free behavior was investigated with a sequential decision making task [Daw et al., 2011]. The task comprised 150 trials with the goal of winning as much money as possible. The structure of the task is depicted in ***Fig. 4***.

Each trial consisted of two stages, in each of which the subject had to pick one symbol (stimulus) out of a pair of symbols. In total, 6 stimuli were employed in the task: one pair of stimuli in the first stage, and two (fixed) pairs in the second stage.

Crucially, the transition between first and second stage was probabilistic: each first-stage stimulus led with 70% probability (= common transition) to a certain second-stage stimulus pair and with only 30% probability (= uncommon transition) to the other second-stage stimulus pair. These common/uncommon transitions remained stable over the whole task - they did not change. Each second-stage stimulus, in turn, led to monetary reward with a certain probability that changed over the course of the task. After each trial, subjects received feedback about whether or not they had achieved a reward. At the end of the task, they received the amount of won money.

Before starting the task, subjects were instructed about the structure of the task. However, they were not told about the exact probabilities and common/uncommon transitions. Instead, they had to learn these associations during the task. To facilitate this process, subjects performed a training run (consisting of 25 trials) before the task.

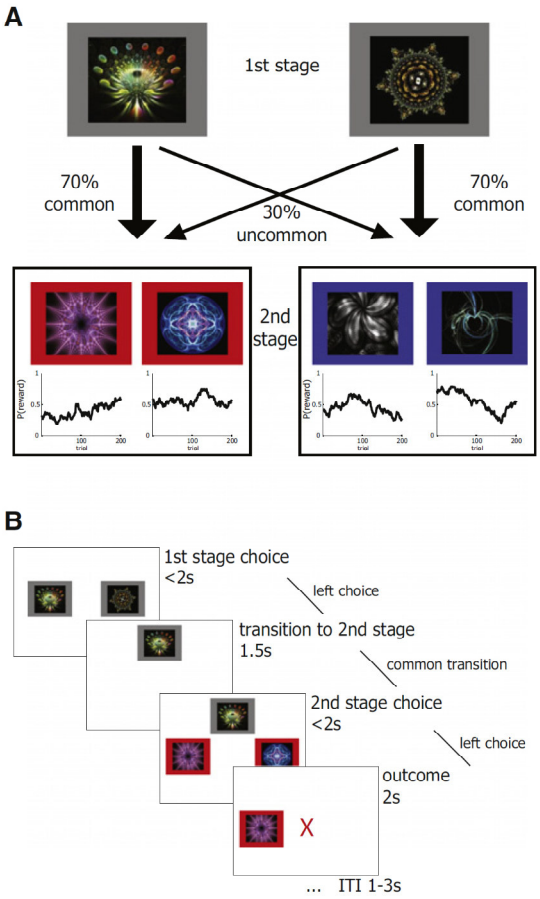


***Figure 4: Structure of the sequential decision making task .***

*(A) Logic and (B) time sequence of one trial. Figure taken from [Wunderlich et al., 2012].*

#### *3.3.3.2 Analysis of stay-switch probability*

First, we checked whether subjects used both model-based and model-free decision making strategies. Therefore, we analyzed their stay-switch behavior. More specifically, we looked at the probability of selecting the same first-stage stimulus as in the trial before (= stay probability). This probability is influenced by two factors: reward (i.e., reward or no reward in the trial before), and transition (i.e., common or uncommon transition between first and second stage in the trial before).

If someone acted purely model-free, then only reward would influence her/his behavior: if s/he has received a reward in the trial before, s/he will choose the same first-stage stimulus again, regardless of whether the transition from first to second stage was common (70%) or uncommon (30%).

However, if someone also acted model-based, we would expect that the transition in the trial before plays an important role, too. This means that when a certain first-stage stimulus has led to a reward via an uncommon transition, one would switch to the other first-stage stimulus in the next trial to increase the probability of winning a reward. In the same vein, no reward after a rare transition would not trigger a switch, since in the next trial one can expect a common transition again, which will likely lead to a reward again. This suggests that model-based decision making is influenced by an interaction of reward and transition.

To quantify subjects' behavior, stay probabilities for four categories were calculated: reward and common transition, reward and uncommon transition, no reward and common transition, no reward and uncommon transition. Then, a repeated-measures ANOVA was conducted with the factors reward and transition. For model-based behavior, a main effect of reward is expected. For model-based behavior, an significant interaction between reward and transition is expected [Daw et al., 2011].

#### *3.3.3.3 Computational modeling of decision making behavior*

Second, in order to quantify the balance between model-based and model-free behavior, subjects' decision making behavior was computationally modeled. Following previous studies [Daw et al., 2011; Deserno et al., 2015; Wunderlich et al., 2012], we employed a hybrid model-free/model-based algorithm. The basic idea of such reinforcement algorithms is to define a value for each action (i.e., selection of a certain stimulus) which quantifies the expected reward. These values are updated after each trial using the prediction error, i.e., the difference

between actual and expected reward. In a second step, values are translated into action probabilities using a softmax function.

In the *second stage*, values were updated in the same way for both model-based and model-free decision making, since the two strategies did not differ at this stage. A SARSA(λ) temporal difference learning algorithm was used [Rummery & Niranjan, 1994]. Value $V_{s2}$ at time point t+1 is defined as:

$$V_{s2}(a_{2,t+1}) = V_{s2}(a_{2,t}) + \alpha_2(r(t) - V_{s2}(a_{2,t}))$$

where $a_2$ is the second-stage action (selection of second-stage stimulus), $\alpha_2$ the second-stage learning rate, and r(t) the reward obtained at time point t.

*First-stage* values were computed as a weighted combination of model-free and model-based values:

$$V_{s1}^{Hybrid} = \omega V_{s1}^{MB} + (1-\omega)V_{s1}^{MF}$$

where ω is a weighting factor quantifying the balance between model-based and model-free decision making (1 means purely model-based, 0 means purely model-free).

First-stage *model-free* values were updated using SARSA(λ) temporal difference learning [Rummery & Niranjan, 1994]. In the first stage, stimulus values were updated on a trial-by-trial basis using the following formula:

$$V_{s1}^{MF}(a_{1,t+1}) = V_{s1}^{MF}(a_{1,t}) + \alpha_1\left(V_{s2}^{MF}(a_{2,t}) - V_{s1}^{MF}(a_{1,t})\right) + \lambda\alpha_1(r(t) - V_{s2}(a_{2,t}))$$

where $a_1$ is the first-stage action (selection of first-stage stimulus), $\alpha_1$ the first-stage learning rate, and λ an eligibility parameter quantifying how much first-stage values are influenced by second-stage prediction errors.

First-stage *model-based* values were updated taking into account the transition probabilities between the two stages [Daw et al., 2011]:

$$V_1^{MB}(a_{1,t+1}) = 0.7 \times \max\left(V_3^{MF}(t), V_4^{MF}(t)\right) + 0.3 \times \max\left(V_5^{MF}(t), V_6^{MF}(t)\right)$$

In this case, first-stage stimulus 1 leads with a probability of 70% to second-stage stimuli 3 and 4, and with 30% probability to second-stage stimuli 5 and 6.

Values were transformed into action probabilities using the following formula:

$$P(a_{i,t} = a | s_{i,t}) = \frac{\exp\left(\beta_i\left[V^{Hybrid}(s_{i,t}, a) + \pi \times rep(a)\right]\right)}{\sum_{a'}\exp\left(\beta_i\left[V^{Hybrid}(s_{i,t}, a') + \pi \times rep(a')\right]\right)}$$

where β represents the softmax temperature (can be interpreted as performance [Maia & Frank, 2017]) and π describes perseverance (choosing the same or a different first-stage stimulus in the next trial).

In summary, the modeling algorithms had seven parameters: first-stage learning rate $\alpha_1$, second-stage learning rate $\alpha_2$, first-stage performance $\beta_1$, second-stage performance $\beta_2$, perseverance $\pi$, eligibility parameter $\lambda$, and model-based/model-free weighting $\omega$.

Parameters were transformed to normal distributions using logistic (for $\alpha$, $\lambda$, $\omega$) or exponential (for $\beta$, $\pi$) functions. Models were first fitted for each subject individually using maximum likelihood and then refitted using the population distribution to ensure normal distribution. The best model was selected using Bayesian Information Criterion (BIC).

Group comparisons and correlations analyses were restricted to $\omega$, which prevented multiple testing problems.

### 3.3.4 Correlation between FDOPA-PET and decision making parameters

To test for associations between presynaptic dopamine synthesis and decision making, Pearson correlations between $k_i^{cer}$ measures of striatal subdivisions and the model-based/model-free weighting parameter $\omega$ were computed.

To test whether these associations differed between patients and controls, interaction analyses (linear regressions) were conducted, with $\omega$ as dependent variable and group, $k_i^{cer}$, and group*$k_i^{cer}$ as independent variables. In such analyses, a significant interaction group*$k_i^{cer}$ indicates a group-differential association between dopamine synthesis and model-based/model-free balance.

# 4 Results

## 4.1 Project 1

In total, the literature search yielded a sample of 22 CRC studies, in which subjects had to resist craving towards a reinforcing stimulus, with 741 subjects (***Table 2***, ***Fig. 2A***) and 47 CER studies, in which subjects had to downregulate their emotional responses to aversive visual stimuli using reappraisal strategies, with 1455 subjects (***Table 3***, ***Fig. 2B***).

| Author, year | Subjects (n) | Gender | Mean age | Stimulus type |
|---|---|---|---|---|
| Brody et al. (2007) | 42 | 12 F, 30 M | 38 | Cigarette videos |
| Crockett et al. (2013) | 28 | 28 M | 18-35 | Erotic pictures |
| Diekhof et al. (2012) | 32 | 16 F, 16 M | 24.5 | Desire reason task |
| Dietrich et al. (2016) | 43 | 43 F | 26.7 | Food pictures |
| Dong et al. (2016) | 27 | 27 F | 21.56 | Food delayed discounting |
| Giuliani et al. (2014) | 50 | 33 F, 17 M | 21.77 | Food pictures |
| Giuliani et al. (2015) | 60 | 60 F | 16.66 | Food pictures |
| Harding et al. (2018) | 30 | 14 F, 16 M | 24.17 | Food pictures |
| Hare et al. (2011) | 33 | 23 F, 10 M | 24.8 | Food pictures |
| Hartwell et al. (2011) | 32 | 19 F, 14 M | 33.5 | Pictures of people smoking |
| He et al. (2014) | 30 | 17 F, 13 M | 19.7 | Food pictures |
| Hill et al. (2017) | 26 | 19 F, 7 M | 24 | Monetary reward |
| Hollmann et al. (2012) | 17 | 17 F | 25.3 | Food pictures |
| Hutcherson et al. (2012) | 26 | 9 F, 17 M | 22 | Food pictures |
| Kober et al. (2010) | 21 | 9 F, 12 M | 26.8 | Food and cigarette pictures |
| McClure et al. (2004) | 14 | 9 F, 5 M | 21.4 | Monetary reward |
| Norman et al. (2017) | 20 | 20 M | 12-18 | Monetary reward: delay discounting task |
| Petit et al. (2016) | 23 | 10 F,13 M | 25.91 | Food pictures |
| Silvers et al. (2014) | 105 | 71 F, 34 M | 14.27 | Food pictures |
| Tuulari et al. (2015) | 41 | 41 F | 44.9 | Food pictures |
| Van der Laan et al. (2014) | 20 | 20 F | 21.2 | Food pictures |
| Yokum et al. (2013) | 21 | 13 F, 8 M | 15.2 | Food pictures |

***Table 2: Studies included in the CRC meta-analysis.***

*F = female, M = male.*

| Author, year | Subjects (n) | Gender | Mean age | Stimulus type |
|---|---|---|---|---|
| Belden et al. (2014) | 19 | 8 F, 11M | 10.05 | Pictures: IAPS |
| Denny et al. (2015) | 17 | 12 F, 5 M | 24.1 | Pictures: IAPS |
| Domes et al. (2010) | 33 | 17 F, 16 M | 24.9 | Pictures: IAPS |
| Dörfel et al. (2014) | 36 | 36 F | 18-39 | Pictures: IAPS |
| Doré et al. (2017) | 20 | 12 F, 8 M | 24.6 | Pictures: IAPS |
| Eippert et al. (2007) | 24 | 24 F | 23.30 | Pictures: IAPS |
| Engen et al (2015) | 15 | 5 F, 10 M | 56.1 | Film clip |
| Erk et al. (2010) | 17 | 8 F, 9 M | 43.9 | Pictures: IAPS |
| Goldin et al. (2008) | 17 | 17 F | 22.7 | Videos |
| Hallam et al. (2015) | 40 | 20 F, 20 M | 20 | Pictures: IAPS |
| Hayes et al. (2010) | 25 | 11 F, 14 M | 21.6 | Pictures: IAPS |
| Koenigsberg et al. (2009) + (2010) | 16 | 9 F, 7 M | 31.8 | Pictures: IAPS |
| Krendl et al. (2012) | 16 | 10 F, 6 M | 21.6 | Pictures: IAPS |
| Lang et al. (2012) | 15 | 15 F | 24.73 | Scripts: ANET |
| Leiberg et al. (2012) | 24 | 24 F | 24.1 | Pictures: IAPS |
| Mak et al. (2009a) | 12 | 12 F | 24 | Pictures: IAPS |
| Mak et al. (2009b) | 24 | 12 F, 12 M | 24 | Pictures: IAPS |
| McRae et al. (2008) | 25 | 13 F, 12 M | 20.6 | Pictures: IAPS |
| McRae et al. (2010) | 18 | 18 F | 24.4 | Pictures: IAPS |
| McRae et al. (2012) | 38 | 21 F, 17M | 16.5 | Pictures: IAPS |
| Modinos et al. (2010) | 18 | 7 F, 11M | 21.1 | Pictures: IAPS |
| Morawetz et al. (2016a) | 59 | 20 F, 39 M | 32.47 | Film clip |
| Morawetz et al. (2016b) | 60 | 30 F, 30 M | 30.48 | Pictures: FACES |
| Morawetz et al. (2017a) | 23 | 12 F, 11 M | 25.70 | Pictures: IAPS |
| Mulej Bratec et al. (2015) | 20 | 20 F | 24.8 | Pictures: IAPS |
| Nelson et al. (2015) | 22 | 11 F, 11 M | 25.2 | Pictures |
| New et al. (2009) | 14 | 14 F | 31.7 | Pictures: IAPS |
| Ochsner et al. (2002) | 15 | 15 F | 21.9 | Pictures: IAPS |
| Ochsner et al. (2004) | 24 | 24 F | 20.6 | Pictures: IAPS |
| Paschke et al. (2016) | 108 | 55 F | 26.12 | Pictures: EPS |
| Perlman et al. (2012) | 14 | 6 F, 8 M | 15.1 | Pictures: IAPS |
| Phan et al. (2005) | 14 | 8 F, 6 M | 27.6 | Pictures: IAPS |
| Pitskel et al. (2011) | 15 | 6 F, 9 M | 13.03 | Pictures: IAPS |
| Qu et al. (2017) | 29 | 14 F, 15 M | 19.2 | Photos |
| Sarkheil et al. (2015) | 14 | 8 F, 6 M | 20-27 | Pictures: IAPS |
| Schulze et al. (2011) | 15 | 15 F | 24.53 | Pictures: IAPS |
| Silvers et al. (2015a) | 56 | 31 F, 25 M | 16.45 | Pictures: IAPS |
| Silvers et al. (2015b) | 30 | 13 F, 17 M | 21.97 | Pictures: IAPS |
| Silvers et al. (2017) | 112 | 65 F, 47 M | 15.73 | Pictures: IAPS |
| Sripada et al. (2014) | 49 | 23 F, 26 M | 23.63 | Pictures: IAPS |
| Stephanou et al. (2016) + (2017) | 78 | 44 F, 34 M | 19.91 | Pictures: IAPS |
| Uchida et al. (2015) | 62 | 32 F, 30 M | 22.3 | Pictures: IAPS |
| Vanderhasselt et al. (2013) | 42 | 42 F | 21.26 | Pictures: IAPS |

| | | | | |
|---|---|---|---|---|
| Walter et al. (2009) | 18 | 18 F | 24 | Pictures: IAPS |
| Winecoff et al. (2011) | 42 | n.a. | 25 | Pictures: IAPS |
| Winecoff et al. (2013) | 31 | 21 F, 10 M | F: 23.1<br>M: 69 | Pictures: IAPS |
| Zaehringer et al. (2018) | 20 | 13 F, 7 M | 39.65 | Pictures: IAPS |

***Table 3: Studies included in the CER meta-analysis.***

*ANET: Affective Norms for English Text, EPS: Emotional Picture Set, F = female, IAPS: International Affective Picture System, M = male.*

### 4.1.1 Meta-analysis of cognitive reward control: CRC > Reward baseline

Significant stronger activation during CRC compared to reward baseline (i.e., craving towards a rewarding stimulus without regulation) was found for bilateral supplementary motor area (SMA), pre-SMA, dlPFC, vlPFC, anterior insulae, and angular gyrus (***Fig. 5A***).

### 4.1.2 Meta-analysis of cognitive emotion regulation: CER > Emotional baseline

We found significant stronger activation during CER compared to baseline emotion (i.e., attending to an aversive stimulus without regulation) mainly in bilateral dlPFC, vlPFC, SMA, and pre-SMA (***Fig. 5B***). Additional clusters were located in temporal gyrus (superior, middle, and inferior), angular gyrus, anterior and posterior cingulate cortex, precentral gyrus, caudate nucleus, occipital cortex, and cerebellum.

### 4.1.3 Common activation patterns of CRC and CER

To test for brain regions that are activated during both CRC and CER, we conducted a conjunction analysis of the contrasts "CRC > Reward baseline" and "CER > Emotional baseline". We found significant overlap in the following regions: bilateral SMA, pre-SMA, dlPFC, vlPFC, and anterior insulae, as well as left angular and superior temporal gyrus (***Fig. 5C***).

### 4.1.4 Differential activation patterns of CRC and CER

To complement the conjunction analysis, we also tested for regions with increased stronger activation during CER compared to CRC and vice versa.

#### *4.1.4.1 (CER > Emotional baseline) > (CRC > Reward baseline)*

We identified clusters with significantly stronger activation during CER than during CRC in bilateral angular gyrus, left superior and medial temporal gyrus, and parts of left vlPFC and pre-SMA (***Fig. 5D***).

#### *4.1.4.2 (CRC > Reward baseline) > (CER > Emotional baseline)*

No brain regions showed significantly stronger activation during CRC than during CER (***Fig. 5D***).

### 4.1.5 Post-hoc control analyses for both CRC and CER

Jackknife analyses showed that no single study had a significant effect on the results of the individual, i.e., "CRC > Reward baseline" and "CER > Emotional baseline", or difference, i.e., "(CER > Emotional baseline) > (CRC > Reward baseline)", meta-analyses (p≥0.78 for each significant result cluster across all contrasts). Therefore, the reported results include all studies. Further post-hoc analyses revealed no disproportionate influence of the variables gender (p≥0.51), age (p≥0.31), cognitive control strategy (p≥0.44), and stimulus type (p≥0.36).

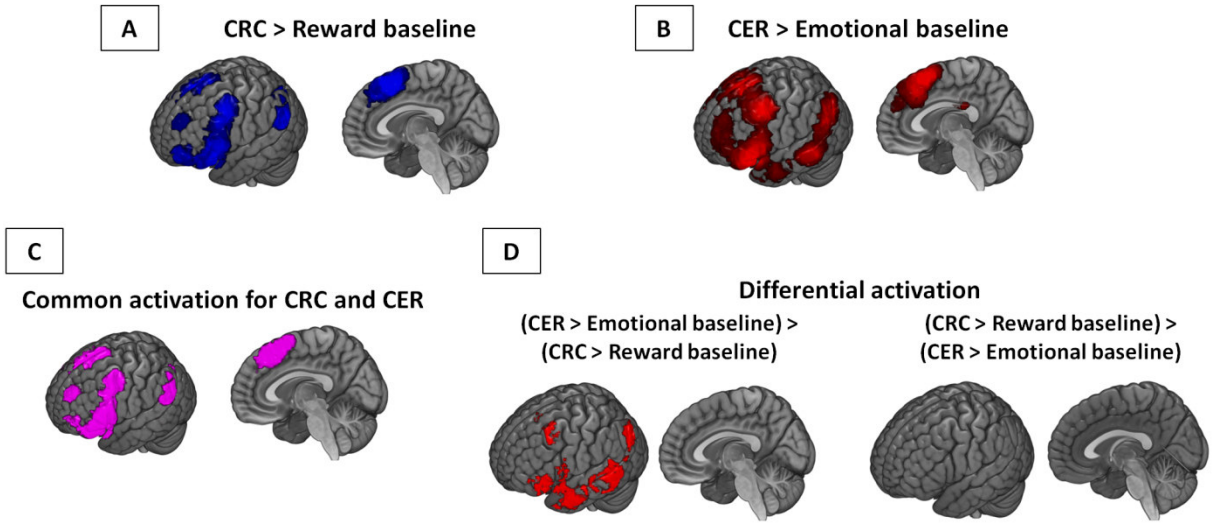


***Figure 5: Brain activation of CRC and CER.***

*Top row: Brain regions showing consistent activation during cognitive reward control (A) and cognitive emotion regulation (B). Results were calculated by Multilevel Kernel Density Analysis (MKDA) meta-analysis and are significant for p<0.05 (both height-based and extent-based threshold).*

*Bottom row: (C) Brain regions of common activation during both CRC and CER, calculated by conjunction of both single meta-analytic result-maps (p<0.005). (D) Brain regions showing differential activation between CER and CRC. Results were calculated by Multilevel Kernel Density Analysis (MKDA) meta-analysis and are significant for p<0.05 (both height-based and extent-based threshold).*

## 4.2 Project 2

### 4.2.1 CER success

To control for CER accomplishment, we assessed CER success via emotional intensity rating scores. After each trial, subjects rated the intensity of their emotions on a scale from -3 to +3 (with intervals of 1; set to 0 on each trial, negative scores reflect negative valence) via button press. These emotional intensity scores were then, for each condition, averaged over all trials and compared via paired two-sample t-test between Attend and Regulate conditions. During the Regulate condition, emotional intensity scores were significantly less negative than during the Attend condition ($p<0.0001$), indicating successful CER across subjects.

### 4.2.2 Increased global participation across network modules during successful CER

To perform a whole-brain graph-analytical approach on CER neurobiology, we parcellated the brain into 286 cortical and subcortical nodes. Edges were constructed from gPPI, reflecting task-dependent functional connectivity [McLaren et al., 2012]. For each subject, this procedure resulted in two 286x286 connectivity matrices representing the whole-brain graph, once for the Attend and once for the Regulate condition (***Fig. 3C***). Graphs were thresholded at different costs (i.e., connection densities) from 10 to 50% (intervals of 5%) and network topology was investigated by graph analysis, which was focused on community structure quantified by both global participation coefficient [Guimera & Amaral, 2005b] and modularity [Newman, 2004]. To control for the specificity of findings, we also examined global measures of segregation (i.e., global clustering coefficient) and integration (i.e., characteristic path length) [Watts & Strogatz, 1998] and related CER-sensitive whole-brain graph results with emotional intensity rating scores across subjects.

As expected, we found that modularity (i.e., decomposability of the graph into network modules) was unchanged across Attend and Regulate conditions (***Fig. 6A***; Wilcoxon's signed-rank test, $p=0.687$); for both conditions, we found three stable modules, which were very consistent (though not completely identical) across conditions (***Fig. 3C***). On the group level, only 10% of the nodes switched modules from the Attend to the Regulate condition. The normalized mutual information (NMI) between the group-level modular partitions in the two conditions was 0.64 (NMI is a measure of similarity that is 1 if two modular partitions are identical and 0 if they are totally independent [Kuncheva & Hadjitodorov, 2004; Meunier et al., 2009]). To visualize this modular consistency, we colored the nodes according to both their anatomical position (i.e., brain location) and functional network membership (i.e., sub-graphs such as the default mode network, derived from Power et al. 2011); the coloring thus shows, for example, a "yellow" module of the graph (***Fig. 3C***), built up con-

sistently of nodes belonging to the default mode, the fronto-parietal task control, and the salience network.

Critically, and in contrast to module decomposability, we found that global participation across network modules (i.e., the overall connectivity of nodes of one module with nodes of other modules) was increased during CER (Wilcoxon's signed-rank test, p=0.022) (***Fig. 6A***). This finding indicates that CER is associated with an increased interaction across functional brain network modules.

These results were not influenced by: (i) a specific cost, since they were consistent over the whole cost range, and usage of the area under the curve (representing the entire cost range) confirmed the result of significantly increased global participation during CER (p=0.032); (ii) the testing procedure, since permutation testing confirmed the finding of significantly increased global participation during CER (p=0.035); (iii) the preprocessing protocol concerning smoothing, since results were stable over different sizes of smoothing kernels. (iv) Furthermore, in order to get further evidence that increased global participation was related with CER in terms of CER success, we correlated the global participation coefficient with the mean emotional intensity rating score over all trials. In the Regulate condition, global participation showed an at-trend-significant positive Pearson correlation with emotional intensity (r=0.43, p=0.069); robustness against outliers was confirmed by Grubbs' test [Grubbs, 1969]. However, this correlation could be confounded by low statistical power due to the rather low number of subjects.

Moreover, global clustering coefficient, a key measure of network segregation describing the interconnectedness of neighboring nodes (Wilcoxon's signed-rank test, p=0.376), and characteristic path length, a key measure of network integration describing the average distance between nodes (Wilcoxon's signed-rank test, p=0.314), were not affected by CER (***Fig. 6A***). This result suggests that the interaction increase during CER was specific for interactions across network modules and not simply across neighboring nodes or node pairs. Taken together, results indicate that the brain's global modular structure remains stable during CER, compared to during attending to emotional stimuli. Emotional processing both with and without CER is thus likely based on the same functional brain network modular structure. Notably, however, during CER, interaction across these networks increases, underlying the successful cognitive regulation of aversive emotions.

## 4.2.3 Nodal participation and connector hub analysis

### *4.2.3.1 Increased nodal participation of amygdala and cuneus during CER*

To investigate the community structure further at nodal levels, we first focused on nodes that drove the increase of global participation during CER. Note that global participation coefficient is defined as the average nodal participation coefficient of all nodes of the graph [Godwin et al., 2015]. Nodal par-

ticipation coefficient, in turn, quantifies the ratio of a node's between-module edges to all edges connected to this node [Guimera & Amaral, 2005b]. To address the question of which nodes showed increased nodal participation during CER, we applied Wilcoxon's signed-rank testing ($p<0.05$, FDR-corrected for multiple testing across 286 nodes). Left basolateral amygdala ($p=0.0002$) and right cuneus ($p=0.0003$) showed significantly increased nodal participation in the Regulate compared to the Attend condition (***Fig. 6B***). At a more liberal correction for multiple testing (i.e., threshold $p<0.0035$ equal to 1/286 nodes [Lynall et al., 2010]), additionally the left centromedial amygdala ($p=0.0013$) and left cuneus ($p=0.0022$) showed increased nodal participation during CER (***Fig. 6B***). Results indicate that during CER, it is specifically left amygdala and cuneus that become more closely connected to nodes in other brain network modules.

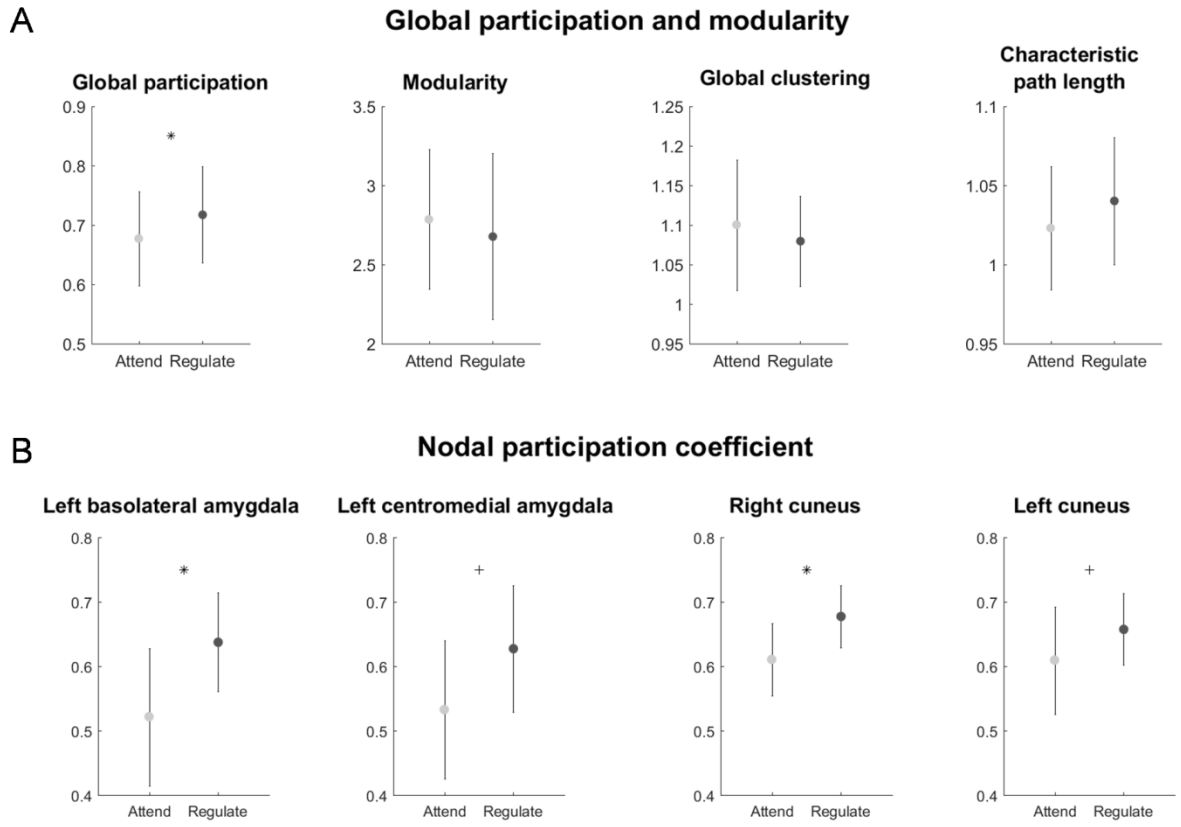


***Figure 6: Increased global and nodal interaction across modules during CER.***

*(A) Comparison of normalized global graph scores between Regulate and Attend conditions (mean and SD). * = significant difference between Regulate and Attend (Wilcoxon's signed-rank test, p<0.05). (B) Nodes with significantly higher nodal participation coefficient in the Regulate compared to the Attend condition; means and SDs are shown. * = significant using Wilcoxon's signed-rank test (p<0.05, FDR-corrected for multiple comparisons). + = significant at a more liberal correction for multiple comparisons (Wilcoxon's signed-rank test, p<0.0035 (=1/286 nodes)).*

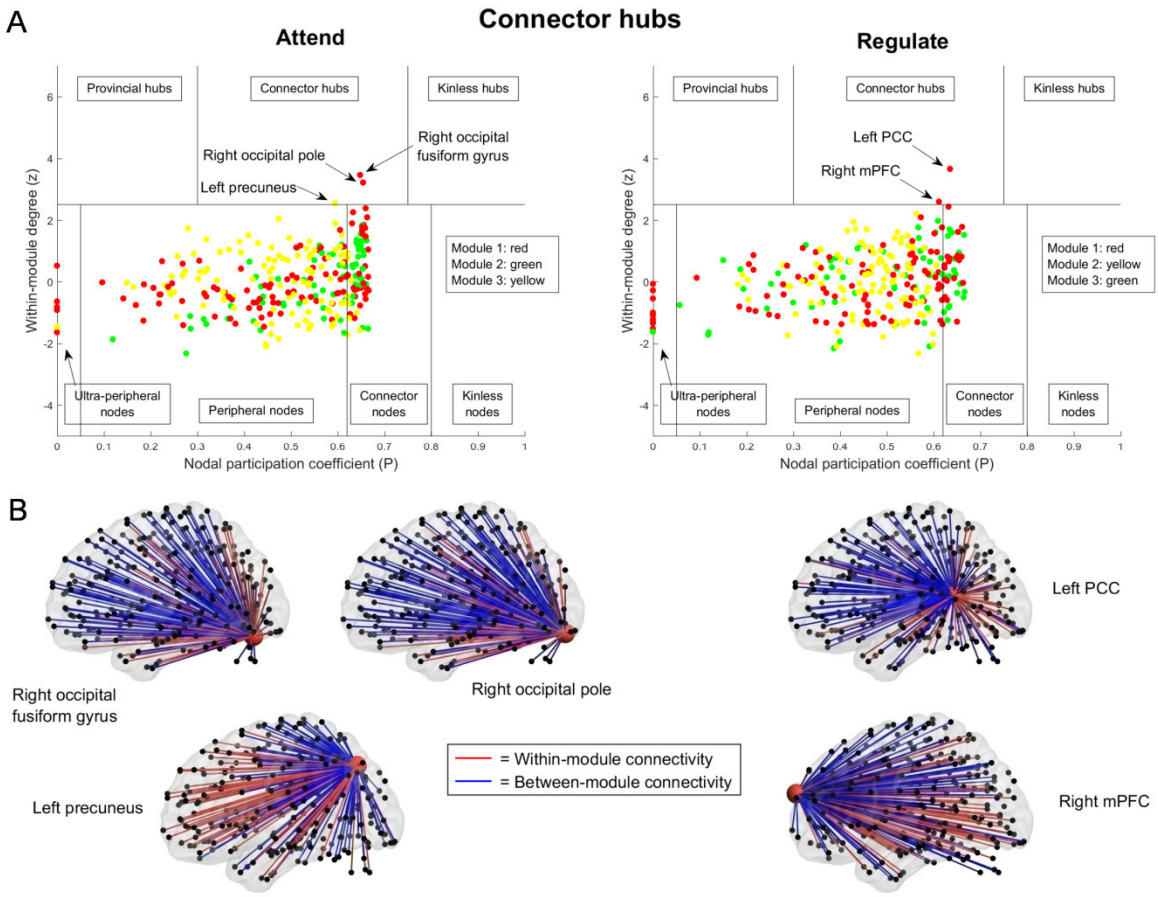


***Figure 7: Connector hubs during emotions with and without CER.***

*(A) Topological node roles based on within- and between-module connectivity in the group-level graphs of Attend and Regulate conditions. Nodes are grouped into 7 different categories according to their position on the z-P plane (z refers to within-module degree z-score reflecting within-module connectivity; P refers to nodal participation coefficient reflecting between-module connectivity). Anatomical positions of connector hubs are labeled with arrows. The color of each node shows its modular affiliation; module numbers and colors are consistent with* ***Fig. 3****. PCC = posterior cingulate cortex, mPFC = medial prefrontal cortex. (B) Within- and between-module edges of connector hubs in Attend and Regulate conditions. Within-module edges appear in red, between-module edges in blue.*

### *4.2.3.2 Distinct nodes act as connector hubs in Regulate and Attend conditions*

Nodal participation quantifies between-module connectivity; however, it provides no information about a node's within-module connectivity. To get a more complete picture of a node's role in the community structure of the whole-brain graph, we combined nodal participation and within-module degree. The within-module degree of a node, normalized over all nodes of its module, reflects its within-module connectivity [Guimera & Amaral, 2005b]. Within-module degree *z* and nodal participation coefficient *P* define a two-dimensional parameter space, the *z-P* plane. Plotting all nodes on

the *z-P* plane allows for classification of nodes according to their within- and between-module connectivity (***Fig. 7A***). Crucially, nodes classified as so-called connector hubs have both high within- and high between-module connectivity and are assumed to mediate communication between their own module and other modules [Guimera & Amaral, 2005b]. As an example, the major airport hubs in the world are connector hubs [Guimera et al., 2005]. ***Fig. 7*** shows the node roles in group-level graphs for the Attend and the Regulate condition, respectively. We observed a different set of connector hubs for each condition. During the Attend condition, connector hubs were located in posterior parts of the brain (i.e., right occipital fusiform gyrus, right occipital pole, left precuneus) (***Fig. 7A/B***). In the Regulate condition, however, connector hubs were located in relatively more anterior regions of the brain (right anterior medial PFC (mPFC), left posterior cingulate cortex (PCC)) (***Fig. 7A/B***). This result indicates that when simply attending to visual-emotional stimuli, the communication across modules is mainly mediated by nodes in visual-occipital cortices. During CER, in contrast, between-module information transfer occurs mainly through nodes in more anterior regions, such as mPFC and PCC. Interestingly, the mPFC node "switched" from module 3 (consisting mainly of default mode, fronto-parietal task control, and salience network nodes) in the Attend condition to module 1 (consisting mainly of visual and subcortical nodes) in the Regulate condition. This switch across modules during CER might indicate that the mPFC thus enabled regulatory control over areas processing visual emotional stimuli. Acting as a connector hub in its "new" module, it could perfectly mediate information flow between other brain modules and the "visual-subcortical module".

### 4.2.4 Spatial overlap of nodal functional embedding into the whole brain and specialized local activity during aversive emotional processing

Finally, we tested whether nodes sensitive for changes in functional embedding (i.e., nodal participation or connector hub properties) overlapped with areas whose local activity is specialized for emotional processing with and without CER. We applied canonical voxel-wise paired t-testing to contrast activation β-maps at a threshold of $p<0.005$ (uncorrected), and found typical activation patterns for emotional processing with CER (Regulate - Attend) and without CER (Attend - Regulate), in line with previous findings [Buhle et al., 2014; Ochsner et al., 2002; Wager et al., 2008]. Critically, amygdala and cuneus nodes, which showed increased nodal participation during CER, overlapped with clusters of decreased activation during CER (Attend - Regulate) (***Fig. 8A***). This result indicates that increased embedding of these nodes into the whole-brain network during CER is accompanied by suppression of local activity. Concerning connector hub properties, neither did connector hubs of the Attend condition overlap with activation clusters for the contrast Attend - Regulate, nor did connector hubs of the Regulate condition overlap with activation clusters for the contrast Regulate - Attend (***Fig. 8B***).

Results suggest that complex node properties incorporating both inter- and intra-modular connectivity during CER are not directly represented by patterns of specialized local activity.

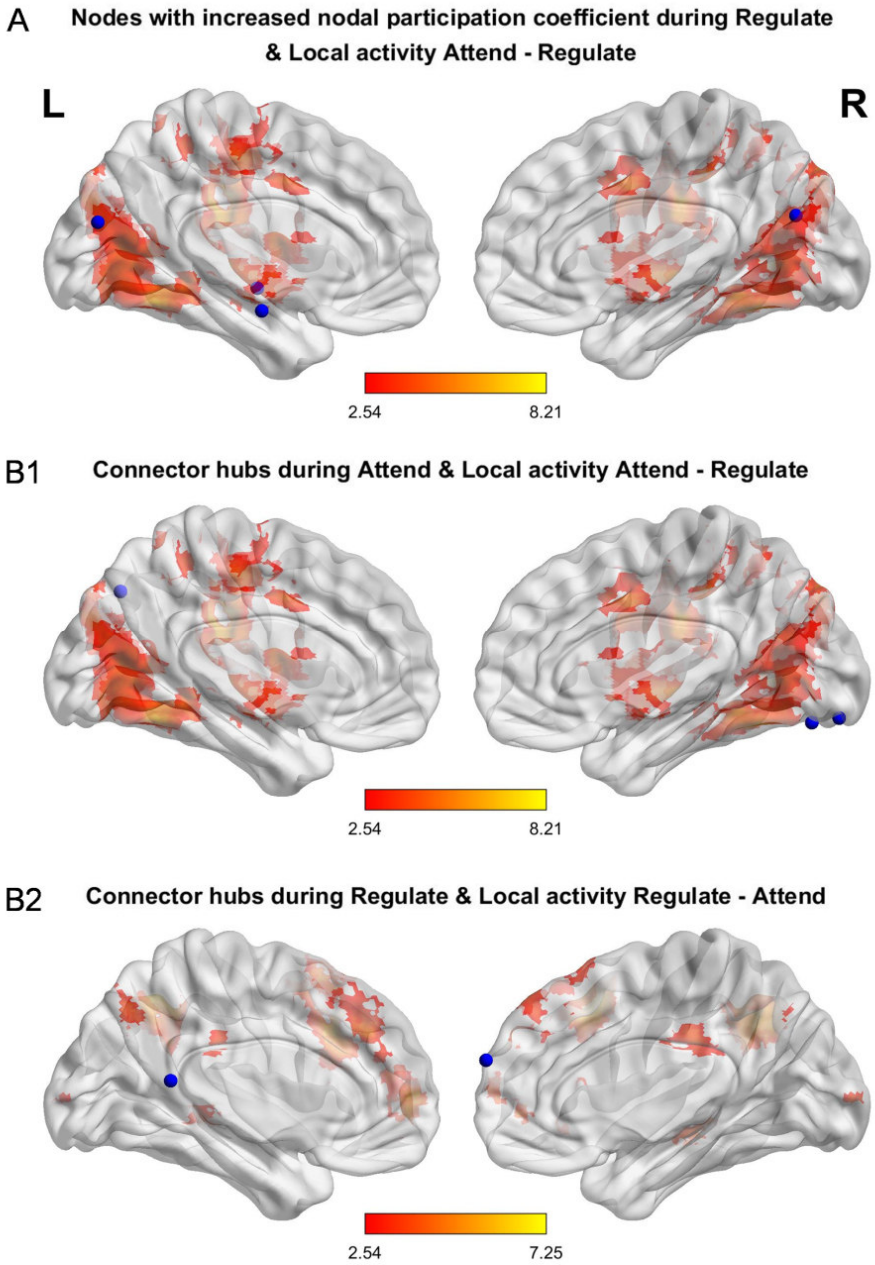


***Figure 8: Linking global and local properties of CER.***

*(A) Overlap of nodes with increased nodal participation during the Regulate condition and clusters of differential local activity (Attend - Regulate, p<0.005). (B) Overlap of connector hubs and clusters of differential local activity. (B1) Overlap of connector hubs during the Attend condition and clusters of differential local activity (Attend - Regulate, p<0.005). (B2) Overlap of connector hubs during the Regulate condition and clusters of differential local activity (Regulate - Attend, p<0.005).*

## 4.3 Project 3

### 4.3.1 Decision making and dopamine in healthy subjects

#### *4.3.1.1 Stay-switch behavior*

The repeated-measures ANOVA of stay probability in healthy subjects showed a significant main effect of reward (p=0.01) and a significant interaction reward*transition (p=0.046). The main effect of reward indicates significant model-free behavior, the interaction between reward and transition significant model-based behavior. So both model-free and model-based components contributed to decision making behavior in healthy subjects (***Fig. 9***).

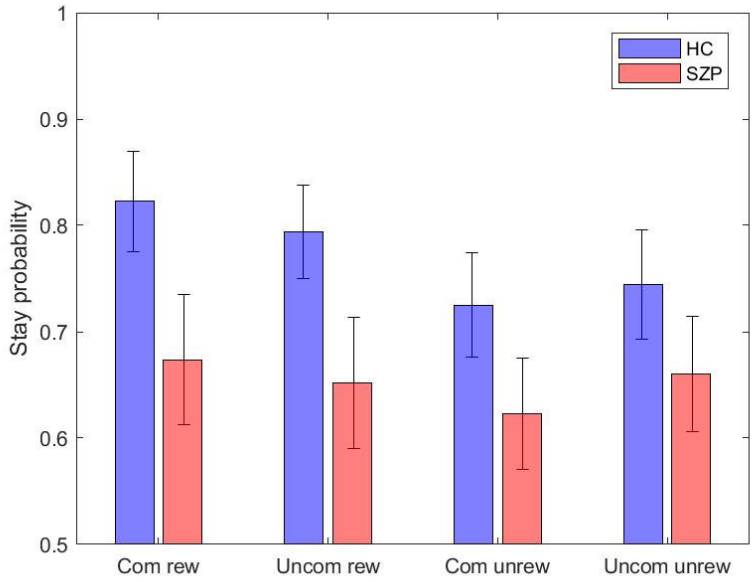


***Figure 9: Stay-switch behavior.***

*Stay probability of healthy controls (HC) and patients with schizophrenia (SZP) shown for 4 categories: com rew = common transition and reward in the trial before; uncom rew = uncommon transition and reward in the trial before; com unrew = common transition and no reward in the trial before; uncom unrew = uncommon transition and no reward in the trial before.*

#### *4.3.1.2 Association between decision making and dopamine synthesis*

To validate our approach based on the results from [Deserno et al., 2015], we tested whether we could replicate their findings of a positive association of dopamine synthesis capacity in nucleus accumbens and the tendency towards model-based behavior. Indeed, we also found a positive Pearson correlation between limbic striatal (covering primarily nucleus accumbens) $k_i^{cer}$ and the weighting parameter ω between model-based and model-free behavior (r=0.43, p=0.04).

## 4.3.2 Impaired decision making and aberrant dopamine in schizophrenia

### *4.3.2.1 Demographic and clinical characteristics*

Patients with schizophrenia and healthy controls did not significantly differ regarding age (p=0.76, two-sample t-test) or gender (p=1, $\chi^2$-test). Patients' mean PANSS score was 46.1.

### *4.3.2.2 Stay-switch behavior*

The repeated-measures ANOVA of stay probability in patients showed a significant interaction reward*transition (p=0.027), but no significant main effect of reward (p=0.27) (***Fig. 9***). A mixed ANOVA comprising both subject groups revealed a significant interaction reward*group (p=0.048), indicating group-differential model-free behavior. In contrast, there was no significant interaction reward*transition*group (p=0.7), indicating preserved model-based decision making in schizophrenia.

### *4.3.2.3 Computational modeling of decision making*

Decision making parameters were fitted using a computational model that described subjects' decision making behavior. We restricted group comparisons to the model-based/model-free weighting parameter ω to avoid multiple comparison problems. ω was significantly higher in patients (p=0.02, two-sample t-test), indicating an increased tendency towards model-based behavior in schizophrenia.

### *4.3.2.4 Striatal dopamine synthesis capacity*

The FDOPA-PET analysis showed significantly reduced $k_i^{cer}$ in associative striatum (p=0.001, two-sample t-test; patients: 0.0120$min^{-1}$; controls: 0.0143$min^{-1}$) and sensorimotor striatum (p=0.007; patients: 0.0129$min^{-1}$; controls: 0.0153$min^{-1}$) for patients with schizophrenia. No significant difference was observed for limbic striatum (p=0.58; patients: 0.0125$min^{-1}$; controls: 0.0127$min^{-1}$).

### *4.3.2.5 Association between decision making and dopamine synthesis*

For patients, no significant correlations between the model-based/model-free weighting parameter ω and FDOPA $k_i^{cer}$ were found. Next, we conducted interaction analyses to test for group-differential associations between model-based/model-free balance and dopamine synthesis. We observed significant interactions group*$k_i^{cer}$ for limbic striatum (p=0.04) and sensorimotor striatum (p=0.03).

# 5 Discussion

## 5.1 Project 1

This study investigated two complementary questions; first, is there a consistent pattern of brain activation in CRC across stimulus types? Second, inspired by the idea of a common neurocognitive mechanism generating cognitive regulation of both rewarding stimuli and negative emotions, does a common activation pattern exist for both CRC and CER? We collected fMRI activation studies in CRC and CER and conducted a coordinate-based meta-analysis followed by conjunction to assess brain areas recruited by CRC and CER. First, we identified consistent CRC activation across stimulus types mainly in supplementary motor area, pre-supplementary motor area, ventrolateral and dorsolateral prefrontal cortices. Second, we found that this activation pattern overlapped largely with CER-related activation. This link between CRC and CER supports models of a common neurocognitive mechanism for CRC and CER, generating cognitive control of both reward and negative emotions. A candidate for such a common mechanism is model-based decision making for actions that alter either one's craving towards consumption of a rewarding stimulus or one's emotional state.

### 5.1.1 Consistent activation in CRC across stimulus types

The CRC meta-analysis revealed that brain regions in bilateral SMA, pre-SMA, vlPFC, dlPFC, anterior insula, and angular gyrus were consistently more strongly activated during CRC than during reward cue exposure without control (***Fig. 5A***). This is the first coordinate-based meta-analysis of fMRI-studies in the field of CRC that investigated studies across stimulus types. The included literature was restricted to studies using paradigms in which subjects viewed pictures/videos of rewarding stimuli and had to control their craving towards these stimuli in the "CRC" condition [Brody et al., 2007; Kelley et al., 2015; Kober et al., 2010]. Distinct paradigms, e.g., involving depletion of self-regulatory resources [Wagner et al., 2013], were not considered in order to avoid methodological inconsistencies. We ensured maximal coverage of the existing literature by including studies with a wide range of rewarding stimuli, for example money, food, sex, or cigarette smoking (***Table 2***). To ensure that no particular stimulus type (e.g., food pictures) had a disproportionate influence on the results, we conducted post-hoc analyses to control for this factor. These analyses showed no significant effect of a specific stimulus type. Further control analyses demonstrated that neither any single study nor the factors age, gender, or cognitive control strategy (i.e., antecedent- or postcedent-focused) had a significant influence on results.

The results support recent theoretical suggestions and a qualitative review by Kelley et al., hypothesizing that lateral PFC, ventromedial PFC, and anterior cingulate cortex are critical for CRC (their concept of "self-regulation" is very akin to our concept of CRC) [Kelley et al., 2015]. While we could confirm consistent activation in lateral prefrontal cortices during CRC, we did not observe robust activation in ventromedial PFC and anterior cingulate. Lateral PFC is thought to be more involved in cognitive aspects of self-regulation (e.g., planning), while ventromedial PFC activation might rather reflect adverse consequences of excessive behavior [Kelley et al., 2015]. As we restricted studies to be based on paradigms of *cognitive* reward control, our results seem well in line with these predictions.

Furthermore, our findings extend the recent meta-analysis of Han et al., who reported consistent activation in SMA, pre-SMA, lateral PFC, insula, and parietal cortices during dietary self-control [Han et al., 2018]. We also included other stimuli like cigarettes or erotic pictures and observed a similar pattern, although more extended in lateral PFC. This suggests that the activation pattern relevant for food-control is comprised within a slightly larger pattern for domain-general cognitive control of hedonic stimuli. So in summary, results indicate that SMA, pre-SMA, and lateral fronto-parietal cortices are consistently activated during CRC across a wide range of rewarding stimuli.

### 5.1.2 Common activation in both CRC and CER

Combining the results of the CRC meta-analysis with the CER meta-analysis, we showed that activation patterns of CRC and CER converged on bilateral SMA, pre-SMA, dlPFC, and vlPFC, as well as on insular, parietal, and temporal cortices (***Fig. 5C***).

This result is composed of several subresults: (i) Consistent activation during CER comprised bilateral vlPFC, dlPFC, SMA, pre-SMA, cingulate, temporal, parietal, and subcortical regions (***Fig. 5B***). These results confirm almost exactly results of several previous meta-analyses of reappraisal studies, which also highlighted regions in dlPFC, vlPFC, SMA, pre-SMA, temporal, and parietal cortices [Buhle et al., 2014; Kohn et al., 2014; Langner et al., 2018; Morawetz et al., 2017b], thereby confirming the reliability of our meta-analytic approach. Moreover, the findings were not affected by any single study, age, gender, or regulation strategy, as shown by post-hoc control analyses.

(ii) We linked CRC and CER activation via conjunction analysis. This analysis revealed a common multi-regional activation pattern in bilateral SMA, pre-SMA, dlPFC, vlPFC as well as anterior insula, left angular and superior temporal gyrus (***Fig. 5C***). While CRC controls approach behavior towards rewarding stimuli, CER controls avoidance behavior regarding aversive stimuli [Corr & McNaughton, 2012]. This conceptualization suggests overlapping mechanisms and complementary activation patterns. According to appraisal models of emotions [Gross & Barrett, 2011], negative emotions arise from the valuation of an aversive stimulus, which then leads to avoidance behavior. In emotion regu-

lation, in turn, the emotion itself becomes the subject of valuation, and emotional reactivity represents the outcome action to be altered [Etkin et al., 2015]. In CER, for example, the emotion is cognitively reappraised, contrary to other regulation strategies like response inhibition [Gross & Barrett, 2011]. Similarly, rewarding stimuli are valued, leading to approach behavior. In CRC, in turn, this valuation itself is valued and modulated. This renders CRC akin to CER reappraisal; we likewise restricted CRC to cognitive re-valuation, as opposed to response inhibition strategies [Han et al., 2018].

Deepening this line of thought in terms of cognitive mechanisms of reappraisal, common activation across CER and CRC is consistent with a recent theory suggesting shared model-based control mechanisms for CER and reward-related decision-making such as CRC [Etkin et al., 2015]. Etkin and colleagues suggested particularly that vlPFC, dlPFC, SMA, and pre-SMA are critically involved in CER due to their typical involvement in reward model-based decision-making. This overlap of suggested and observed common activation across CER and CRC with its implications for underlying model-based control mechanisms will be discussed in detail below in paragraph 5.1.3.

(iii) When testing for differences in activation patterns between CRC and CER, CER was found to recruit a larger activation pattern than CRC in bilateral angular gyrus, left superior and medial temporal gyrus, and parts of left vlPFC and pre-SMA (***Fig. 5D***). In contrast, CRC did not show any differentially larger activation pattern than CER. A possible explanation for the selectively larger activation pattern of CER in predominantly left-sided cortical regions, which are essentially involved in language functions [Knecht et al., 2000], might be an association between language function and CER-reappraisal. CER-reappraisals comprise re-interpretation of a stimulus and its situation, which is often guided by language-based re-formulation (e.g. 'this stimulus is not real, but part of an experiment') and which therefore may recruit relatively more language-relevant regions than CRC [Ochsner et al., 2012].

Notably, a very recent meta-analysis published during data analysis addressed a related question: do neural patterns of CER overlap with cognitive action control (comprising a wide range of tasks like response inhibition, response conflicts, or task switching) [Langner et al., 2018]? Langner et al. found overlapping activation in pre-SMA, vlPFC, insula, and temporoparietal junction, but rather extended activation differences in prefrontal and parietal cortices. Our study differed in several ways from their approach, in that our questions were more focused: first, we restricted CER to downregulation of emotion, whereas they also allowed for upregulation, and to cognitive reappraisal, whereas they also included other strategies like response suppression. Second, their concept of cognitive action control comprised a wide range of tasks, whereas we restricted CRC tasks to the cognitive control of rewarding stimuli. Thus, we addressed a more specific question. Our results showed a slightly different pattern: the pattern of overlapping activation was more pronounced, while the activation differences were more restricted (however, results from Langner et al. were also dominated by greater activation during CER).

### 5.1.3 Potential common model-based mechanisms of CER and CRC

Our finding of shared neural correlates of CRC and CER is consistent with the idea of a common neurocognitive mechanism of CER and CRC. One candidate for such a shared mechanism is model-based control: Etkin et al. have recently transferred empirically supported concepts from reward-based learning to emotion regulation, suggesting that model-based control strategies might underlie both CER and CRC [Etkin et al., 2015]. This approach provides a unifying framework for the investigation of CER and CRC, and maybe even for further distinct instances of cognitive control/self-regulation, such as cognitive task control. In concepts of model-based reward decision making such as CRC, decisions about action selection are driven by internal models, which take into account information about stimulus value, context, short- and long-term goals etc. [Daw et al., 2005; Dolan & Dayan, 2013]. Likewise, in CER, decisions about which emotion-regulatory action to select for achieving a desired emotional state might be guided by such a cognitive model [Etkin et al., 2015]. Thus, both model-based control strategies involve decisions about actions, which alter either one's emotional state or one's craving towards consumption of a reinforcing stimulus. Our data provide empirical evidence for these theories by identifying shared neural correlates of CER and CRC, which might underlie shared mechanisms based on model-based decision making.

Speculatively, this finding might also extend to other domains of model-based cognitive control, such as task switching [Braver et al., 2003; Sohn et al., 2000]. Coordinate-based meta-analyses of task-switching showed a consistent domain-general frontoparietal activation pattern [Derrfuss et al., 2005; Kim et al., 2012]. Moreover, another meta-analysis observed common activation in frontoparietal cortices across a wide range of cognitive control task domains [Niendam et al., 2012]. This suggests shared neural correlates for CER, CRC, and other instances of cognitive control, possibly hinting at shared neural mechanisms. Future studies/meta-analyses are needed to address this question.

To sum up, our finding of shared neural correlates of CER and CRC provides evidence for common underlying mechanisms, which might be model-based decision making mechanisms. However, future studies are needed to specifically test this hypothesis by comparing CER and CRC decision making mechanisms with a suitable task paradigm.

### 5.1.4 Cognitive control and intrinsic brain networks

The common activation pattern of CRC and CER resembles multi-regional activation patterns during top-down cognitive control and top-down attention tasks [Corbetta & Shulman, 2002; Dosenbach et al., 2006; Duncan & Owen, 2000; Sohn et al., 2000]. Remarkably, these 'task-control systems', recruited during task states, link systematically with spatial patterns of correlated, slowly fluctuating brain activity during rest (i.e., so-called intrinsic functional connectivity networks as measured by

resting-state fMRI) across frontal and parietal cortices [Power et al., 2011]. In other words, intrinsic fronto-parietal networks, whose coherent ongoing activity mirrors the spatial outline of distinct task-control systems, both reflect *previous* cognitive control performances and support *future* cognitive control requirements [Cole et al., 2014]. This specific issue mirrors a more general theme, namely that organized ongoing brain activity reflects and shapes cognitive task activations in general [Berkes et al., 2011; Cole et al., 2016; Rosenberg et al., 2016; Smith et al., 2009; Tavor et al., 2016]. Future studies are needed to test whether the same intrinsic domain-general networks underlie multiple forms of model-based decision-making ranging from CRC, CER, to cognitive control of perceptual tasks. Indeed, a recent meta-analytic approach has provided first hints of a 'core network' underlying cognitive control across a wide range of tasks [Langner et al., 2018].

### 5.1.5 Limitations

The following limitations are worth noting. First, studies differed with regard to demographic factors like age and gender. We controlled for these variables by post-hoc analyses, finding no disproportionate effects. Second, our meta-analytic approach is limited in testing whether both CRC and CER represent model-based decision making. We have suggested this interpretation based on overlapping neural substrates and theoretical models [Etkin et al., 2015]. But certainly, future task-fMRI studies are needed to specifically address this question by directly comparing CRC and CER, for example with model-based decision making paradigms.

### 5.1.6 Conclusion

We show a consistent brain activation pattern for cognitive reward control focused on prefrontal cortices, which largely overlaps with the activation pattern of cognitive emotion regulation. This common activation pattern suggests a common neurocognitive mechanism for the control of both emotion and reward.

## 5.2 Project 2

This project provides first evidence that global interaction changes across brain networks spanning the whole brain contribute to human CER, more specifically that global participation across stable functional brain network modules increases during successful CER. The increase in global participation was critically driven by medial PFC and amygdala nodes, which overlapped with specialized local activity. These findings indicate the complementary global-local nature of human CER.

### 5.2.1 Increased global interaction of stable functional modules during CER

On a global whole-brain scale, we found that during CER, in comparison to emotional processing without regulation, global participation significantly increased, whereas modularity (i.e., decomposability into functional modules with high within-module connectivity) remained stable (***Fig. 6A***). Modules' composition was largely the same during emotions with and without CER (***Fig. 3C***). The behavioral significance of the increase in global participation was supported by its at-trend significant positive correlation with emotional intensity scores reflecting CER success, even though this analysis suffered from low statistical power. Both global clustering coefficient and characteristic path length remained unchanged during CER in comparison to emotions without CER, indicating that CER is specifically linked with an interaction increase between functional brain modules and not with interaction increases in general (***Fig. 6A***). These results suggest that CER is associated with an increased global interaction of stable functional whole-brain networks. Global models of CER anticipated that CER emerges from changing interactions of stable functional whole-brain networks [Barrett, 2009; James, 1884]. As we have shown, the composition of functional network modules indeed remains largely identical across conditions with and without CER (***Fig. 3C***); what changes is their interaction on a global level (***Fig. 6A***). This interaction increase across modules is consistent with previous network-focused results by Sripada et al. [Sripada et al., 2014], who found increased region-to-region connectivity between regions of a visual network and those of cortical control networks during CER while participants observed aversive pictures. In addition, global theories of CER further assume that CER arises from interactions of domain-general brain networks [Lindquist & Barrett, 2012]. This indicates that these networks are not limited to subserving distinct mental "faculties" (i.e., specific functions or emotions) [Touroutoglou et al., 2015]. This view is supported by our finding that each of the three brain modules in the current study comprised nodes in brain regions associated with a wide variety of functional domains (***Fig. 3C***). Therefore, one should note that the term "brain module", as it is used in this study, has to be clearly distinguished from domain-specific cognitive modules hypothesized in faculty psychology approaches [Fodor, 1983].

### 5.2.2 Global interaction increase is pronounced in specific nodes

The increase in global interaction across functional brain networks during CER was driven by key nodes of increased functional embedding, quantified by both nodal participation and connector hub properties (***Fig. 6B and 7***). The left basolateral and centromedial amygdala, for example, showed increased nodal participation during the cognitive regulation of aversive emotions, indicating an increased embedding in the functional whole-brain network (***Fig. 6B***). The amygdala has widespread structural [McDonald, 1998] and functional [Robinson et al., 2010] connections with both cortical and subcortical regions of the brain, thus acting as a hub in the whole-brain network [Mears & Pollard, 2016]. Beyond widespread connectivity, the amygdala is particularly involved in the processing of visual emotional stimuli [Adolphs et al., 1994]. In studies testing global emotion theories, particularly the left amygdala showed increased centrality or hubness during emotional processing [Koelsch & Skouras, 2014; Wheelock et al., 2014; Zhang et al., 2015]. Our results extend these findings by showing that during CER, specifically the left amygdala becomes more strongly embedded in the whole-brain network. This increased functional embedding occurs both in the basolateral and the centromedial amygdala (***Fig. 6B***). These two subregions can be distinguished based on their differential connectivity patterns with cortical and subcortical regions [Swanson & Petrovich, 1998]. Both amygdala subdivisions form part of brain circuits that enable adaptive behavior in response to aversive stimuli [Gross & Canteras, 2012; LeDoux, 2012].

The bilateral cuneus similarly exhibited increased nodal participation in the Regulate compared to the Attend condition (***Fig. 6B***). The cuneus contains brain regions associated with primary and higher visual processing [Felleman & Van Essen, 1991]. Its structural and functional connectivity with amygdala and prefrontal cortices provides support for its involvement in the processing of aversive visual stimuli [Narumoto et al., 2000]. We found that the cuneus was more tightly embedded in the functional whole-brain network during CER than during emotional processing without CER.

Connector hubs differed between Regulate and Attend conditions (***Fig. 7***). Exhibiting both high within-module and high between-module connectivity, connector hubs are critical for mediating intermodular information transfer, much like airport hubs [Guimera et al., 2005]. During emotional processing without regulation, connector hubs were located in posterior regions of the brain, especially in the occipital cortex. This brain part is strongly involved in the processing of aversive visual stimuli [Sabatinelli et al., 2011]. During CER, however, the role of connector hubs was taken over by more anterior parts of the brain, particularly the medial PFC and the PCC. Crucially, the medial PFC node switched from a cortical control module to a visual-subcortical module during CER, possibly to enable regulatory control over areas involved in emotional processing. In this way, the medial PFC could control 'information flow' between its new module and other brain modules during CER. One should

also note that medial PFC and PCC are important constituents of the default mode network, which is specifically associated with emotional decisions [Andrews-Hanna et al., 2010], cortical fear representation [Gross & Canteras, 2012], and emotion regulation [Sheline et al., 2009].

### 5.2.3 Linking global and local theories of CER

Nodes with increased nodal participation, i.e., amygdala and cuneus, overlapped with clusters of decreased local activity during CER compared to emotional processing without regulation (***Fig. 8A***). Suppression of local amygdala activity is consistently found in studies testing local theories of CER [Buhle et al., 2014]. Our results thus suggest that increased whole-brain participation of amygdala and cuneus might be accompanied by suppressed local activity during CER. In contrast, connector hubs of either the Attend or the Regulate condition did not overlap with clusters of specialized local activity during CER (***Fig. 8B***). Connector hub status reflects both high within- and between-module connectivity [Guimera & Amaral, 2005b]. Therefore, it is possible that this complex node property might not be directly represented by patterns of specialized local activity.

In summary, increased nodal participation was associated with specialized local activity, thus linking global and local models of CER. So far, local and global theories of CER have coexisted as - potentially contradictory - extremes in a continuum of theoretical perspectives of CER [Gross & Barrett, 2011]. Our study now provides initial experimental evidence that local and global models of CER may instead be viewed as complementary aspects of CER, rather than dichotomous perspectives.

### 5.2.4 Clinical implications

Our results may carry implications for the integration of distinct neurobiological models of affective disorders, particularly major depressive disorder (MDD). On the one hand, *local* neurobiological models of MDD are based on *local* perspectives of CER, which is a core symptom of depression [Hamilton et al., 2012; Mayberg, 1997]. For example, medial PFC and amygdala exhibit abnormalities in major depression, such as grey matter volume loss [Hamilton et al., 2008; Koolschijn et al., 2009] or simultaneous amygdala hyperactivation and mPFC hypoactivation [Siegle et al., 2002]; these alterations are thought to underlie impaired PFC control over amygdala activity as a central mechanism of impaired CER in particular and major depression in general [Mayberg, 1997]. On the other hand, *global* accounts of MDD propose major depression as a disorder of the human connectome [Gong & He, 2015]. Substantially altered structural and intrinsic functional large-scale brain organization has been found in MDD, including aberrant mPFC and amygdala hubness [Jin et al., 2011; Singh et al., 2013]. Such connectome-related changes are relevant for the course of MDD [Meng et al., 2014].

However, these different conceptualizations of major depression have been largely unrelated to each other. Linking global and local accounts of CER, our result can likewise provide a link between global and local neurobiological accounts of major depression in the context of impaired CER. For example, aberrant local amygdala activity during emotional processing in depressed patients might be not only due to impaired local control by PFC [Erk et al., 2010], but also due to the amygdala's impaired global functional embedding [Jin et al., 2011], which is relevant for effective CER (***Fig. 6B***). Likewise, structural and functional abnormalities of the medial PFC [Bludau et al., 2016] might not only impair the control over local amygdala activity during CER [Erk et al., 2010], but also affect impaired global interaction within and across modules (***Fig. 7***). Suggestively, the impairment of CER in major depression might be characterized by processes we found in healthy subjects during emotions without CER, such that across-module interaction might be dominated by occipital nodes (***Fig. 7***). Interestingly, such 'occipital dominance' of changes in several brain modalities has been reported in major depression, for example regarding reduced volume [Peterson et al., 2009], functional hubness [Meng et al., 2014], and metabolism [Sanacora et al., 2004]. Future studies focusing on a global perspective of CER impairments in major depression should test these suggestions.

### 5.2.5 Limitations and future directions

The following limitations should be considered for the correct evaluation of results.

First, we used a rather small sample size of 19 subjects. Low sample sizes decrease statistical power, inflate effect sizes, and lead to an increased rate of false positive results [Button et al., 2013]. This issue has been highlighted particularly for correlation analyses and therefore affects particularly the correlation results between graph scores and CER success [Yarkoni, 2009]. Moreover, the low sample size might limit the universal validity of our findings. On the other hand, this study is, to our knowledge, the first graph-based fMRI study in the field of cognitive emotion regulation, providing a proof of principle. Future studies are needed to test the replicability of results in independent subject samples.

Second, we used a typical experimental design to investigate CER via Attend vs. Regulate contrasts, which had already been employed extensively before [Buhle et al., 2014; Ochsner et al., 2002; Wager et al., 2008]. An inherent problem of this design is that actively regulating one's emotions could be cognitively more demanding than simply attending to a stimulus, or in other words: cognitive cost may confound results. The current study cannot fully exclude this confound. Nevertheless, a) results fit both expected hypothesis and other studies' findings, as discussed above, and b) we made an effort to minimize this possible confound as much as possible by applying an antecedent-focused reappraisal strategy [Gross, 2002; Sheppes & Meiran, 2008], and by using young healthy female partici-

pants, whose high Reappraisal scores on the Emotion Regulation Questionnaires (normative female mean = 4.61 [SD = 1.02, N = 1483], current study mean = 5.12 [SD = 0.52, N = 20]); t (1501) = 2.25, p = 0.025; normative mean taken from Gross & John (2003)) signify that they used reappraisal with minimal associated cognitive costs. Future studies of more rigorous design, additionally controlling for difficulty, are necessary to support our observations.

Third, we included only female subjects to exclude any gender influences concerning emotion processing and regulation [McRae et al., 2008b], a strategy applied by numerous other studies in the field [Frank et al., 2014]. Therefore, inferences of our results to the human brain as a whole should be treated carefully. Future studies could address this issue by examining male subjects or mixed groups with subgroup and comparison analyses.

Fourth, future studies could also investigate how global interaction changes during downregulation of responses to pleasant emotional stimuli or during upregulation of emotional responses. We speculate that results on a global level might be similar to our results. However, on a nodal level, regulation of positive emotions might implicate a changed participation of the ventral striatum [Buhle et al., 2014], while emotional upregulation, typically associated with enhanced amygdala local activity [Frank et al., 2014], might go along with decreased nodal participation of the amygdala.

### 5.2.6 Conclusion

Cognitive emotion regulation is associated with an increased global interaction of stable functional brain networks. This interaction is mainly driven by an increased embedding of specific nodes, such as amygdala, cuneus, medial prefrontal and posterior cingulate cortex, in the functional whole-brain network. As these key nodes partly coincide with regions involved in specialized local activation during CER, current results link global and local views on human CER as complementary perspectives.

## 5.3 Project 3

This study employed a sequential decision making task and FDOPA-PET in healthy subjects and patients with schizophrenia. Task data were used to describe subjects' decision making behavior via stay-switch probability and computational modeling. PET data were used to derive striatal dopamine synthesis capacity via graphical Patlak analysis. In this way, several connected questions were investigated: first, is the balance between model-based and model-free decision making associated with striatal dopamine synthesis (confirming previous studies)? Second, is the balance between model-based and model-free decision making altered in schizophrenia? Third, is such an aberrant balance associated with striatal dopamine synthesis? We found a positive correlation between the tendency towards model-based behavior and ventral striatal dopamine synthesis in healthy controls. In patients with schizophrenia, specifically model-free decision making was impaired and appeared to be particularly associated with reduced dorsal striatal dopamine synthesis.

### 5.3.1 Decision making and striatal dopamine synthesis in healthy subjects

We found a positive correlation between FDOPA $k_i^{cer}$ of limbic striatum and the tendency towards model-based behavior in healthy subjects. This means that the higher the dopamine synthesis, the more a subject acts in a model-based way. The model-based/model-free balance parameter was calculated with a well-established computational model [Daw et al., 2011; Deserno et al., 2015; Wunderlich et al., 2012]. The functional subdivision used in this study (limbic striatum) covers mostly the ventral striatum, particularly the nucleus accumbens. Therefore, our results are consistent with previous findings by Deserno et al., who reported a positive correlation between model-based/model-free balance and FDOPA-PET $k_i^{cer}$ in the nucleus accumbens [Deserno et al., 2015]. This consistency supports the validity of our approach. Further support for such claims comes from the pattern of stay-switch probability (***Fig. 9***): this analysis quantified how likely a subject was to select the same first-stage stimulus in the next trial again, depending on reward and transition in the trial before. Results showed that healthy subjects acted both in a model-free and a model-based fashion. This finding is in line with previous studies and theories stating that everyone uses both decision making strategies - what varies is the balance between the two.

### 5.3.2 Model-based/model-free decision making in schizophrenia

Computational modeling results showed that patients with schizophrenia exhibited a significantly increased tendency towards model-based behavior. The stay-switch analysis revealed that model-free decision making was significantly different between patients and controls, whereas model-based

behavior was not changed. Taken together, these two subresults suggest that in schizophrenia, specifically model-free decision making is impaired. As a consequence, patients' decision making balance seems to be relatively (or maybe as compensation) shifted towards model-based behavior, which explains the computational modeling result. This result is contrary to findings by Culbreth et al., who reported specifically aberrant model-based decision making in patients with schizophrenia [Culbreth et al., 2016]. However, the patients used in this thesis were in remission of psychotic symptoms, whereas patients in Culbreth et al. were psychotic. Thus, during psychosis, it seems that complex decisions requiring model-based computations are impaired. This might reflect a temporary disease state. In contrast, remission of (usually fluctuating) psychotic symptoms, but presence of negative and cognitive symptoms, might represent a disease trait, as such a constellation often persists for long periods. In such patients, model-free decision making is impaired. This could explain cognitive impairments: patients have to rely on computationally expensive model-based behavior instead of the faster, automatized model-free one. Future studies should elucidate this possible connection.

### 5.3.3 Decision making and striatal dopamine synthesis in schizophrenia

We observed no significant correlation between model-based/model-free balance and dopamine synthesis in patients with schizophrenia. However, when conducting an interaction analysis to look whether associations differ between patients and healthy controls, we found significant interactions for limbic and sensorimotor striatum. Focusing first on the limbic striatum, this result shows that the positive correlation between dopamine synthesis and tendency towards model-based behavior in healthy subjects is not present in patients with schizophrenia. However, dopamine synthesis was not significantly different across groups for limbic striatum. Therefore, abnormal ventral striatal dopamine transmission might not be the primary factor leading to impaired decision making in schizophrenia. In contrast, dopamine synthesis in the sensorimotor striatum was significantly reduced in patients. The sensorimotor striatum ROI covered mostly putamen (dorsolateral striatum). This corresponds with theories positing that model-free decision making is mainly associated with dorsolateral striatum [Daw et al., 2005; Dolan & Dayan, 2013; Graybiel, 2008; Striedter, 2016]. So, aberrant dorsal striatal dopamine synthesis might be a crucial factor in the specific impairment of model-free decision making in schizophrenia.

### 5.3.4 Conclusion

Results suggest that model-free decision making is specifically impaired in schizophrenia (during remission of psychotic symptoms) and associated with altered dopamine synthesis in dorsal striatum.

# 6 Conclusion

This thesis investigated neural correlates of cognitive control of motivated behavior. Cognitive control was conceptualized as model-based decision making, i.e., the selection of context-appropriate behaviors based on a internal model of the world.

In Project 1, we could show a consistent and overlapping brain activation pattern for two instances of cognitive control, namely cognitive regulation of aversive emotions and cognitive control of impulses towards rewarding stimuli. This pattern, identified via coordinate-based meta-analysis of task fMRI studies, comprised mainly prefrontal cortices. Such a common activation pattern suggests a common model-based mechanism for the control of both emotion and reward.

In Project 2, we investigated whether - additionally to such regional brain activations - also global interaction among functional brain networks is important for successful cognitive control. This was done paradigmatically for cognitive emotion regulation via graph analysis of task fMRI data. Indeed, we observed increased global interaction of stable functional brain networks, mainly driven by an increased embedding of specific nodes, such as amygdala, cuneus, medial prefrontal and posterior cingulate cortex, into the functional whole-brain network. These key nodes partly coincided with regions of local activation during cognitive emotion regulation, suggesting a link between global and local theories of cognitive control.

In Project 3, the link between ventral striatal dopamine transmission and model-based decision making was confirmed via a sequential decision making task coupled with FDOPA-PET. Patients with schizophrenia, however, showed specifically impaired model-free decision making behavior, which was associated with aberrant dopamine synthesis in the dorsal striatum.

Taken together, these findings support conceptualizations of cognitive control as model-based decision making, which - apart from local brain activation - also involves global processes. In schizophrenia, however, aberrant striatal dopamine transmission seems to impair rather model-free behavior.

# 7 References


Abi-Dargham, A., Martinez, D., Mawlawi, O., Simpson, N., Hwang, D.R., Slifstein, M., Anjilvel, S., Pidcock, J., Guo, N.N., Lombardo, I., Mann, J.J., Van Heertum, R., Foged, C., Halldin, C., Laruelle, M. (2000): Measurement of striatal and extrastriatal dopamine D1 receptor binding potential with [11C]NNC 112 in humans: validation and reproducibility. *J Cereb Blood Flow Metab* 20, 225-243.

Adolphs, R., Tranel, D., Damasio, H., Damasio, A. (1994): Impaired recognition of emotion in facial expressions following bilateral damage to the human amygdala. *Nature* 372, 669-672.

Alexander, G.E., DeLong, M.R., Strick, P.L. (1986): Parallel organization of functionally segregated circuits linking basal ganglia and cortex. *Annu Rev Neurosci* 9, 357-381.

Amunts, K., Kedo, O., Kindler, M., Pieperhoff, P., Mohlberg, H., Shah, N.J., Habel, U., Schneider, F., Zilles, K. (2005): Cytoarchitectonic mapping of the human amygdala, hippocampal region and entorhinal cortex: intersubject variability and probability maps. *Anat Embryol (Berl)* 210, 343-352.

Andreasen, N.C., Carpenter, W.T., Jr., Kane, J.M., Lasser, R.A., Marder, S.R., Weinberger, D.R. (2005): Remission in schizophrenia: proposed criteria and rationale for consensus. *Am J Psychiatry* 162, 441-449.

Andrews-Hanna, J.R., Reidler, J.S., Sepulcre, J., Poulin, R., Buckner, R.L. (2010): Functional-anatomic fractionation of the brain's default network. *Neuron* 65, 550-562.

Attwell, D., Buchan, A.M., Charpak, S., Lauritzen, M., Macvicar, B.A., Newman, E.A. (2010): Glial and neuronal control of brain blood flow. *Nature* 468, 232-243.

Barrett, L.F. (2009): The Future of Psychology: Connecting Mind to Brain. *Perspect Psychol Sci* 4, 326-339.

Barrett, L.F., Wilson-Mendenhall, C.D., Barsalou, L.W., 2014. A psychological construction account of emotion regulation and dysregulation: The role of situated conceptualizations, in: Gross, J.J. (Ed.), Handbook of Emotion Regulation. Guilford, New York, pp. 447-465.

Belden, A.C., Luby, J.L., Pagliaccio, D., Barch, D.M. (2014): Neural activation associated with the cognitive emotion regulation of sadness in healthy children. *Dev Cogn Neurosci* 9, 136-147.

Bellman, R. (1957): Dynamic Programming. Princeton University Press, Princeton, NJ.

Benjamini, Y., Hochberg, Y. (1995): Controlling the false discovery rate: a practical and powerful approach to multiple testing. *Journal of the Royal Statistical Society, Series B* 57, 289–300.

Berkes, P., Orban, G., Lengyel, M., Fiser, J. (2011): Spontaneous cortical activity reveals hallmarks of an optimal internal model of the environment. *Science* 331, 83-87.

Bloomfield, M.A., Pepper, F., Egerton, A., Demjaha, A., Tomasi, G., Mouchlianitis, E., Maximen, L., Veronese, M., Turkheimer, F., Selvaraj, S., Howes, O.D. (2014): Dopamine function in cigarette smokers: an [(1)(8)F]-DOPA PET study. *Neuropsychopharmacology* 39, 2397-2404.

Bludau, S., Bzdok, D., Gruber, O., Kohn, N., Riedl, V., Sorg, C., Palomero-Gallagher, N., Muller, V.I., Hoffstaedter, F., Amunts, K., Eickhoff, S.B. (2016): Medial Prefrontal Aberrations in Major Depressive Disorder Revealed by Cytoarchitectonically Informed Voxel-Based Morphometry. *Am J Psychiatry* 173, 291-298.

Braver, T.S., Reynolds, J.R., Donaldson, D.I. (2003): Neural Mechanisms of Transient and Sustained Cognitive Control during Task Switching. *Neuron* 39, 713-726.

Breier, A., Su, T.P., Saunders, R., Carson, R.E., Kolachana, B.S., de Bartolomeis, A., Weinberger, D.R., Weisenfeld, N., Malhotra, A.K., Eckelman, W.C., Pickar, D. (1997): Schizophrenia is associated with elevated amphetamine-induced synaptic dopamine concentrations: evidence from a novel positron emission tomography method. *Proc Natl Acad Sci U S A* 94, 2569-2574.

Brody, A.L., Mandelkern, M.A., Olmstead, R.E., Jou, J., Tiongson, E., Allen, V., Scheibal, D., London, E.D., Monterosso, J.R., Tiffany, S.T., Korb, A., Gan, J.J., Cohen, M.S. (2007): Neural substrates of resisting craving during cigarette cue exposure. *Biol Psychiatry* 62, 642-651.

Buhle, J.T., Silvers, J.A., Wager, T.D., Lopez, R., Onyemekwu, C., Kober, H., Weber, J., Ochsner, K.N. (2014): Cognitive reappraisal of emotion: a meta-analysis of human neuroimaging studies. *Cereb Cortex* 24, 2981-2990.

Bullmore, E.T., Bassett, D.S. (2011): Brain graphs: graphical models of the human brain connectome. *Annu Rev Clin Psychol* 7, 113-140.

Bullmore, E.T., Sporns, O. (2009): Complex brain networks: graph theoretical analysis of structural and functional systems. *Nat Rev Neurosci* 10, 186-198.

Button, K.S., Ioannidis, J.P., Mokrysz, C., Nosek, B.A., Flint, J., Robinson, E.S., Munafo, M.R. (2013): Power failure: why small sample size undermines the reliability of neuroscience. *Nat Rev Neurosci* 14, 365-376.

Cardoso, M.M., Sirotin, Y.B., Lima, B., Glushenkova, E., Das, A. (2012): The neuroimaging signal is a linear sum of neurally distinct stimulus- and task-related components. *Nat Neurosci* 15, 1298-1306.

Carlsson, A., Lindqvist, M., Magnusson, T. (1957): 3,4-Dihydroxyphenylalanine and 5-hydroxytryptophan as reserpine antagonists. *Nature* 180, 1200.

Cauli, B., Tong, X.K., Rancillac, A., Serluca, N., Lambolez, B., Rossier, J., Hamel, E. (2004): Cortical GABA interneurons in neurovascular coupling: relays for subcortical vasoactive pathways. *J Neurosci* 24, 8940-8949.

Cisler, J.M., Bush, K., Steele, J.S. (2014): A comparison of statistical methods for detecting context-modulated functional connectivity in fMRI. *Neuroimage* 84, 1042-1052.

Cole, M.W., Bassett, D.S., Power, J.D., Braver, T.S., Petersen, S.E. (2014): Intrinsic and task-evoked network architectures of the human brain. *Neuron* 83, 238-251.

Cole, M.W., Ito, T., Bassett, D.S., Schultz, D.H. (2016): Activity flow over resting-state networks shapes cognitive task activations. *Nat Neurosci* 19, 1718-1726.

Conti, M., Eriksson, L. (2016): Physics of pure and non-pure positron emitters for PET: a review and a discussion. *EJNMMI Phys* 3, 8.

Corbetta, M., Shulman, G.L. (2002): Control of goal-directed and stimulus-driven attention in the brain. *Nat Rev Neurosci* 3, 201-215.

Corr, P.J., McNaughton, N. (2012): Neuroscience and approach/avoidance personality traits: a two stage (valuation-motivation) approach. *Neurosci Biobehav Rev* 36, 2339-2354.

Creese, I., Burt, D.R., Snyder, S.H. (1976): Dopamine receptor binding predicts clinical and pharmacological potencies of antischizophrenic drugs. *Science* 192, 481-483.

Crockett, M.J., Braams, B.R., Clark, L., Tobler, P.N., Robbins, T.W., Kalenscher, T. (2013): Restricting temptations: neural mechanisms of precommitment. *Neuron* 79, 391-401.

Culbreth, A.J., Westbrook, A., Daw, N.D., Botvinick, M., Barch, D.M. (2016): Reduced model-based decision-making in schizophrenia. *J Abnorm Psychol* 125, 777-787.

Davis, K.L., Kahn, R.S., Ko, G., Davidson, M. (1991): Dopamine in schizophrenia: a review and reconceptualization. *Am J Psychiatry* 148, 1474-1486.

Daw, N.D., Gershman, S.J., Seymour, B., Dayan, P., Dolan, R.J. (2011): Model-based influences on humans' choices and striatal prediction errors. *Neuron* 69, 1204-1215.

Daw, N.D., Niv, Y., Dayan, P. (2005): Uncertainty-based competition between prefrontal and dorsolateral striatal systems for behavioral control. *Nat Neurosci* 8, 1704-1711.

Denny, B.T., Inhoff, M.C., Zerubavel, N., Davachi, L., Ochsner, K.N. (2015): Getting Over It: Long-Lasting Effects of Emotion Regulation on Amygdala Response. *Psychol Sci* 26, 1377-1388.

Derrfuss, J., Brass, M., Neumann, J., von Cramon, D.Y. (2005): Involvement of the inferior frontal junction in cognitive control: meta-analyses of switching and Stroop studies. *Hum Brain Mapp* 25, 22-34.

Deserno, L., Huys, Q.J., Boehme, R., Buchert, R., Heinze, H.J., Grace, A.A., Dolan, R.J., Heinz, A., Schlagenhauf, F. (2015): Ventral striatal dopamine reflects behavioral and neural signatures of model-based control during sequential decision making. *Proc Natl Acad Sci U S A* 112, 1595-1600.

Di Martino, A., Scheres, A., Margulies, D.S., Kelly, A.M., Uddin, L.Q., Shehzad, Z., Biswal, B., Walters, J.R., Castellanos, F.X., Milham, M.P. (2008): Functional connectivity of human striatum: a resting state FMRI study. *Cereb Cortex* 18, 2735-2747.

Diedrichsen, J., Balsters, J.H., Flavell, J., Cussans, E., Ramnani, N. (2009): A probabilistic MR atlas of the human cerebellum. *Neuroimage* 46, 39-46.

Diekhof, E.K., Keil, M., Obst, K.U., Henseler, I., Dechent, P., Falkai, P., Gruber, O. (2012): A functional neuroimaging study assessing gender differences in the neural mechanisms underlying the ability to resist impulsive desires. *Brain Res* 1473, 63-77.

Dietrich, A., Hollmann, M., Mathar, D., Villringer, A., Horstmann, A. (2016): Brain regulation of food craving: relationships with weight status and eating behavior. *Int J Obes (Lond)* 40, 982-989.

Dolan, R.J., Dayan, P. (2013): Goals and habits in the brain. *Neuron* 80, 312-325.

Domes, G., Schulze, L., Bottger, M., Grossmann, A., Hauenstein, K., Wirtz, P.H., Heinrichs, M., Herpertz, S.C. (2010): The neural correlates of sex differences in emotional reactivity and emotion regulation. *Hum Brain Mapp* 31, 758-769.

Dong, D., Wang, Y., Jackson, T., Chen, S., Wang, Y., Zhou, F., Chen, H. (2016): Impulse control and restrained eating among young women: Evidence for compensatory cortical activation during a chocolate-specific delayed discounting task. *Appetite* 105, 477-486.

Doré, B.P., Boccagno, C., Burr, D., Hubbard, A., Long, K., Weber, J., Stern, Y., Ochsner, K.N. (2017): Finding Positive Meaning in Negative Experiences Engages Ventral Striatal and Ventromedial Prefrontal Regions Associated with Reward Valuation. *Journal of Cognitive Neuroscience* 29, 235-244.
Dorfel, D., Lamke, J.P., Hummel, F., Wagner, U., Erk, S., Walter, H. (2014): Common and differential neural networks of emotion regulation by Detachment, Reinterpretation, Distraction, and Expressive Suppression: a comparative fMRI investigation. *Neuroimage* 101, 298-309.
Dosenbach, N.U., Visscher, K.M., Palmer, E.D., Miezin, F.M., Wenger, K.K., Kang, H.C., Burgund, E.D., Grimes, A.L., Schlaggar, B.L., Petersen, S.E. (2006): A core system for the implementation of task sets. *Neuron* 50, 799-812.
Duncan, J., Owen, A.M. (2000): Common regions of the human frontal lobe recruited by diverse cognitive demands. *Trends Neurosci* 23, 475-483.
Eippert, F., Veit, R., Weiskopf, N., Erb, M., Birbaumer, N., Anders, S. (2007): Regulation of emotional responses elicited by threat-related stimuli. *Hum Brain Mapp* 28, 409-423.
Engen, H.G., Singer, T. (2015): Compassion-based emotion regulation up-regulates experienced positive affect and associated neural networks. *Soc Cogn Affect Neurosci* 10, 1291-1301.
Erk, S., Mikschl, A., Stier, S., Ciaramidaro, A., Gapp, V., Weber, B., Walter, H. (2010): Acute and sustained effects of cognitive emotion regulation in major depression. *J Neurosci* 30, 15726-15734.
Etkin, A., Buchel, C., Gross, J.J. (2015): The neural bases of emotion regulation. *Nat Rev Neurosci* 16, 693-700.
Etkin, A., Wager, T.D. (2007): Functional neuroimaging of anxiety: a meta-analysis of emotional processing in PTSD, social anxiety disorder, and specific phobia. *Am J Psychiatry* 164, 1476-1488.
Farde, L., Hall, H., Ehrin, E., Sedvall, G. (1986): Quantitative analysis of D2 dopamine receptor binding in the living human brain by PET. *Science* 231, 258-261.
Felleman, D.J., Van Essen, D.C. (1991): Distributed hierarchical processing in the primate cerebral cortex. *Cereb Cortex* 1, 1-47.
Fodor, J.A. (1983): The Modularity of Mind: An Essay on Faculty Psychology. MIT Press, Cambridge.
Frank, D.W., Dewitt, M., Hudgens-Haney, M., Schaeffer, D.J., Ball, B.H., Schwarz, N.F., Hussein, A.A., Smart, L.M., Sabatinelli, D. (2014): Emotion regulation: quantitative meta-analysis of functional activation and deactivation. *Neurosci Biobehav Rev* 45, 202-211.
Fuertinger, S., Horwitz, B., Simonyan, K. (2015): The Functional Connectome of Speech Control. *PLoS Biol* 13, e1002209.
Garnett, E.S., Firnau, G., Nahmias, C. (1983): Dopamine visualized in the basal ganglia of living man. *Nature* 305, 137-138.
Gerchen, M.F., Bernal-Casas, D., Kirsch, P. (2014): Analyzing task-dependent brain network changes by whole-brain psychophysiological interactions: a comparison to conventional analysis. *Hum Brain Mapp* 35, 5071-5082.
Girouard, H., Iadecola, C. (2006): Neurovascular coupling in the normal brain and in hypertension, stroke, and Alzheimer disease. *J Appl Physiol (1985)* 100, 328-335.
Girvan, M., Newman, M.E. (2002): Community structure in social and biological networks. *Proc Natl Acad Sci U S A* 99, 7821-7826.
Giuliani, N.R., Mann, T., Tomiyama, A.J., Berkman, E.T. (2014): Neural systems underlying the reappraisal of personally craved foods. *J Cogn Neurosci* 26, 1390-1402.
Giuliani, N.R., Pfeifer, J.H. (2015): Age-related changes in reappraisal of appetitive cravings during adolescence. *Neuroimage* 108, 173-181.
Godwin, D., Barry, R.L., Marois, R. (2015): Breakdown of the brain's functional network modularity with awareness. *Proc Natl Acad Sci U S A* 112, 3799-3804.
Goldin, P.R., McRae, K., Ramel, W., Gross, J.J. (2008): The neural bases of emotion regulation: reappraisal and suppression of negative emotion. *Biol Psychiatry* 63, 577-586.
Gong, Q., He, Y. (2015): Depression, Neuroimaging and Connectomics: A Selective Overview. *Biol Psychiatry* 77, 223-235.
Grace, A.A., Bunney, B.S. (1984a): The control of firing pattern in nigral dopamine neurons: burst firing. *J Neurosci* 4, 2877-2890.
Grace, A.A., Bunney, B.S. (1984b): The control of firing pattern in nigral dopamine neurons: single spike firing. *J Neurosci* 4, 2866-2876.
Graybiel, A.M. (2008): Habits, rituals, and the evaluative brain. *Annu Rev Neurosci* 31, 359-387.
Grezellschak, S., Lincoln, T.M., Westermann, S. (2015): Cognitive emotion regulation in patients with schizophrenia: Evidence for effective reappraisal and distraction. *Psychiatry Res* 229, 434-439.
Gross, C.T., Canteras, N.S. (2012): The many paths to fear. *Nat Rev Neurosci* 13, 651-658.

Gross, J.J. (1998): The emerging field of emotion regulation: an integrative review. *Review of General Psychology* 2, 271-299.
Gross, J.J. (2002): Emotion regulation: affective, cognitive, and social consequences. *Psychophysiology* 39, 281-291.
Gross, J.J., Barrett, L.F. (2011): Emotion Generation and Emotion Regulation: One or Two Depends on Your Point of View. *Emot Rev* 3, 8-16.
Gross, J.J., John, O.P. (2003): Individual differences in two emotion regulation processes: implications for affect, relationships, and well-being. *J Pers Soc Psychol* 85, 348-362.
Grubbs, F. (1969): Procedures for Detecting Outlying Observations in Samples. *Technometrics* 11, 1-21.
Guimera, R., Amaral, L.A.N. (2005a): Cartography of complex networks: modules and universal roles. *J Stat Mech* 2005, nihpa35573.
Guimera, R., Amaral, L.A.N. (2005b): Functional cartography of complex metabolic networks. *Nature* 433, 895-900.
Guimera, R., Mossa, S., Turtschi, A., Amaral, L.A.N. (2005): The worldwide air transportation network: Anomalous centrality, community structure, and cities' global roles. *Proc Natl Acad Sci U S A* 102, 7794-7799.
Haber, S.N. (2016): Corticostriatal circuitry. *Dialogues Clin Neurosci* 18, 7-21.
Hallam, G.P., Webb, T.L., Sheeran, P., Miles, E., Wilkinson, I.D., Hunter, M.D., Barker, A.T., Woodruff, P.W., Totterdell, P., Lindquist, K.A., Farrow, T.F. (2015): The neural correlates of emotion regulation by implementation intentions. *PLoS One* 10, e0119500.
Hamilton, J.P., Etkin, A., Furman, D.J., Lemus, M.G., Johnson, R.F., Gotlib, I.H. (2012): Functional neuroimaging of major depressive disorder: a meta-analysis and new integration of base line activation and neural response data. *Am J Psychiatry* 169, 693-703.
Hamilton, J.P., Siemer, M., Gotlib, I.H. (2008): Amygdala volume in major depressive disorder: a meta-analysis of magnetic resonance imaging studies. *Mol Psychiatry* 13, 993-1000.
Han, J.E., Boachie, N., Garcia-Garcia, I., Michaud, A., Dagher, A. (2018): Neural correlates of dietary self-control in healthy adults: A meta-analysis of functional brain imaging studies. *Physiol Behav* 192, 98-108.
Harding, I.H., Andrews, Z.B., Mata, F., Orlandea, S., Martinez-Zalacain, I., Soriano-Mas, C., Stice, E., Verdejo-Garcia, A. (2018): Brain substrates of unhealthy versus healthy food choices: influence of homeostatic status and body mass index. *Int J Obes (Lond)* 42, 448-454.
Hare, T.A., Malmaud, J., Rangel, A. (2011): Focusing attention on the health aspects of foods changes value signals in vmPFC and improves dietary choice. *J Neurosci* 31, 11077-11087.
Hartwell, K.J., Johnson, K.A., Li, X., Myrick, H., LeMatty, T., George, M.S., Brady, K.T. (2011): Neural correlates of craving and resisting craving for tobacco in nicotine dependent smokers. *Addict Biol* 16, 654-666.
Hayes, J.P., Morey, R.A., Petty, C.M., Seth, S., Smoski, M.J., McCarthy, G., Labar, K.S. (2010): Staying cool when things get hot: emotion regulation modulates neural mechanisms of memory encoding. *Front Hum Neurosci* 4, 230.
He, Q., Xiao, L., Xue, G., Wong, S., Ames, S.L., Schembre, S.M., Bechara, A. (2014): Poor ability to resist tempting calorie rich food is linked to altered balance between neural systems involved in urge and self-control. *Nutrition Journal*.
Heatherton, T.F. (2011): Neuroscience of self and self-regulation. *Annu Rev Psychol* 62, 363-390.
Hill, P.F., Yi, R., Spreng, R.N., Diana, R.A. (2017): Neural congruence between intertemporal and interpersonal self-control: Evidence from delay and social discounting. *Neuroimage* 162, 186-198.
Hillman, E.M. (2014): Coupling mechanism and significance of the BOLD signal: a status report. *Annu Rev Neurosci* 37, 161-181.
Hofmann, S.G., Sawyer, A.T., Fang, A., Asnaani, A. (2012): Emotion Dysregulation Model of Mood and Anxiety Disorders. *Depression and Anxiety* 29, 409-416.
Hofmann, W., Friese, M., Strack, F. (2009): Impulse and Self-Control From a Dual-Systems Perspective. *Perspect Psychol Sci* 4, 162-176.
Hollmann, M., Hellrung, L., Pleger, B., Schlogl, H., Kabisch, S., Stumvoll, M., Villringer, A., Horstmann, A. (2012): Neural correlates of the volitional regulation of the desire for food. *Int J Obes (Lond)* 36, 648-655.
Howes, O.D., Kambeitz, J., Kim, E., Stahl, D., Slifstein, M., Abi-Dargham, A., Kapur, S. (2012): The nature of dopamine dysfunction in schizophrenia and what this means for treatment. *Arch Gen Psychiatry* 69, 776-786.
Howes, O.D., Kapur, S. (2009): The dopamine hypothesis of schizophrenia: version III--the final common pathway. *Schizophr Bull* 35, 549-562.

Howes, O.D., Montgomery, A.J., Asselin, M.C., Murray, R.M., Valli, I., Tabraham, P., Bramon-Bosch, E., Valmaggia, L., Johns, L., Broome, M., McGuire, P.K., Grasby, P.M. (2009): Elevated striatal dopamine function linked to prodromal signs of schizophrenia. *Arch Gen Psychiatry* 66, 13-20.

Humphries, M.D., Gurney, K., Prescott, T.J. (2006): The brainstem reticular formation is a small-world, not scale-free, network. *Proc Biol Sci* 273, 503-511.

Hutcherson, C.A., Plassmann, H., Gross, J.J., Rangel, A. (2012): Cognitive regulation during decision making shifts behavioral control between ventromedial and dorsolateral prefrontal value systems. *J Neurosci* 32, 13543-13554.

James, W. (1884): What is an emotion? *Mind* 9, 188-205.

Jauhar, S., Nour, M.M., Veronese, M., Rogdaki, M., Bonoldi, I., Azis, M., Turkheimer, F., McGuire, P., Young, A.H., Howes, O.D. (2017): A Test of the Transdiagnostic Dopamine Hypothesis of Psychosis Using Positron Emission Tomographic Imaging in Bipolar Affective Disorder and Schizophrenia. *JAMA Psychiatry* 74, 1206-1213.

Jin, C., Gao, C., Chen, C., Ma, S., Netra, R., Wang, Y., Zhang, M., Li, D. (2011): A preliminary study of the dysregulation of the resting networks in first-episode medication-naive adolescent depression. *Neurosci Lett* 503, 105-109.

Joormann, J., Gotlib, I.H. (2010): Emotion regulation in depression: relation to cognitive inhibition. *Cogn Emot* 24, 281-298.

Kahn, I., Andrews-Hanna, J.R., Vincent, J.L., Snyder, A.Z., Buckner, R.L. (2008): Distinct cortical anatomy linked to subregions of the medial temporal lobe revealed by intrinsic functional connectivity. *J Neurophysiol* 100, 129-139.

Kaiser, R.H., Andrews-Hanna, J.R., Wager, T.D., Pizzagalli, D.A. (2015): Large-Scale Network Dysfunction in Major Depressive Disorder: A Meta-analysis of Resting-State Functional Connectivity. *JAMA Psychiatry* 72, 603-611.

Kay, S.R., Fiszbein, A., Opler, L.A. (1987): The positive and negative syndrome scale (PANSS) for schizophrenia. *Schizophr Bull* 13, 261-276.

Kelley, W.M., Wagner, D.D., Heatherton, T.F. (2015): In search of a human self-regulation system. *Annu Rev Neurosci* 38, 389-411.

Kernighan, B.W., Lin, S. (1970): An efficient heuristic procedure for partitioning graphs. *Bell System Technical Journal* 49, 291–307.

Kim, C., Cilles, S.E., Johnson, N.F., Gold, B.T. (2012): Domain general and domain preferential brain regions associated with different types of task switching: a meta-analysis. *Hum Brain Mapp* 33, 130-142.

Kinnison, J., Padmala, S., Choi, J.M., Pessoa, L. (2012): Network analysis reveals increased integration during emotional and motivational processing. *J Neurosci* 32, 8361-8372.

Knecht, S., Deppe, M., Drager, B., Bobe, L., Lohmann, H., Ringelstein, E., Henningsen, H. (2000): Language lateralization in healthy right-handers. *Brain* 123 ( Pt 1), 74-81.

Kober, H., Mende-Siedlecki, P., Kross, E.F., Weber, J., Mischel, W., Hart, C.L., Ochsner, K.N. (2010): Prefrontal-striatal pathway underlies cognitive regulation of craving. *Proc Natl Acad Sci U S A* 107, 14811-14816.

Koelsch, S., Skouras, S. (2014): Functional centrality of amygdala, striatum and hypothalamus in a "small-world" network underlying joy: an fMRI study with music. *Hum Brain Mapp* 35, 3485-3498.

Koenigsberg, H.W., Fan, J., Ochsner, K.N., Liu, X., Guise, K., Pizzarello, S., Dorantes, C., Tecuta, L., Guerreri, S., Goodman, M., New, A., Flory, J., Siever, L.J. (2010): Neural correlates of using distancing to regulate emotional responses to social situations. *Neuropsychologia* 48, 1813-1822.

Koenigsberg, H.W., Fan, J., Ochsner, K.N., Liu, X., Guise, K.G., Pizzarello, S., Dorantes, C., Guerreri, S., Tecuta, L., Goodman, M., New, A., Siever, L.J. (2009): Neural correlates of the use of psychological distancing to regulate responses to negative social cues: a study of patients with borderline personality disorder. *Biol Psychiatry* 66, 854-863.

Kohn, N., Eickhoff, S.B., Scheller, M., Laird, A.R., Fox, P.T., Habel, U. (2014): Neural network of cognitive emotion regulation--an ALE meta-analysis and MACM analysis. *Neuroimage* 87, 345-355.

Koolschijn, P.C., van Haren, N.E., Lensvelt-Mulders, G.J., Hulshoff Pol, H.E., Kahn, R.S. (2009): Brain volume abnormalities in major depressive disorder: a meta-analysis of magnetic resonance imaging studies. *Hum Brain Mapp* 30, 3719-3735.

Krendl, A.C., Kensinger, E.A., Ambady, N. (2012): How does the brain regulate negative bias to stigma? *Soc Cogn Affect Neurosci* 7, 715-726.

Kuncheva, L., Hadjitodorov, S. (2004): Using Diversity in Cluster Ensembles. *IEEE Int. Conf. Syst. Man. Cybern.* 2, 1214–1219.

Laakso, A., Bergman, J., Haaparanta, M., Vilkman, H., Solin, O., Hietala, J. (1998): [18F]CFT [(18F)WIN 35,428], a radioligand to study the dopamine transporter with PET: characterization in human subjects. *Synapse* 28, 244-250.

Lang, P.J., Bradley, M.M., Cuthbert, B.N. (1997): International Affective Picture System (IAPS): Technical Manual and Affective Ratings. NIMH Center for the Study of Emotion and Attention.

Lang, S., Kotchoubey, B., Frick, C., Spitzer, C., Grabe, H.J., Barnow, S. (2012): Cognitive reappraisal in trauma-exposed women with borderline personality disorder. *Neuroimage* 59, 1727-1734.

Langner, R., Leiberg, S., Hoffstaedter, F., Eickhoff, S.B. (2018): Towards a human self-regulation system: Common and distinct neural signatures of emotional and behavioural control. *Neurosci Biobehav Rev* 90, 400-410.

Laruelle, M., Abi-Dargham, A., van Dyck, C.H., Rosenblatt, W., Zea-Ponce, Y., Zoghbi, S.S., Baldwin, R.M., Charney, D.S., Hoffer, P.B., Kung, H.F., et al. (1995): SPECT imaging of striatal dopamine release after amphetamine challenge. *J Nucl Med* 36, 1182-1190.

Laruelle, M., D'Souza, C.D., Baldwin, R.M., Abi-Dargham, A., Kanes, S.J., Fingado, C.L., Seibyl, J.P., Zoghbi, S.S., Bowers, M.B., Jatlow, P., Charney, D.S., Innis, R.B. (1997): Imaging D2 receptor occupancy by endogenous dopamine in humans. *Neuropsychopharmacology* 17, 162-174.

LeDoux, J. (2012): Rethinking the emotional brain. *Neuron* 73, 653-676.

Leiberg, S., Eippert, F., Veit, R., Anders, S. (2012): Intentional social distance regulation alters affective responses towards victims of violence: an FMRI study. *Hum Brain Mapp* 33, 2464-2476.

Lieberman, J.A., Kane, J.M., Alvir, J. (1987): Provocative tests with psychostimulant drugs in schizophrenia. *Psychopharmacology (Berl)* 91, 415-433.

Lima, B., Cardoso, M.M., Sirotin, Y.B., Das, A. (2014): Stimulus-related neuroimaging in task-engaged subjects is best predicted by concurrent spiking. *J Neurosci* 34, 13878-13891.

Lindquist, K.A., Barrett, L.F. (2012): A functional architecture of the human brain: emerging insights from the science of emotion. *Trends Cogn Sci* 16, 533-540.

Logothetis, N.K. (2008): What we can do and what we cannot do with fMRI. *Nature* 453, 869-878.

Logothetis, N.K., Pauls, J., Augath, M., Trinath, T., Oeltermann, A. (2001): Neurophysiological investigation of the basis of the fMRI signal. *Nature* 412, 150-157.

Logothetis, N.K., Wandell, B.A. (2004): Interpreting the BOLD signal. *Annu Rev Physiol* 66, 735-769.

Lynall, M.E., Bassett, D.S., Kerwin, R., McKenna, P.J., Kitzbichler, M., Muller, U., Bullmore, E. (2010): Functional connectivity and brain networks in schizophrenia. *J Neurosci* 30, 9477-9487.

Maia, T.V. (2009): Reinforcement learning, conditioning, and the brain: Successes and challenges. *Cogn Affect Behav Neurosci* 9, 343-364.

Maia, T.V., Frank, M.J. (2017): An Integrative Perspective on the Role of Dopamine in Schizophrenia. *Biol Psychiatry* 81, 52-66.

Mak, A.K., Hu, Z.G., Zhang, J.X., Xiao, Z., Lee, T.M. (2009a): Sex-related differences in neural activity during emotion regulation. *Neuropsychologia* 47, 2900-2908.

Mak, A.K., Hu, Z.G., Zhang, J.X., Xiao, Z.W., Lee, T.M. (2009b): Neural correlates of regulation of positive and negative emotions: an fmri study. *Neurosci Lett* 457, 101-106.

Matsui, T., Murakami, T., Ohki, K. (2016): Transient neuronal coactivations embedded in globally propagating waves underlie resting-state functional connectivity. *Proc Natl Acad Sci U S A* 113, 6556-6561.

Mayberg, H.S. (1997): Limbic-cortical dysregulation: a proposed model of depression. *J Neuropsychiatry Clin Neurosci* 9, 471-481.

McClure, S.M., Laibson, D.I., Loewenstein, G., Cohen, J.D. (2004): Separate neural systems value immediate and delayed monetary rewards. *Science* 306, 503-507.

McDonald, A.J. (1998): Cortical pathways to the mammalian amygdala. *Prog Neurobiol* 55, 257-332.

McLaren, D.G., Ries, M.L., Xu, G., Johnson, S.C. (2012): A generalized form of context-dependent psychophysiological interactions (gPPI): a comparison to standard approaches. *Neuroimage* 61, 1277-1286.

McRae, K., Gross, J.J., Weber, J., Robertson, E.R., Sokol-Hessner, P., Ray, R.D., Gabrieli, J.D., Ochsner, K.N. (2012): The development of emotion regulation: an fMRI study of cognitive reappraisal in children, adolescents and young adults. *Soc Cogn Affect Neurosci* 7, 11-22.

McRae, K., Hughes, B., Chopra, S., Gabrieli, J.D., Gross, J.J., Ochsner, K.N. (2010): The neural bases of distraction and reappraisal. *J Cogn Neurosci* 22, 248-262.

McRae, K., Ochsner, K.N., Mauss, I.B., Gabrieli, J.D., Gross, J.J. (2008a): Gender Differences in Emotion Regulation: An fMRI Study of Cognitive Reappraisal. *Group Processes & Intergroup Relations* 11, 143-162.

McRae, K., Ochsner, K.N., Mauss, I.B., Gabrieli, J.J.D., Gross, J.J. (2008b): Gender differences in emotion regulation: An fMRI study of cognitive reappraisal. *Group Processes & Intergroup Relations* 11, 143-162.

Mears, D., Pollard, H.B. (2016): Network science and the human brain: Using graph theory to understand the brain and one of its hubs, the amygdala, in health and disease. *J Neurosci Res*.

Meng, C., Brandl, F., Tahmasian, M., Shao, J., Manoliu, A., Scherr, M., Schwerthoffer, D., Bauml, J., Forstl, H., Zimmer, C., Wohlschlager, A.M., Riedl, V., Sorg, C. (2014): Aberrant topology of striatum's connectivity is associated with the number of episodes in depression. *Brain* 137, 598-609.

Meunier, D., Lambiotte, R., Fornito, A., Ersche, K.D., Bullmore, E.T. (2009): Hierarchical modularity in human brain functional networks. *Front Neuroinform* 3, 37.

Modinos, G., Ormel, J., Aleman, A. (2010): Individual differences in dispositional mindfulness and brain activity involved in reappraisal of emotion. *Soc Cogn Affect Neurosci* 5, 369-377.

Morawetz, C., Bode, S., Baudewig, J., Heekeren, H.R. (2017a): Effective amygdala-prefrontal connectivity predicts individual differences in successful emotion regulation. *Soc Cogn Affect Neurosci* 12, 569-585.

Morawetz, C., Bode, S., Baudewig, J., Jacobs, A.M., Heekeren, H.R. (2016a): Neural representation of emotion regulation goals. *Hum Brain Mapp* 37, 600-620.

Morawetz, C., Bode, S., Derntl, B., Heekeren, H.R. (2017b): The effect of strategies, goals and stimulus material on the neural mechanisms of emotion regulation: A meta-analysis of fMRI studies. *Neurosci Biobehav Rev* 72, 111-128.

Morawetz, C., Kellermann, T., Kogler, L., Radke, S., Blechert, J., Derntl, B. (2016b): Intrinsic functional connectivity underlying successful emotion regulation of angry faces. *Soc Cogn Affect Neurosci* 11, 1980-1991.

Mulej Bratec, S., Xie, X., Schmid, G., Doll, A., Schilbach, L., Zimmer, C., Wohlschlager, A., Riedl, V., Sorg, C. (2015): Cognitive emotion regulation enhances aversive prediction error activity while reducing emotional responses. *Neuroimage* 123, 138-148.

Narumoto, J., Yamada, H., Iidaka, T., Sadato, N., Fukui, K., Itoh, H., Yonekura, Y. (2000): Brain regions involved in verbal or non-verbal aspects of facial emotion recognition. *Neuroreport* 11, 2571-2576.

Nelson, B.D., Fitzgerald, D.A., Klumpp, H., Shankman, S.A., Phan, K.L. (2015): Prefrontal engagement by cognitive reappraisal of negative faces. *Behav Brain Res* 279, 218-225.

New, A.S., Fan, J., Murrough, J.W., Liu, X., Liebman, R.E., Guise, K.G., Tang, C.Y., Charney, D.S. (2009): A functional magnetic resonance imaging study of deliberate emotion regulation in resilience and posttraumatic stress disorder. *Biol Psychiatry* 66, 656-664.

Newman, M.E. (2004): Fast algorithm for detecting community structure in networks. *Phys Rev E Stat Nonlin Soft Matter Phys* 69, 066133.

Newman, M.E. (2006): Modularity and community structure in networks. *Proc Natl Acad Sci U S A* 103, 8577-8582.

Niendam, T.A., Laird, A.R., Ray, K.L., Dean, Y.M., Glahn, D.C., Carter, C.S. (2012): Meta-analytic evidence for a superordinate cognitive control network subserving diverse executive functions. *Cogn Affect Behav Neurosci* 12, 241-268.

Norman, L.J., Carlisi, C.O., Christakou, A., Chantiluke, K., Murphy, C., Simmons, A., Giampietro, V., Brammer, M., Mataix-Cols, D., Rubia, K. (2017): Neural dysfunction during temporal discounting in paediatric Attention-Deficit/Hyperactivity Disorder and Obsessive-Compulsive Disorder. *Psychiatry Res Neuroimaging* 269, 97-105.

O'Herron, P., Chhatbar, P.Y., Levy, M., Shen, Z., Schramm, A.E., Lu, Z., Kara, P. (2016): Neural correlates of single-vessel haemodynamic responses in vivo. *Nature* 534, 378-382.

Ochsner, K.N., Bunge, S.A., Gross, J.J., Gabrieli, J.D. (2002): Rethinking feelings: an FMRI study of the cognitive regulation of emotion. *J Cogn Neurosci* 14, 1215-1229.

Ochsner, K.N., Ray, R.D., Cooper, J.C., Robertson, E.R., Chopra, S., Gabrieli, J.D., Gross, J.J. (2004): For better or for worse: neural systems supporting the cognitive down- and up-regulation of negative emotion. *Neuroimage* 23, 483-499.

Ochsner, K.N., Silvers, J.A., Buhle, J.T. (2012): Functional imaging studies of emotion regulation: a synthetic review and evolving model of the cognitive control of emotion. *Ann N Y Acad Sci* 1251, E1-24.

Ogawa, S., Lee, T.M., Kay, A.R., Tank, D.W. (1990): Brain magnetic resonance imaging with contrast dependent on blood oxygenation. *Proc Natl Acad Sci U S A* 87, 9868-9872.

Owen, M.J., Sawa, A., Mortensen, P.B. (2016): Schizophrenia. *Lancet* 388, 86-97.

Pan, W.J., Thompson, G.J., Magnuson, M.E., Jaeger, D., Keilholz, S. (2013): Infraslow LFP correlates to resting-state fMRI BOLD signals. *Neuroimage* 74, 288-297.

Paschke, L.M., Dorfel, D., Steimke, R., Trempler, I., Magrabi, A., Ludwig, V.U., Schubert, T., Stelzel, C., Walter, H. (2016): Individual differences in self-reported self-control predict successful emotion regulation. *Soc Cogn Affect Neurosci* 11, 1193-1204.

Patlak, C.S., Blasberg, R.G., Fenstermacher, J.D. (1983): Graphical evaluation of blood-to-brain transfer constants from multiple-time uptake data. *J Cereb Blood Flow Metab* 3, 1-7.

Pavlov, I.P. (1927): Conditioned Reflexes. Oxford University Press, London.

Peppiatt, C.M., Howarth, C., Mobbs, P., Attwell, D. (2006): Bidirectional control of CNS capillary diameter by pericytes. *Nature* 443, 700-704.

Perlman, G., Simmons, A.N., Wu, J., Hahn, K.S., Tapert, S.F., Max, J.E., Paulus, M.P., Brown, G.G., Frank, G.K., Campbell-Sills, L., Yang, T.T. (2012): Amygdala response and functional connectivity during emotion regulation: a study of 14 depressed adolescents. *J Affect Disord* 139, 75-84.

Peterson, B.S., Warner, V., Bansal, R., Zhu, H., Hao, X., Liu, J., Durkin, K., Adams, P.B., Wickramaratne, P., Weissman, M.M. (2009): Cortical thinning in persons at increased familial risk for major depression. *Proc Natl Acad Sci U S A* 106, 6273-6278.

Petit, O., Merunka, D., Anton, J.L., Nazarian, B., Spence, C., Cheok, A.D., Raccah, D., Oullier, O. (2016): Health and Pleasure in Consumers' Dietary Food Choices: Individual Differences in the Brain's Value System. *PLoS One* 11, e0156333.

Phan, K.L., Fitzgerald, D.A., Nathan, P.J., Moore, G.J., Uhde, T.W., Tancer, M.E. (2005): Neural substrates for voluntary suppression of negative affect: a functional magnetic resonance imaging study. *Biol Psychiatry* 57, 210-219.

Pitskel, N.B., Bolling, D.Z., Kaiser, M.D., Crowley, M.J., Pelphrey, K.A. (2011): How grossed out are you? The neural bases of emotion regulation from childhood to adolescence. *Dev Cogn Neurosci* 1, 324-337.

Power, J.D., Cohen, A.L., Nelson, S.M., Wig, G.S., Barnes, K.A., Church, J.A., Vogel, A.C., Laumann, T.O., Miezin, F.M., Schlaggar, B.L., Petersen, S.E. (2011): Functional network organization of the human brain. *Neuron* 72, 665-678.

Qu, Y., Telzer, E.H. (2017): Cultural differences and similarities in beliefs, practices, and neural mechanisms of emotion regulation. *Cultur Divers Ethnic Minor Psychol* 23, 36-44.

Radua, J., Romeo, M., Mataix-Cols, D., Fusar-Poli, P. (2013): A general approach for combining voxel-based meta-analyses conducted in different neuroimaging modalities. *Curr Med Chem* 20, 462-466.

Reiser, M., Kuhn, F.-P., Debus, J. (2011): Duale Reihe Radiologie. Thieme, Stuttgart.

Robinson, J.L., Laird, A.R., Glahn, D.C., Lovallo, W.R., Fox, P.T. (2010): Metaanalytic connectivity modeling: delineating the functional connectivity of the human amygdala. *Hum Brain Mapp* 31, 173-184.

Rosenberg, M.D., Finn, E.S., Scheinost, D., Papademetris, X., Shen, X., Constable, R.T., Chun, M.M. (2016): A neuromarker of sustained attention from whole-brain functional connectivity. *Nat Neurosci* 19, 165-171.

Rubinov, M., Sporns, O. (2010): Complex network measures of brain connectivity: uses and interpretations. *Neuroimage* 52, 1059-1069.

Rummery, G.A., Niranjan, M. (1994): On-line Q-learning using connectionist systems. Cambridge University Engineering Department.

Sabatinelli, D., Fortune, E.E., Li, Q., Siddiqui, A., Krafft, C., Oliver, W.T., Beck, S., Jeffries, J. (2011): Emotional perception: meta-analyses of face and natural scene processing. *Neuroimage* 54, 2524-2533.

Sanacora, G., Gueorguieva, R., Epperson, C.N., Wu, Y.T., Appel, M., Rothman, D.L., Krystal, J.H., Mason, G.F. (2004): Subtype-specific alterations of gamma-aminobutyric acid and glutamate in patients with major depression. *Arch Gen Psychiatry* 61, 705-713.

Sanchez-Gonzalez, M.A., Garcia-Cabezas, M.A., Rico, B., Cavada, C. (2005): The primate thalamus is a key target for brain dopamine. *J Neurosci* 25, 6076-6083.

Sarkheil, P., Zilverstand, A., Kilian-Hutten, N., Schneider, F., Goebel, R., Mathiak, K. (2015): fMRI feedback enhances emotion regulation as evidenced by a reduced amygdala response. *Behav Brain Res* 281, 326-332.

Schneider, F., Fink, G. (2013): Funktionelle MRT in Psychiatrie und Neurologie, 2 ed. Springer, Berlin (u.a.).

Schulze, L., Domes, G., Kruger, A., Berger, C., Fleischer, M., Prehn, K., Schmahl, C., Grossmann, A., Hauenstein, K., Herpertz, S.C. (2011): Neuronal correlates of cognitive reappraisal in borderline patients with affective instability. *Biol Psychiatry* 69, 564-573.

Sheline, Y.I., Barch, D.M., Price, J.L., Rundle, M.M., Vaishnavi, S.N., Snyder, A.Z., Mintun, M.A., Wang, S., Coalson, R.S., Raichle, M.E. (2009): The default mode network and self-referential processes in depression. *Proc Natl Acad Sci U S A* 106, 1942-1947.

Sheppes, G., Meiran, N. (2008): Divergent cognitive costs for online forms of reappraisal and distraction. *Emotion* 8, 870-874.

Shulman, R.G., Rothman, D.L., Behar, K.L., Hyder, F. (2004): Energetic basis of brain activity: implications for neuroimaging. *Trends Neurosci* 27, 489-495.
Sibson, N.R., Dhankhar, A., Mason, G.F., Rothman, D.L., Behar, K.L., Shulman, R.G. (1998): Stoichiometric coupling of brain glucose metabolism and glutamatergic neuronal activity. *Proc Natl Acad Sci U S A* 95, 316-321.
Siegle, G.J., Steinhauer, S.R., Thase, M.E., Stenger, V.A., Carter, C.S. (2002): Can't shake that feeling: event-related fMRI assessment of sustained amygdala activity in response to emotional information in depressed individuals. *Biol Psychiatry* 51, 693-707.
Silvers, J.A., Insel, C., Powers, A., Franz, P., Helion, C., Martin, R.E., Weber, J., Mischel, W., Casey, B.J., Ochsner, K.N. (2017): vlPFC-vmPFC-Amygdala Interactions Underlie Age-Related Differences in Cognitive Regulation of Emotion. *Cereb Cortex* 27, 3502-3514.
Silvers, J.A., Insel, C., Powers, A., Franz, P., Weber, J., Mischel, W., Casey, B.J., Ochsner, K.N. (2014): Curbing craving: behavioral and brain evidence that children regulate craving when instructed to do so but have higher baseline craving than adults. *Psychol Sci* 25, 1932-1942.
Silvers, J.A., Shu, J., Hubbard, A.D., Weber, J., Ochsner, K.N. (2015a): Concurrent and lasting effects of emotion regulation on amygdala response in adolescence and young adulthood. *Dev Sci* 18, 771-784.
Silvers, J.A., Wager, T.D., Weber, J., Ochsner, K.N. (2015b): The neural bases of uninstructed negative emotion modulation. *Soc Cogn Affect Neurosci* 10, 10-18.
Singh, M.K., Kesler, S.R., Hadi Hosseini, S.M., Kelley, R.G., Amatya, D., Hamilton, J.P., Chen, M.C., Gotlib, I.H. (2013): Anomalous gray matter structural networks in major depressive disorder. *Biol Psychiatry* 74, 777-785.
Smith, S.M., Fox, P.T., Miller, K.L., Glahn, D.C., Fox, P.M., Mackay, C.E., Filippini, N., Watkins, K.E., Toro, R., Laird, A.R., Beckmann, C.F. (2009): Correspondence of the brain's functional architecture during activation and rest. *Proc Natl Acad Sci U S A* 106, 13040-13045.
Sohn, M.H., Ursu, S., Anderson, J.R., Stenger, V.A., Carter, C.S. (2000): The role of prefrontal cortex and posterior parietal cortex in task switching. *Proc Natl Acad Sci U S A* 97, 13448-13453.
Spielberg, J.M., Miller, G.A., Heller, W., Banich, M.T. (2015): Flexible brain network reconfiguration supporting inhibitory control. *Proc Natl Acad Sci U S A* 112, 10020-10025.
Sripada, C., Angstadt, M., Kessler, D., Phan, K.L., Liberzon, I., Evans, G.W., Welsh, R.C., Kim, P., Swain, J.E. (2014): Volitional regulation of emotions produces distributed alterations in connectivity between visual, attention control, and default networks. *Neuroimage* 89, 110-121.
Stephanou, K., Davey, C.G., Kerestes, R., Whittle, S., Harrison, B.J. (2017): Hard to look on the bright side: neural correlates of impaired emotion regulation in depressed youth. *Soc Cogn Affect Neurosci* 12, 1138-1148.
Stephanou, K., Davey, C.G., Kerestes, R., Whittle, S., Pujol, J., Yucel, M., Fornito, A., Lopez-Sola, M., Harrison, B.J. (2016): Brain functional correlates of emotion regulation across adolescence and young adulthood. *Hum Brain Mapp* 37, 7-19.
Striedter, G.F. (2016): Neurobiology: A Functional Approach. Oxford University Press, New York.
Sutton, R.S. (1988): Learning to predict by the methods of temporal differences. *Machine Learning* 3, 9-44.
Sutton, R.S., Barto, A.G. (2018): Reinforcement Learning: An Introduction, 2 ed. The MIT Press, Cambridge, MA.
Swanson, L.W., Petrovich, G.D. (1998): What is the amygdala? *Trends Neurosci* 21, 323-331.
Takano, T., Tian, G.F., Peng, W., Lou, N., Libionka, W., Han, X., Nedergaard, M. (2006): Astrocyte-mediated control of cerebral blood flow. *Nat Neurosci* 9, 260-267.
Tavor, I., Parker Jones, O., Mars, R.B., Smith, S.M., Behrens, T.E., Jbabdi, S. (2016): Task-free MRI predicts individual differences in brain activity during task performance. *Science* 352, 216-220.
Thorndike, E.L. (1898): Animal intelligence: An experimental study of the associative processes in animals. *Psychological Review Monograph Supplements* 2.
Tolman, E.C. (1932): Purposive behavior in animals and men. Appleton Century, New York.
Tolman, E.C. (1948): Cognitive maps in rats and men. *Psychol Rev* 55, 189-208.
Touroutoglou, A., Lindquist, K.A., Dickerson, B.C., Barrett, L.F. (2015): Intrinsic connectivity in the human brain does not reveal networks for 'basic' emotions. *Soc Cogn Affect Neurosci* 10, 1257-1265.
Tuulari, J.J., Karlsson, H.K., Hirvonen, J., Salminen, P., Nuutila, P., Nummenmaa, L. (2015): Neural circuits for cognitive appetite control in healthy and obese individuals: an fMRI study. *PLoS One* 10, e0116640.
Uchida, M., Biederman, J., Gabrieli, J.D., Micco, J., de Los Angeles, C., Brown, A., Kenworthy, T., Kagan, E., Whitfield-Gabrieli, S. (2015): Emotion regulation ability varies in relation to intrinsic functional brain architecture. *Soc Cogn Affect Neurosci* 10, 1738-1748.

van der Laan, L.N., de Ridder, D.T., Charbonnier, L., Viergever, M.A., Smeets, P.A. (2014): Sweet lies: neural, visual, and behavioral measures reveal a lack of self-control conflict during food choice in weight-concerned women. *Front Behav Neurosci* 8, 184.

van Rossum, J.M. (1966): The significance of dopamine-receptor blockade for the mechanism of action of neuroleptic drugs. *Arch Int Pharmacodyn Ther* 160, 492-494.

Vanderhasselt, M.A., Kuhn, S., De Raedt, R. (2013): 'Put on your poker face': neural systems supporting the anticipation for expressive suppression and cognitive reappraisal. *Soc Cogn Affect Neurosci* 8, 903-910.

Verhoeff, N.P., Kapur, S., Hussey, D., Lee, M., Christensen, B., Psych, C., Papatheodorou, G., Zipursky, R.B. (2001): A simple method to measure baseline occupancy of neostriatal dopamine D2 receptors by dopamine in vivo in healthy subjects. *Neuropsychopharmacology* 25, 213-223.

Wager, T.D., Davidson, M.L., Hughes, B.L., Lindquist, M.A., Ochsner, K.N. (2008): Prefrontal-subcortical pathways mediating successful emotion regulation. *Neuron* 59, 1037-1050.

Wager, T.D., Lindquist, M., Kaplan, L. (2007): Meta-analysis of functional neuroimaging data: current and future directions. *Soc Cogn Affect Neurosci* 2, 150-158.

Wagner, D.D., Altman, M., Boswell, R.G., Kelley, W.M., Heatherton, T.F. (2013): Self-regulatory depletion enhances neural responses to rewards and impairs top-down control. *Psychol Sci* 24, 2262-2271.

Walter, H., von Kalckreuth, A., Schardt, D., Stephan, A., Goschke, T., Erk, S. (2009): The temporal dynamics of voluntary emotion regulation. *PLoS One* 4, e6726.

Watts, D.J., Strogatz, S.H. (1998): Collective dynamics of 'small-world' networks. *Nature* 393, 440-442.

Weinstein, J.J., Chohan, M.O., Slifstein, M., Kegeles, L.S., Moore, H., Abi-Dargham, A. (2017): Pathway-Specific Dopamine Abnormalities in Schizophrenia. *Biol Psychiatry* 81, 31-42.

Weishaupt, D., Köchli, V.D., Marincek, B. (2009): Wie funktioniert MRI?, 6 ed. Springer, Heidelberg.

Wheelock, M.D., Sreenivasan, K.R., Wood, K.H., Ver Hoef, L.W., Deshpande, G., Knight, D.C. (2014): Threat-related learning relies on distinct dorsal prefrontal cortex network connectivity. *Neuroimage* 102 Pt 2, 904-912.

Wils, R.S., Gotfredsen, D.R., Hjorthoj, C., Austin, S.F., Albert, N., Secher, R.G., Thorup, A.A., Mors, O., Nordentoft, M. (2017): Antipsychotic medication and remission of psychotic symptoms 10years after a first-episode psychosis. *Schizophr Res* 182, 42-48.

Winecoff, A., Clithero, J.A., Carter, R.M., Bergman, S.R., Wang, L., Huettel, S.A. (2013): Ventromedial prefrontal cortex encodes emotional value. *J Neurosci* 33, 11032-11039.

Winecoff, A., Labar, K.S., Madden, D.J., Cabeza, R., Huettel, S.A. (2011): Cognitive and neural contributors to emotion regulation in aging. *Soc Cogn Affect Neurosci* 6, 165-176.

Wunderlich, K., Smittenaar, P., Dolan, R.J. (2012): Dopamine enhances model-based over model-free choice behavior. *Neuron* 75, 418-424.

Xia, M., Wang, J., He, Y. (2013): BrainNet Viewer: a network visualization tool for human brain connectomics. *PLoS One* 8, e68910.

Yarkoni, T. (2009): Big Correlations in Little Studies: Inflated fMRI Correlations Reflect Low Statistical Power-Commentary on Vul et al. (2009). *Perspect Psychol Sci* 4, 294-298.

Yokum, S., Stice, E. (2013): Cognitive regulation of food craving: effects of three cognitive reappraisal strategies on neural response to palatable foods. *Int J Obes (Lond)* 37, 1565-1570.

Zaehringer, J., Falquez, R., Schubert, A.L., Nees, F., Barnow, S. (2018): Neural correlates of reappraisal considering working memory capacity and cognitive flexibility. *Brain Imaging Behav*.

Zhang, W., Li, H., Pan, X. (2015): Positive and negative affective processing exhibit dissociable functional hubs during the viewing of affective pictures. *Hum Brain Mapp* 36, 415-426.

# 8 Acknowledgments

Parts of this thesis were published in the following article published by Oxford University Press:

Brandl F, Mulej Bratec S, Xie X, Wohlschläger AM, Riedl V, Meng C, Sorg C:
*Increased Global Interaction Across Functional Brain Modules During Cognitive Emotion Regulation.*
Cereb Cortex. 2018 Sep 1;28(9):3082-3094.

I want to thank my supervisor Prof. Dr. Claus Zimmer for supporting me during the last years and the members of my thesis advisory committee, PD Dr. Christine Preibisch and Prof. Dr. Markus Ploner, for helpful discussions of my work.

Moreover, I owe a debt of gratitude to PD Dr. Christian Sorg, who has supervised my research with stimulating ideas and constructive critic, thereby often preventing "wrong turns". Further thanks go to my colleagues who helped to achieve this effort, above all Drs. Mihai Avram, Satja Mulej Bratec, and Chun Meng, as well as to Prof. Dr. Sibylle Ziegler, Prof. Dr. Klaus Wunderlich, and Dr. Mona Mustafa, who provided fruitful feedback. I would also like to mention doctoral student Zarah Le Houcq Corbi, the always helpful Martin Gruber, the MTAs Sylvia Schachoff and Anna Winter, and all subjects who kindly participated in the studies.

Finally, I would like to thank my family for always supporting me and making this work possible.

# 9 List of figures and tables

Figure 1: Hemodynamic response. ..... 10
Figure 2: Flow diagram of literature search. ..... 19
Figure 3: Hypothesis, design, and functional brain network modules during emotions with and without CER. ..... 25
Figure 4: Structure of the sequential decision making task . ..... 33
Figure 5: Brain activation of CRC and CER. ..... 40
Figure 6: Increased global and nodal interaction across modules during CER. ..... 43
Figure 7: Connector hubs during emotions with and without CER. ..... 44
Figure 8: Linking global and local properties of CER. ..... 46
Figure 9: Stay-switch behavior. ..... 47

Table 1: Glossary of graph terms ..... 16
Table 2: Studies included in the CRC meta-analysis. ..... 37
Table 3: Studies included in the CER meta-analysis. ..... 39

# 10 Publications related to this thesis

Brandl F, Mulej Bratec S, Xie X, Wohlschläger AM, Riedl V, Meng C, Sorg C:
*Increased Global Interaction Across Functional Brain Modules During Cognitive Emotion Regulation.*
Cereb Cortex. 2018 Sep 1;28(9):3082-3094.

Brandl F, Le Houcq Corbi Z, Mulej Bratec S, Sorg C:
*Cognitive reward control recruits medial and lateral frontal cortices, which are also involved in cognitive emotion regulation - A coordinate-based meta-analysis of fMRI studies.*
NeuroImage (under review)

Brandl F, Avram M, Cabello J, Leucht C, Scherr M, Mustafa M, Leucht S, Ziegler S, Wunderlich K, Sorg C:
*Association between impaired model-free decision making and dopamine synthesis in schizophrenia.*
in preparation for submission